SAXTON NUCLEAR EXPERIMENTAL CORPORATION

SAFEGUARDS REPORT FOR THE SAXTON REACTOR PARTIAL PLUTONIUM CORE II

March 1965

SAFEGUARDS REPORT

FOR THE SAXTON REACTOR PARTIAL

PLUTONIUM CORE II

MARCH 1965

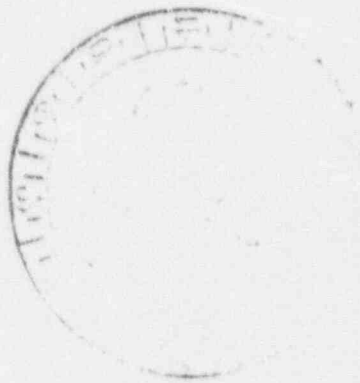

TABLE OF CONTENTS

LIST OF TABLES

LIST OF FIGURES

LIST OF FIGURES (Cont'd)

I. INTRODUCTION

A. OBJECTIVE AND SCOPE

The objectives of the Saxton Plutonium Project are to develop information concerning the utilization of plutonium enriched fuels in a closed cycle water reactor environment and to develop analytical methods and techniques that will reliably predict the in-pile performance and long term behavior of such fuels in large scale reactors.

The scope of the program covers the design and fabrication of mixed PuO_2-UO_2 fuels, evaluation of in-core performance of these fuels and post irradiation examination and evaluation of fuel and clad samples. These fuels will make up part of the core in the Saxton reactor with the remainder of the core made up of UO_2 fuel. The scope also includes pre-irradiation criticals to evaluate the predicted nuclear design.

B. PROGRAM DESCRIPTION

The program goals of extended irradiation exposure and high fuel burnup plus the nuclear and control characteristics of the Saxton reactor are the basic parameters which have been considered in the design of the fuel for the plutonium core. The selection and analysis of various combinations of critical factors assures a fuel design which will not only meet the goals of the program but will also be within the operational limits of the Saxton reactor.

Based on the fuel design and enrichment established, the thermal and hydraulic characteristics of the core have been analyzed and evaluated. In addition, a set of critical experiments have been designed to verify the nuclear parameters of the fuel specified

during the design phase of the program. The results of these criticals, expected by May 1965, will be analyzed and compared with predicted values from the design study before the partial plutonium core is operated.

Additional tests prior to operation at full power in the Saxton reactor include a series of zero and low power tests and physics measurements to obtain and verify actual in-core characteristics and performance. The information to be obtained from these tests and measurements include core excess reactivity, control rod and soluble poison worth characteristics, and temperature, pressure, moderator and power reactivity coefficients. These nuclear characteristics as well as the core thermal and hydraulic characteristics and neutron flux and power distributions will be measured and evaluated at intermediate power levels before operating at full power. Present Saxton in-core instrumentation consisting of pitot tubes, thermocouples and flux wires will be used in obtaining the data.

During the course of the project, a re-determination of these characteristics will be made during several shutdown periods in order to determine characteristic changes with irradiation exposure. Comparisons will be made between measured values and those predicted by analytical methods.

Following the in-core irradiation period, an extensive post-irradiation examination program will be conducted to evaluate fuel performance and to compare actual and predicted performance. Examinations will be made for signs of distortion or wear marks on fuel assembly cans and for broken or distorted grid structures. Fuel rods will be examined for abnormal appearance, wear and dimensional changes. Selected high burnup rods will be examined with a stereomicroscope for evidence of cracking, distortion or other abnormal appearances.

Some rods will be sectioned and examined metallographically to evaluate cladding performance, fuel cracking and radial redistribution. Some selected high burnup rods will be punctured so that gas pressure and clad stress can be calculated and a quantitative analysis performed by mass spectroscopy to determine fission gas releases. Samples of cladding from these rods will be taken for metallographic and mechanical testing. Pellets from several rods will be sampled and examined using mass spectrographic techniques to determine the change in U and Pu isotope concentrations as a function of burnup. Radiochemical analyses will also be performed for selected fission products to determine burnup and radial distribution.

C. PROGRAM SCHEDULE

A tentative schedule for installation of Core II is as follows:

Begin critical experiments - 3/18/65
Complete critical experiments - 6/4/65
Start receipt of fuel at Saxton - 7/10/65
Complete fabrication of all fuel assemblies - 7/1/65
Core loading completed - 8/27/65
Low power testing period - 9/1/65 - 10/1/65

II. NUCLEAR DESIGN

A. INTRODUCTION

1. Objectives

As outlined in Section I, the purpose of the Saxton Plutonium Program is to develop information concerning the use of plutonium enriched fuel in water reactor systems. This purpose is to be achieved by the irradiation of PuO_2-UO_2 fuel in the Saxton reactor and by a supporting program of analysis, experiment and evaluation. The core, composed in part of plutonium fuel, is designed for 8250 megawatt days of operation. Since it is desired to achieve a high burnup in the plutonium fuel, the reference design is one in which nine plutonium fuel assemblies will be installed in the center of the core with the twelve uranium fuel assemblies installed in the peripheral locations.

2. Nuclear Characteristics Summary

When installed in the center of the reactor, the plutonium assemblies influence the nuclear characteristics of the system to a greater extent than if they were installed in peripheral locations. However, the analysis has shown comparatively small changes in reactivity and kinetics characteristics (as compared to an all uranium core) are introduced by the plutonium. The following qualitative statements briefly summarize the major reactivity and kinetic effects that occur with a partial plutonium core.

a) The Saxton plutonium core will have a more negative moderator temperature coefficient than with a conventional uranium loading.

b) The negative Doppler coefficient will be larger with PuO_2-UO_2 fuel than with just UO_2 fuel.

c) The part-plutonium core will have a larger positive pressure coefficient and a more negative void coefficient than the conventional uranium core.

d) Boron worth and control rod worth are decreased in the partial plutonium core.

e) The delayed neutron fraction (β_{eff}) and prompt neutron lifetime when averaged over the core at the beginning of life will be smaller with a partial plutonium loading than with a full loading of uranium fuel. They both remain essentially constant throughout the core life because of the change in radial power distribution and the Pu buildup in the outer uranium assemblies.

As the central plutonium region has a larger absorption cross section than the outer uranium region, the thermal flux undergoes a marked change at region boundaries and peaks to a greater extent than normal in those water slots near the plutonium. In addition, since the fission cross section is larger, local power peaking occurs in the plutonium rods at the boundaries and water slots. Diffusion theory analysis has been used in determining power distribution and power peaking effects. The critical experiments as outlined in paragraph A-4 will determine if the available reactivity and power distributions will permit installation of the plutonium assemblies in the center of the core or if it is necessary to change the reference design to one in which the plutonium assemblies are installed in peripheral locations. Such a change would minimize the differences between a core containing plutonium and a conventional Saxton core.

3. Analytical Methods

The nuclear design of the plutonium loading in the Saxton reactor was based on the use of standard analytic methods developed in the design and operational analysis of a number of pressurized water reactors. These methods have been compared to a large number of water moderated critical experiments. They were also used in the design of the initial uranium loading in the Saxton reactor (Saxton Core I) and in the subsequent comparison of analysis with experimental data from Saxton operation. In addition, the methods were used in the analysis of six mixed-oxide (PuO_2-UO_2) critical and approach-to-critical experiments conducted at Hanford and an allowance for the discrepancy between analysis and experiment was included in the reactivity calculations for the plutonium core. Thus the analysis is based on proven practice, the reactor is one for which experimental information is available, and the extrapolation to a part-plutonium configuration is based, in so far as possible, on applicable critical experiments.

The following paragraphs contain a brief description of the computer programs used in the analysis.

LEOPARD[1]

The LEOPARD computer program determines fast and thermal neutron spectra based on a modified MUFT-SOFOCATE model. The thermal spectrum is the same as that given by a Wigner-Wilkins SOFOCATE calculation except for the treatment of disadvantage factors. Disadvantage factors are determined by using a modified form of the Amouyal-Benoist calculation at 172 energy levels from zero to 0.625 ev. LEOPARD computes a non-thermal spectrum based on a consistent B-1 MUFT IV calculation. The resonance integral for U-238 is determined from a correlation that is in good agreement with Hellstrand's measurements for uranium metal and uranium

(1) R. F. Barry, "LEOPARD - A Spectrum Dependent, Non-Spatial Depletion Code for the IBM-7094," WCAP-3741 (1963.

dioxide at any temperature.

The calculational procedure contained in LEOPARD has been compared to 116 critical and exponential lattices, 55 using UO_2 fuel and 61 using uranium metal fuel. The calculations result in an average k_{eff} of 0.9931 ± 0.0086 for the 116 cases where the quoted errors correspond to one standard deviation.(1)

The code also computes zero-dimensional fuel depletion effects and provides a time dependent microscopic cross-section library for subsequent spatial burnup calculations. The burnup portion of the LEOPARD code has been compared with Yankee Core I spent core data. The plutonium isotopic composition as a function of U-235 depletion is in good agreement with the data.(2)

PDQ-3

Solves the few-group, time independent, neutron diffusion equations in X-Y geometry.

AIM-5

Solves the few-group, time independent, neutron diffusion equation in one dimension.

TURBO*

Solves the few-group, two dimensional (X-Y geometry) neutron diffusion equations in combination with a point-wise burnup calculation to determine reactivity-lifetime relationships. The microscopic library generated in LEOPARD is used to determine time dependent group constants for use in TURBO*.

---

(1) L. E. Strawbridge, "Calculation of Lattice Parameters and Criticality for Uniform Water Moderated Lattices," WCAP-3742 (1963).

(2) "Large Closed-Cycle Water Reactor Research and Development Program Progress Report for the Period July 1, 1964 to September 30, 1964" WCAP-3269-5.

LUX

A modification of the CANDLE one-dimensional few group depletion code and is used to determine reactivity as a function of lifetime. The LEOPARD microscopic library is used.

THERMOS

A cell transport theory code in both space and energy. This program was used as a check on the thermal group calculation contained in LEOPARD. The results from the two calculations were in excellent agreement.

4. Experiment Sequence

Prior to the operation of the plutonium fuel in the Saxton reactor, a critical experiment program with both the PuO_2-UO_2 fuel rods and the UO_2 fuel rods will be carried out at the Westinghouse Reactor Evaluation Center (WREC). The proposed program consists of the following six basic configurations:

Configuration	Type Core	Type Fuel	Type Lattice
1	Single-region, clean core	PuO_2-UO_2	Loose
2	Single-region, clean core	PuO_2-UO_2	Design H/Pu
3	Two-region, clean core	PuO_2-UO_2 Inside UO_2 Outside	Design H/Pu
4	Single-region, borated core	PuO_2-UO_2	Design H/Pu
5	Two-region, borated core	PuO_2-UO_2 Inside UO_2 Outside	Design H/Pu
6	Inverted, two-region, clean and borated cores	UO_2 Inside PuO_2-UO_2 Outside	Design H/Pu

As shown by the table, single-region criticals with the plutonium rods and two-region criticals consisting of separate plutonium and uranium

zones will be carried out. The experiments will include the measurement of system reactivity, power distribution and power peaking effects, flux distributions, control rod and boron worth, and kinetic parameters. These experiments will provide a "clean configuration" check on the analytic methods used in the design of the fuel and reference core. Configuration 6 may not be checked if the first 5 closely verify the analytical results.

Later, low power tests conducted in the Saxton pressure vessel will provide an additional check of the design prior to power operation. These tests will follow procedures developed in the course of previous Saxton startups. The low power tests will include such measurements as the moderator temperature coefficient at several boron concentrations, boron worth, control rod differential worth in a normal withdrawal sequence, and flux distributions.

B. REACTIVITY SUMMARY

1. Available Reactivity

The excess reactivity of the system was determined by means of PDQ-3 two group diffusion calculations in X-Y geometry. The hot, clean reactivity at power is expected to be $10.3 \pm 1.3\% \Delta k/k$. This excess reactivity estimate includes an allowance for the discrepancy between analysis and experiment that is based on the analysis of six variable lattice, mixed-oxide critical and approach-to-critical experiments conducted at Hanford. In this comparison, an average analytical over-prediction of $2.6\% \Delta k/k$ was found. The listed uncertainty of $\pm 1.3\% \Delta k/k$ is an estimate as to the size of the possible error that may occur in initial excess reactivity.

To provide a check on the methods of analysis used in determining the system reactivity, similar PDQ-3 calculations were carried out for

Saxton Core I. A calculated k_{eff} of 0.9997 was determined for the hot, rods-out, just critical configuration containing 1804 ppm boron.

Calculations were also made to determine the clean Core I reactivity at power. The calculated reactivity, 14.82% $\Delta k/k$, is in good agreement with the reactivity as determined from boron worth and power coefficient measurements, 14.4% $\Delta k/k$.

2. Reactivity Lifetime Expected

The available lifetime for the Saxton reactor containing a partial core of plutonium fuel was determined by both one-dimensional (radial) and two-dimensional (x-y) burnup calculations. The reactivity as a function of lifetime as determined from a LUX radial calculation is shown in Figure II-1. This figure also shows the possible variation in lifetime that would result for the maximum and minimum expected values of initial reactivity.

Duplicate lifetime calculations using LUX were carried out for Saxton Core I and were compared to the projected lifetime based on the measured depletion rate. In this comparison, the calculated lifetime is about 1000 hours less than that indicated by the experiment.

3. Lifetime Power and Burnup

The peak power in the core will occur in the plutonium region at the beginning of life. Figure II-2 shows the core radial power distribution as calculated by a PDQ-3 two-dimensional diffusion analysis. The analysis was originally carried out for a plutonium enrichment of 6.5 w/o PuO_2. The difference in power levels for the new reference design of 6.6 w/o enrichment and the 6.5 w/o enrichment design is small, approximately 1% in local power. The local-to-core average power in each fuel rod in the central plutonium assembly is shown in Figure II-3.

The following list summarizes the maximum values of peak rod radial power to core average radial power for both the plutonium and uranium regions as a function of time. The values were determined by means of two-dimensional burnup calculations using TURBO*.

PEAK ROD TO CORE AVERAGE RADIAL POWER

Time, Hours at 23.5 MWt	Pu Region	U Region
0	2.36	1.22
6,000	1.88	1.26
12,000	1.63	1.23
Average for 8250 MWD	2.00	1.24

The initial peak power values in this list and in Figure II-4(a) are higher than those shown in Figures II-2, II-3, in order to correct the calculated peak value to an expected experimental peak value based on a comparison of analytical and experimental results from the original uranium loading. The initial peak power also includes corrections for an increase in coolant boron content to correspond to beginning of life conditions and for the extrapolation from 6.5 w/o enrichment to 6.6 w/o enrichment.

To provide the desired lifetime of 8250 MWD, the specified enrichment is 6.6 w/o PuO_2 and results in an increase in the nuclear hot channel factor over that for a conventional all uranium Saxton core. As a result, it may be necessary to limit the reactor power level initially in order to avoid exceeding the linear power density design of 16 Kw/ft. Figure II-4(a) shows the radial nuclear hot channel factor in the plutonium region as a function of operating time at 23.5 MWt. A reactor operating sequence that does not exceed 16 kw/ft is shown in Figure II-4(b). This figure shows that a power level of 23.5 MWt will be allowed following six months of operation at 21.6 MWt and a load factor of 0.5. The actual initial power level limit to ensure that the design of 16 Kw/ft will not be exceeded will be determined following experimental measurements and calculation of hot channel factors. Thereafter, the maximum linear power density decreases with the reactor at a constant power level of 23.5 MWt and

is expected to be approximately 13.0 kw/ft after 8250 MWD of operation.

A design lifetime objective of 8250 MWD and the listed average value for the peak rod power in each region results in the following predicted peak rod average burnup values.

Maximum burnup, Pu fuel rod = 20,200 MWD/tonne
Maximum burnup, U fuel rod = 11,500 MWD/tonne

4. Reactivity Coefficients

4.1 Doppler Coefficient

Doppler coefficient calculations were carried out as a function of the effective fuel temperature where the effective fuel temperature is defined as that temperature which gives the correct experimental power coefficients of reactivity when employed in standard design calculations. The relationship between pellet temperature and effective fuel temperature is based on the work which correlated effective fuel temperature for Doppler broadening of U-238 resonances with experimental power coefficient measurements in the Yankee, Saxton, and BR-3 reactors. The temperature power relationships developed for the Saxton reactor are shown in Figure II-5.

The Doppler coefficient was determined by completing a series of LEOPARD claculations for values for T_{eff} ranging from 800°F to 2000°F in 200-degree increments. The resulting group constants were then used in AIM-5 radial diffusion calculations. Figure II-6 summarizes the results for variations in T_{eff} alone and for the variation in temperatures shown in Figure II-5. The difference between the two curves is due to the change in moderator content resulting from the small change in clad dimensions with temperature. Figure II-7 shows the derived power coefficient based on the Doppler calculations and the temperature relationships of Figure II-5.

Calculations were also made to determine the fraction of the total Doppler effect due to temperature changes in each region separately. Approximately 70% of the reactivity change due to Doppler is the result of temperature changes in the central plutonium region while 30% is the result of temperature changes in the outer uranium region.

4.2 Moderator Coefficient

The moderator temperature coefficient was determined by a sequence of LEOPARD and AIM-5 calculations. Figure II-8 summarizes the results for partial plutonium core. The figure also includes a comparison of the measured values of the moderator temperature coefficient with the analysis for the conventional Saxton all uranium loading.

4.3 Pressure and Void Coefficient

Table II-1 compares the pressure and void coefficients for the conventional uranium loading with that of the core containing nine plutonium fuel assemblies. The analysis was carried out using a LEOPARD and AIM-5 sequence. Measured values of the pressure coefficient at various boron concentrations are included in the table. The analysis and experiment are in good agreement for comparable conditions.

TABLE II-1

PRESSURE AND VOID COEFFICIENTS

Pressure Coefficient: $\frac{1}{k}\frac{\partial k}{\partial P}$ ($\Delta k/k$ / psi) x 10^6, Moderator = 530°F

Pu Core		CONVENTIONAL CORE			
1000 ppm Boron		Maximum Boron	1000 ppm Boron	Clean 0 Boron	Rodded, 0 Boron
+3.5	Analysis:	+1.30 (2000 ppm)	+2.1	+3.1	+5.6 (all rods)
	Experiment:	+1.45 (1600 ppm)	+2.4		+4.6 (partial rods)

Void Coefficient: $\frac{1}{k} \frac{\partial K}{\partial V}$ (% $\Delta k/k$/% void), Moderator = 530°F

Pu Core		CONVENTIONAL CORE		
1000 ppm Boron	2000 ppm Boron	1000 ppm Boron	Clean 0 Boron	Fully Rodded 0 Boron
-0.27	-0.10	-0.18	-0.26	-0.43

4.4 Boron Worth

The LEOPARD - AIM-5 calculated boron worth as a function of boron concentration is shown in Figure II-9.

C. CONTROLS SUMMARY

The nominal mode of control for the Saxton Plutonium Core II is expected to be chemical shim. However, at times during the program, it may be necessary to employ control rods alone. In any mode of control, soluble poison will be required for cold, clean core shutdown.

1. Reactivity Effects

Control rod worths were established by means of a series of FDQ calculations using a method that accurately determines rod worth in Saxton Core I. The calculated control rod total bank work for the plutonium core is 16.9% $\Delta k/k$. With a maximum predicted initial hot, clean at power excess reactivity of 11.6% $\Delta k/k$, the minimum initial available shutdown margin in the hot reactor is 5.3% $\Delta k/k$. Stuck rod calculations show that the total bank worth with the most effective rod stuck in the fully withdrawn position is 11.7% $\Delta k/k$. The minimum shutdown margin for this condition at the beginning of core life is therefore only 0.1% $\Delta k/k$. Careful evaluation of the critical tests will determine the amount of initial excess reactivity available with the new core. If the initial excess reactivity is greater than 9.7% $\Delta k/k$, then the shutdown criterion of 2% $\Delta k/k$ shutdown margin available with the most reactive rod stuck

will not be met, and it will be necessary to do one or both of the following at the beginning of core life.

a) Restrict rod withdrawal initially by setting existing limit switches to hold the required reactivity in the core as was practiced with the conventional all uranium loading.

b) Use chemical shim for other reactivity effects such as xenon in addition to that required for the temperature defect.

2. Power Effect

Figures II-10 and II-11 show the effect on the beginning of life power distributions for stuck rod and dropped rod conditions. The peak rod power in either figure will be about 3% less for zero boron concentration.

D. KINETIC CHARACTERISTICS

β_{eff} was evaluated throughout life from a TURBO* calculation. A constant value of $\sim$ 0.0049 was found. The β_{eff} was determined by weighting the delayed group yields of the various fissioning materials by the fraction of neutrons from each isotope. An importance factor, derived from LEOPARD calculations using different source spectra, was applied to account for the difference in importance of delayed and prompt neutrons. Table II-2 summarizes the power and neutron source fraction in each of the two regions for each isotope at the beginning of life. The table also includes delayed neutron data and the region and core average β_{eff} and prompt neutron lifetime.

TABLE II-2

ISOTOPIC POWER AND NEUTRON FRACTIONS,
DELAYED NEUTRON DATA, β_{eff} AND PROMPT LIFETIME

Beginning of Life

	Isotopic Power Fractions				Neutron Source Fractions			
Region	U-235	U-238	Pu-239	Pu-241	U-235	U-238	Pu-239	Pu-241
Core Average	0.4301	0.0504	0.5078	0.0112	0.4008	0.0514	0.5352	0.0125
Pu Region(1)	0.1302	0.0503	0.7998	0.0177	0.1188	0.0490	0.8132	0.0190
U Region(2)	0.9390	0.0520	0.0088	0.0001	0.9340	0.056	0.0099	0.0001

Delayed Neutron Data

Delayed Neutron Group, i	λ_i, sec^{-1}		β_i			
	U-235	Pu-239	U-235	U-238	Pu-239	Pu-241 (3)
1	0.0124	0.0128	0.000215	0.000201	0.000074	0.000091
2	0.0305	0.0301	0.001424	0.002151	0.000626	0.000775
3	0.111	0.124	0.001274	0.002543	0.000443	0.000549
4	0.301	0.325	0.002568	0.006092	0.000685	0.000848
5	1.13	1.12	0.000748	0.003533	0.000181	0.000224
6	3.00	2.69	0.000273	0.001178	0.000092	0.000114
			0.0065	0.0157	0.0021	0.0026

β_{eff} and Prompt Neutron Lifetime

Region	β_{eff}	Lifetime, μsec (4)
Core Average	0.0049	11.7 (5)
Pu Region	0.0035 (1)	8.6
U Region	0.0075 (2)	15.7

(1) Includes partially burned uranium fuel followers.

(2) Includes partially burned uranium L-sections.

(3) Relative abundance for Pu-239 used.

(4) Calculation made with core containing 1000 ppm boron.

(5) Weighting based on power fractions of U = .439, contains L-sections and followers, Pu = .561

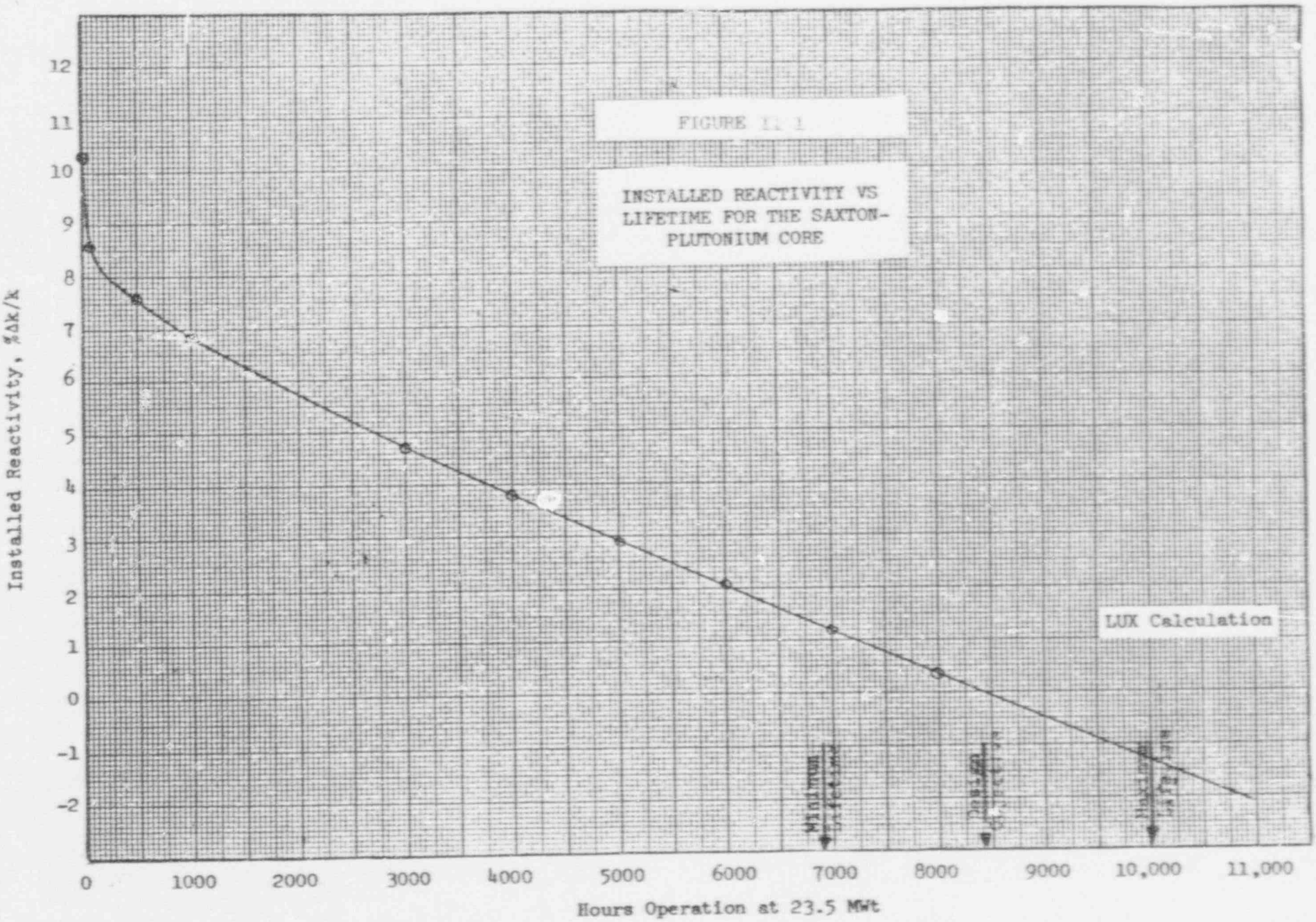
FIGURE 11.1
INSTALLED REACTIVITY VS LIFETIME FOR THE SAXTON-PLUTONIUM CORE
LUX Calculation
Installed Reactivity, %Δk/k
12
11
10
9
8
7
6
5
4
3
2
1
0
-1
-2
0
1000
2000
3000
4000
5000
6000
7000
8000
9000
10,000
11,000
Hours Operation at 23.5 MWt

PDQ Power Distribution

Configuration: 9 PuO_2-UO_2 Assemblies (6.5 w/o PuO_2) in Center Positions
No rods, 1000 ppm Boron, Depleted Followers and L-Sections
λ = 1.08848

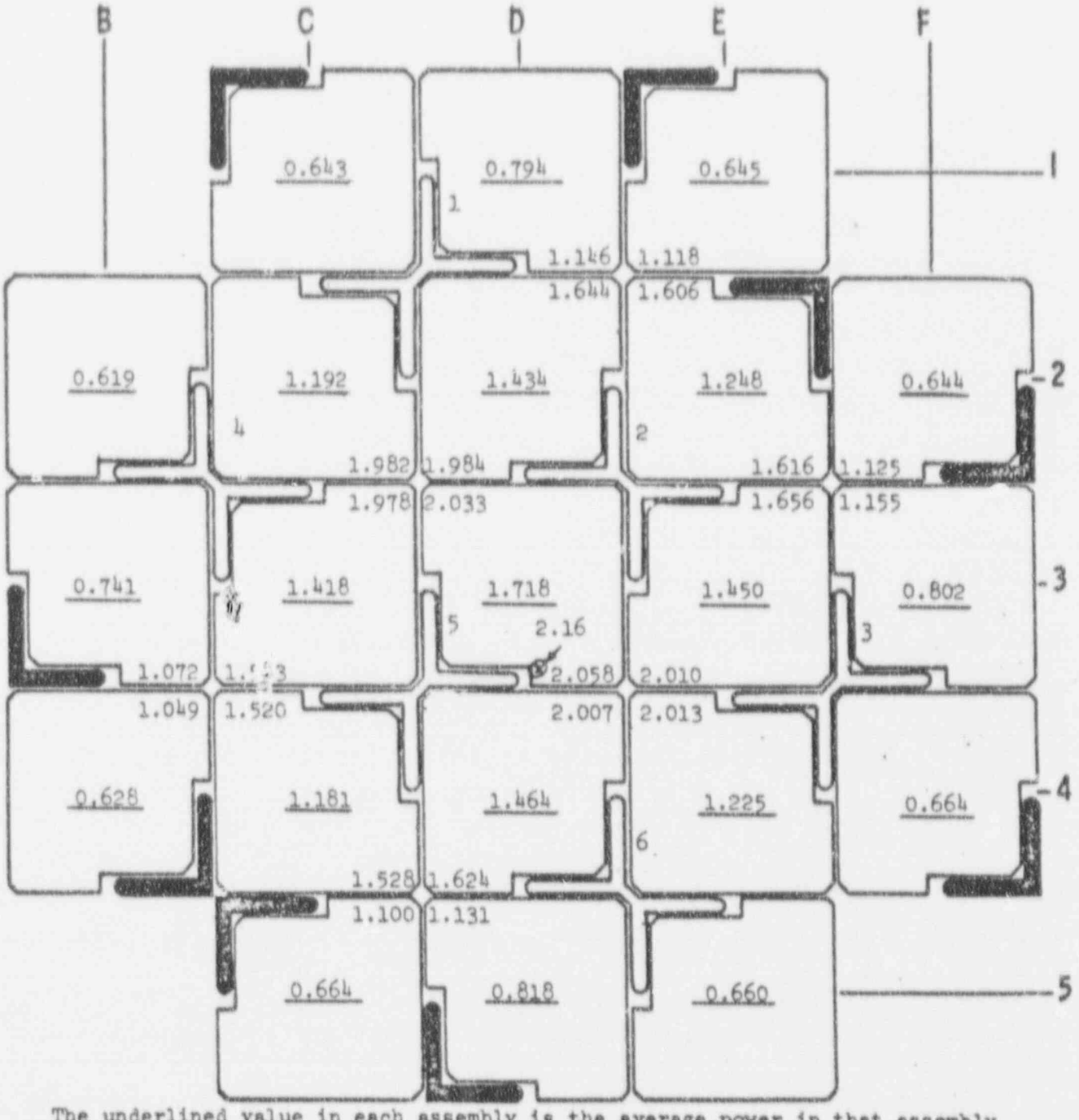

The underlined value in each assembly is the average power in that assembly re'ative to the average power in the core. The relative power is also shown for individual fuel rods near the uncontrolled corners of assemblies (where hot spots usually occur). Maximum Rod Power = 2.36. (This value includes a correction for the discrepancy between analysis and experiment for Saxton Core I and for an increase in boron content to 2400 ppm).

Saxton-Plutonium Core Power Distribution

FIGURE II-5

Conditions: 9 PuO_2-UO_2 Assemblies (6.5 w/o PuO_2) in Center
No Rods, 1000 ppm Boron
Depleted Followers and L-Sections
λ = 1.08848

2.03	1.85	1.88	2.14		2.14	1.91	1.90	2.10
1.84	1.66	1.66	1.76	1.89	1.76	1.67	1.68	1.90
1.87	1.66	1.63	1.64	1.66	1.64	1.63	1.67	1.82
2.15	1.77	1.64	1.62	1.62	1.63	1.65	1.77	2.14
	1.94	1.66	1.63	1.62	1.63	1.66	1.90	
	1.94	1.673	1.63	1.63	1.63	1.65	1.77	2.15
	1.93	1.71	1.68	1.67	1.65	1.64	1.68	1.89
	2.00	1.94	1.95	1.95	1.78	1.67	1.68	1.87
					2.16	1.89	1.96	2.06

Maximum Rod Power = 2.36
(This value includes a correction for the discrepancy between analysis and experiment for Saxton Core I and for an increase in boron content to 2400 ppm).

Center Assembly Power Distribution

FIGURE II-3

FIGURE 11.4(a)

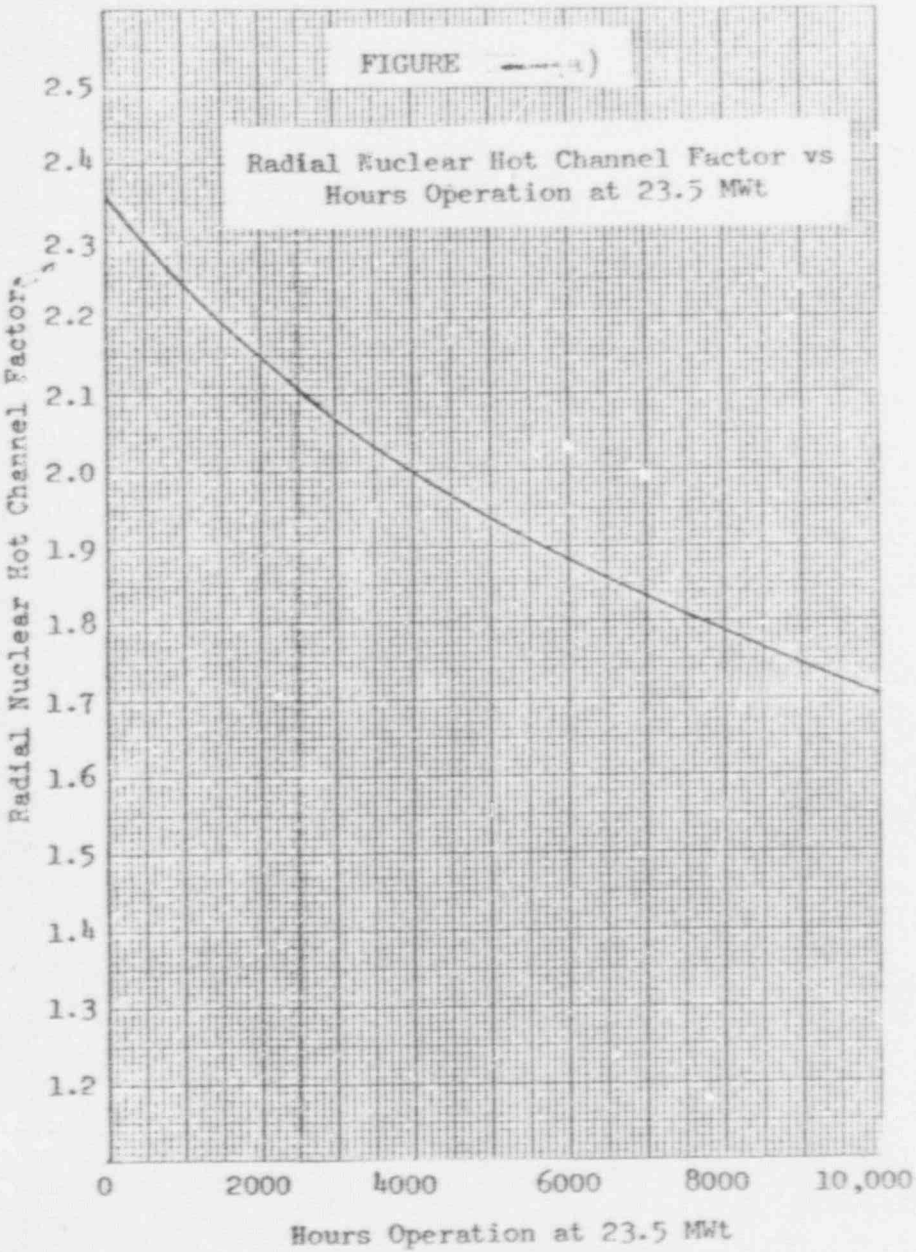

FIGURE 11.4(b)

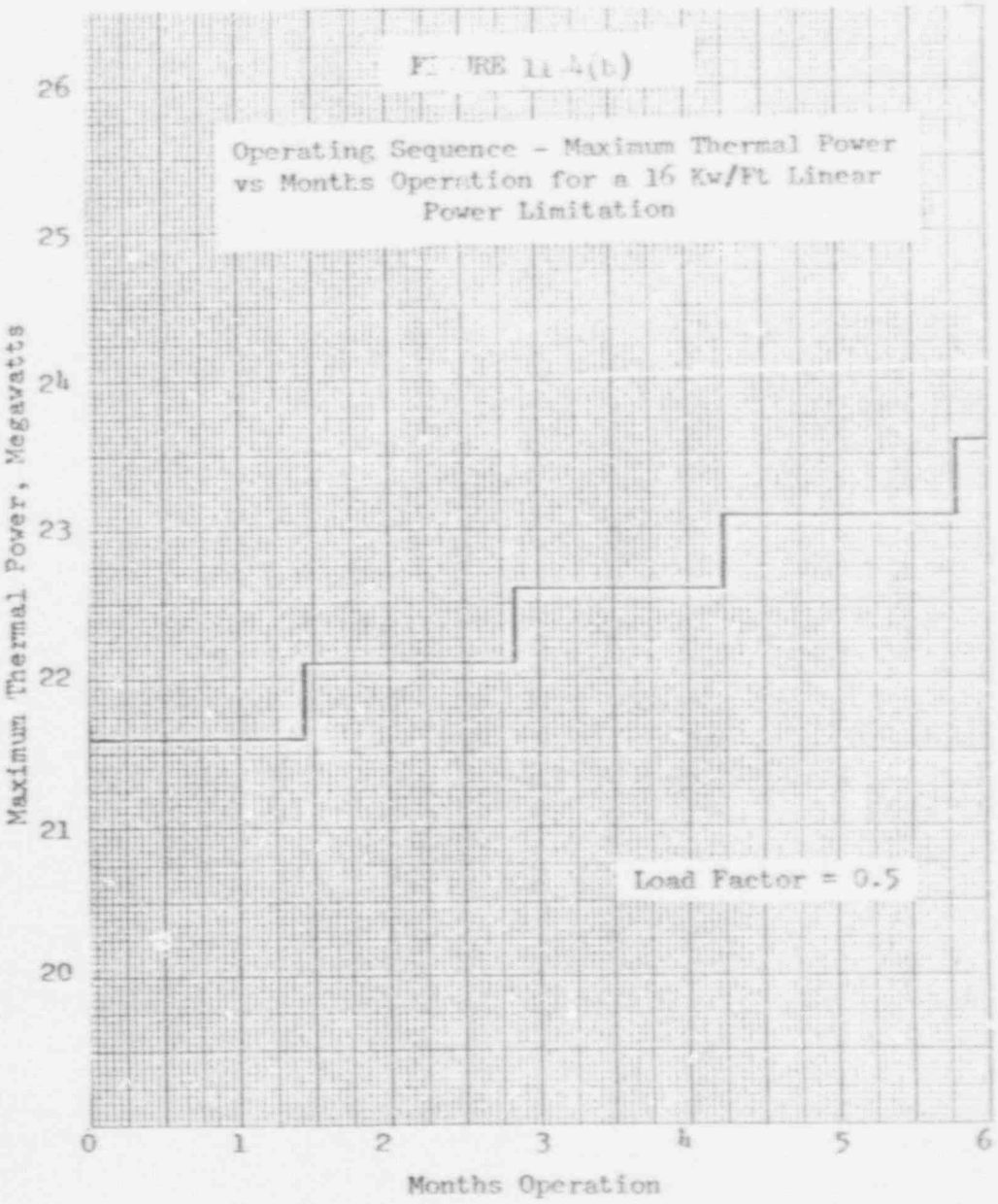

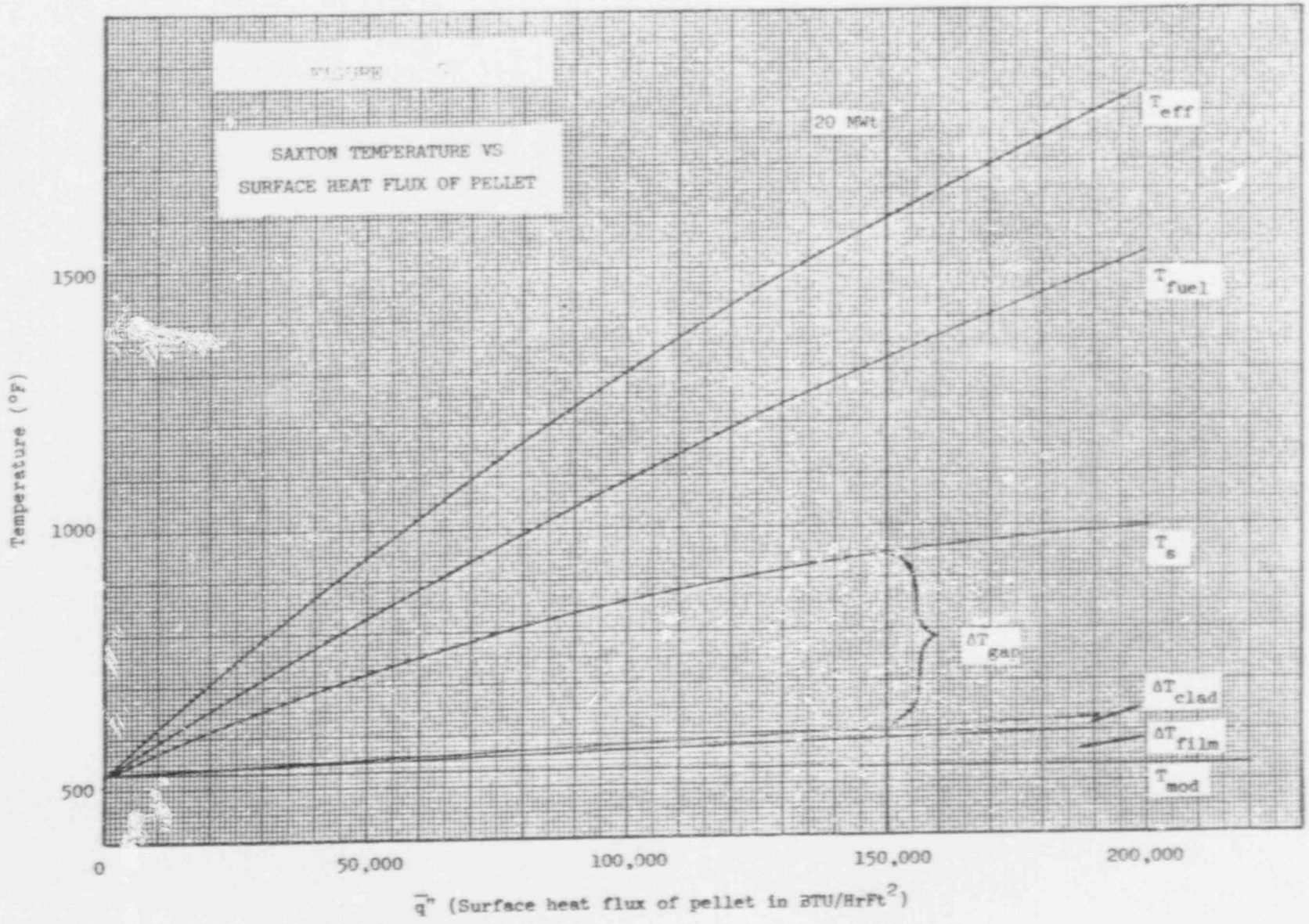
SAXTON TEMPERATURE VS
SURFACE HEAT FLUX OF PELLET
20 MWt
T_{eff}
T_{fuel}
T_s
ΔT_{gap}
ΔT_{clad}
ΔT_{film}
T_{mod}
Temperature (°F)
1500
1000
500
0
50,000
100,000
150,000
200,000
$\bar{q}''$ (Surface heat flux of pellet in BTU/HrFt^2)

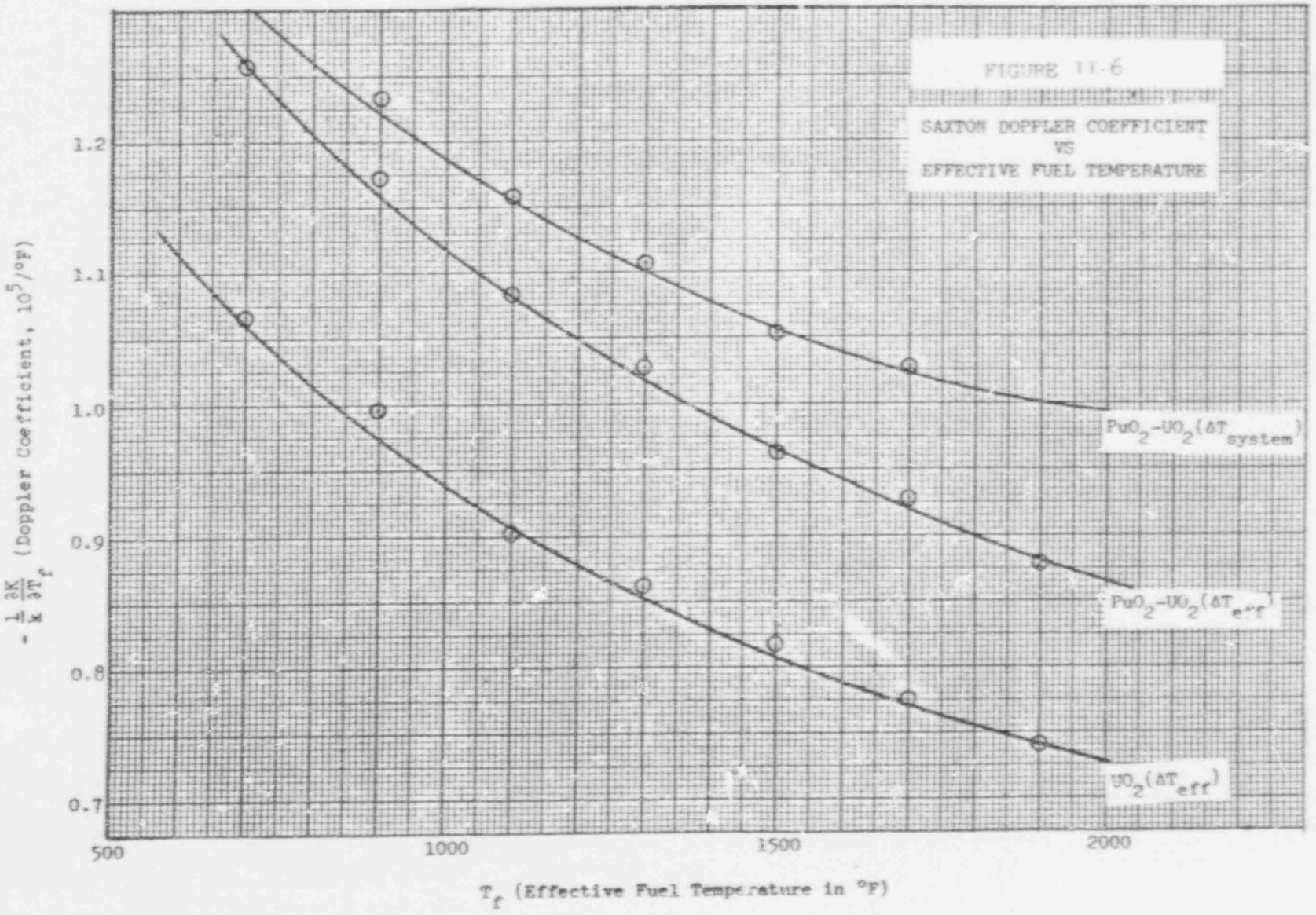
FIGURE II-6
SAXTON DOPPLER COEFFICIENT
VS
EFFECTIVE FUEL TEMPERATURE
PuO_2-UO_2(ΔT_{system})
PuO_2-UO_2(ΔT_{eff})
UO_2(ΔT_{eff})
$-\frac{1}{k}\frac{\partial K}{\partial T_f}$ (Doppler Coefficient, 10^5/°F)
1.2
1.1
1.0
0.9
0.8
0.7
500
1000
1500
2000
T_f (Effective Fuel Temperature in °F)

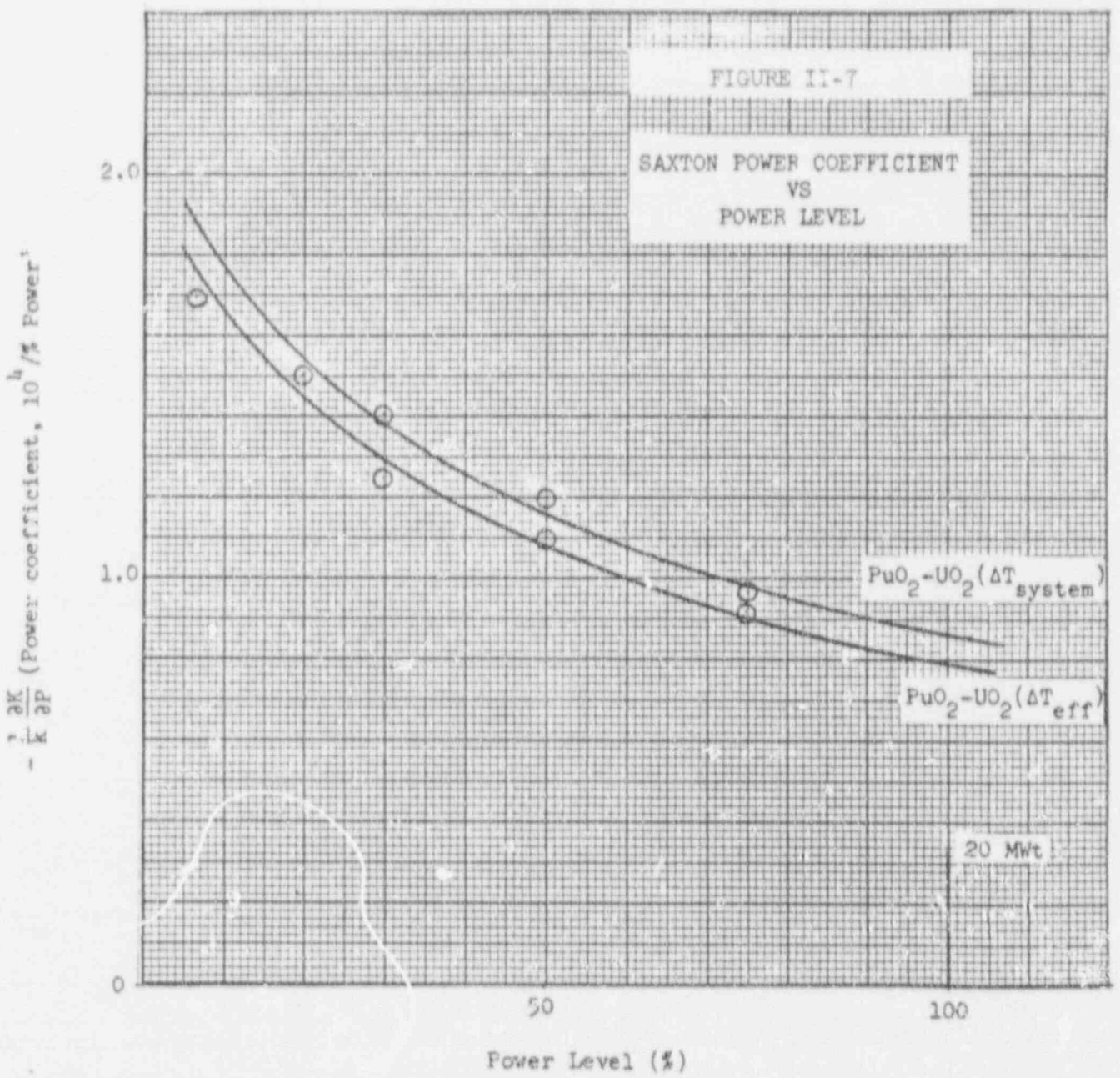
FIGURE II-7
SAXTON POWER COEFFICIENT
VS
POWER LEVEL
2.0
1.0
0
50
100
Power Level (%)
$-\frac{1}{k}\frac{\partial k}{\partial P}$ (Power coefficient, 10^{-4}/% Power)
PuO_2-UO_2(ΔT_{system})
PuO_2-UO_2(ΔT_{eff})
20 MWt

FIGURE II-8

VARIATION OF MODERATOR TEMPERATURE COEFFICIENT WITH TEMPERATURE

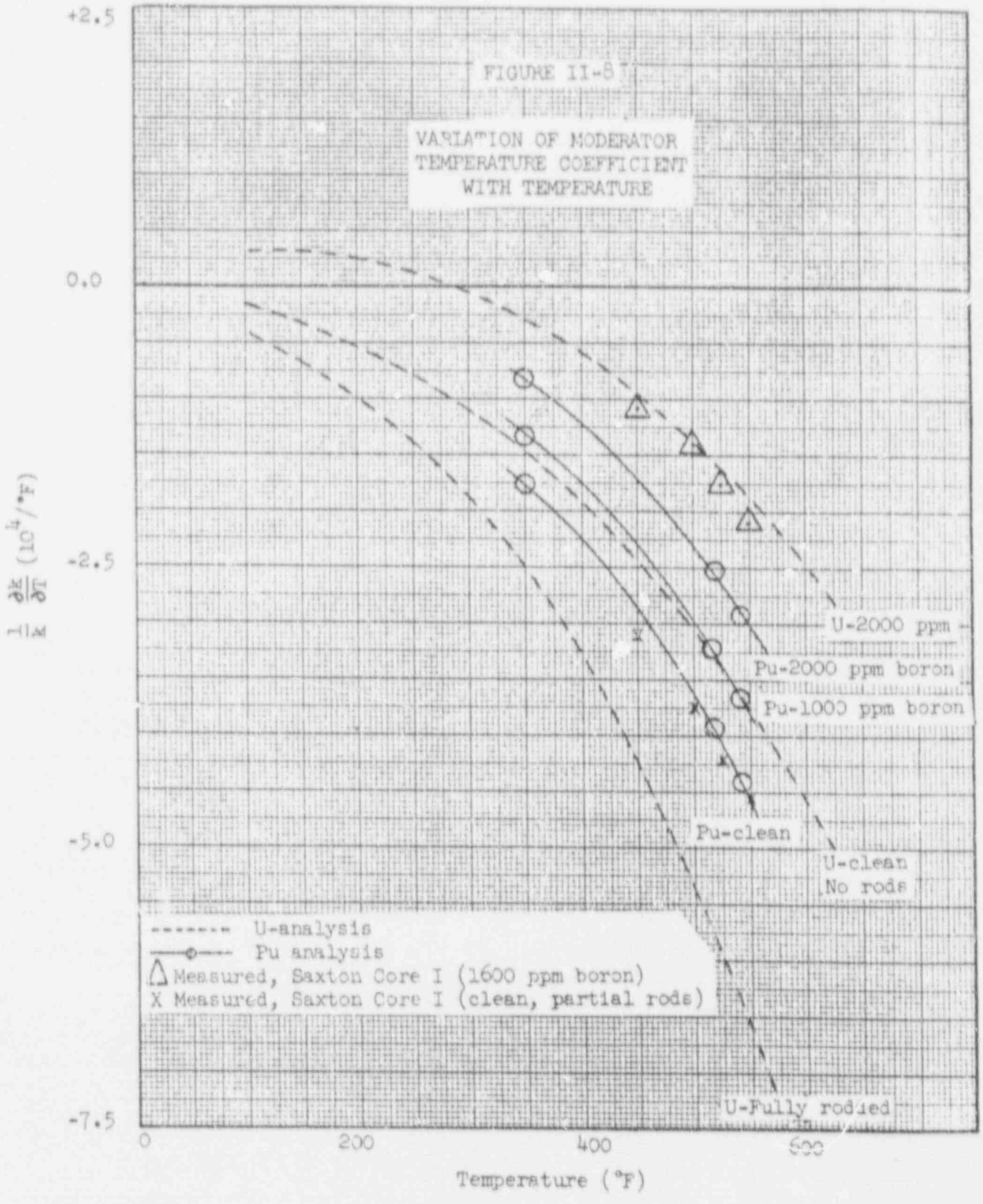

FIGURE II-9

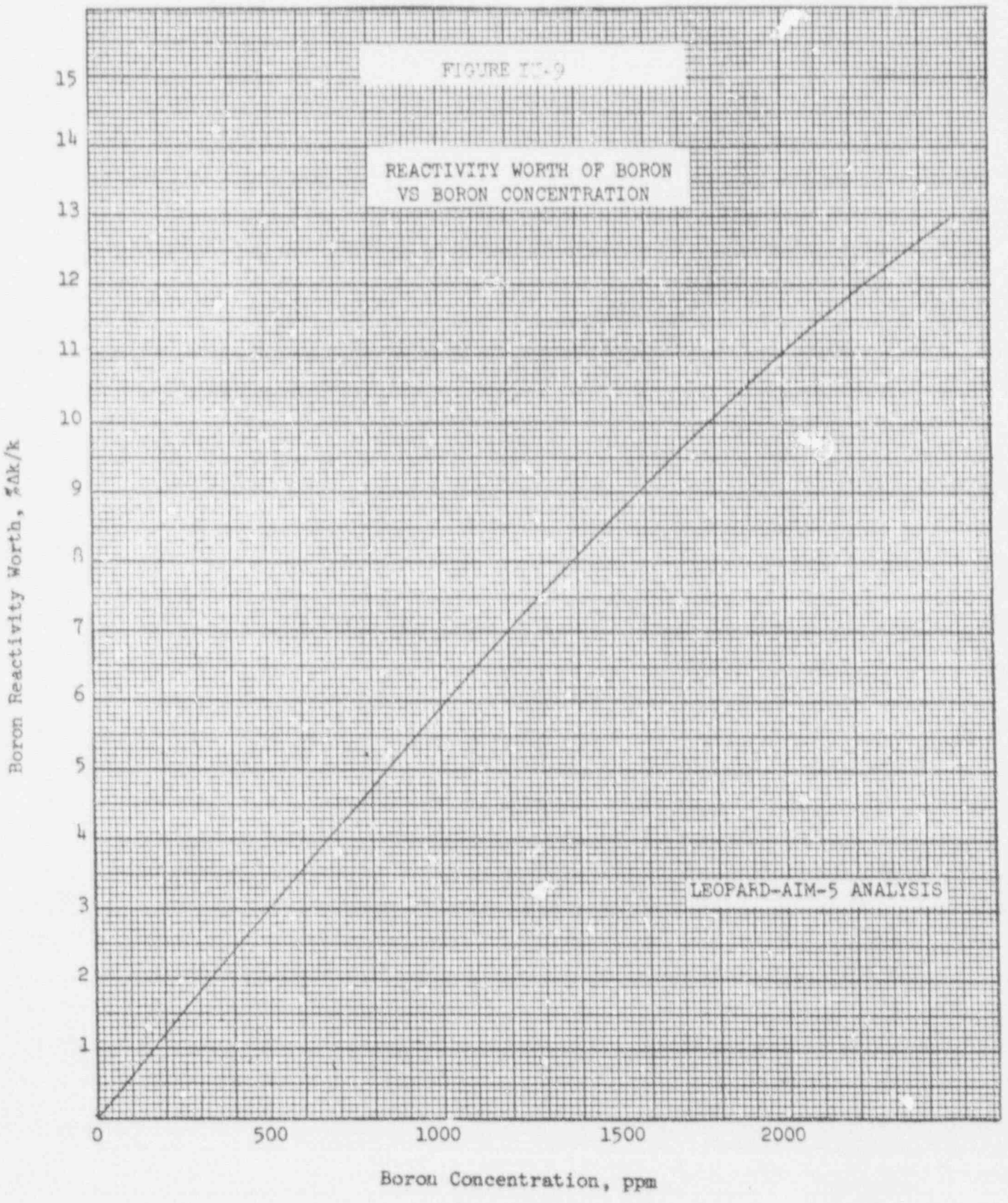
REACTIVITY WORTH OF BORON
VS BORON CONCENTRATION
LEOPARD-AIM-5 ANALYSIS
Boron Reactivity Worth, %Δk/k
Boron Concentration, ppm
0
500
1000
1500
2000
1
2
3
4
5
6
7
8
9
10
11
12
13
14
15

PDQ Power Distribution

Configuration: 9 PuO_2-UO_2 Assemblies (6.5 w/o PuO_2) in center positions. Rods 1,2,3,4,6 in, 1000 ppm boron, Depleted Followers and L-sections

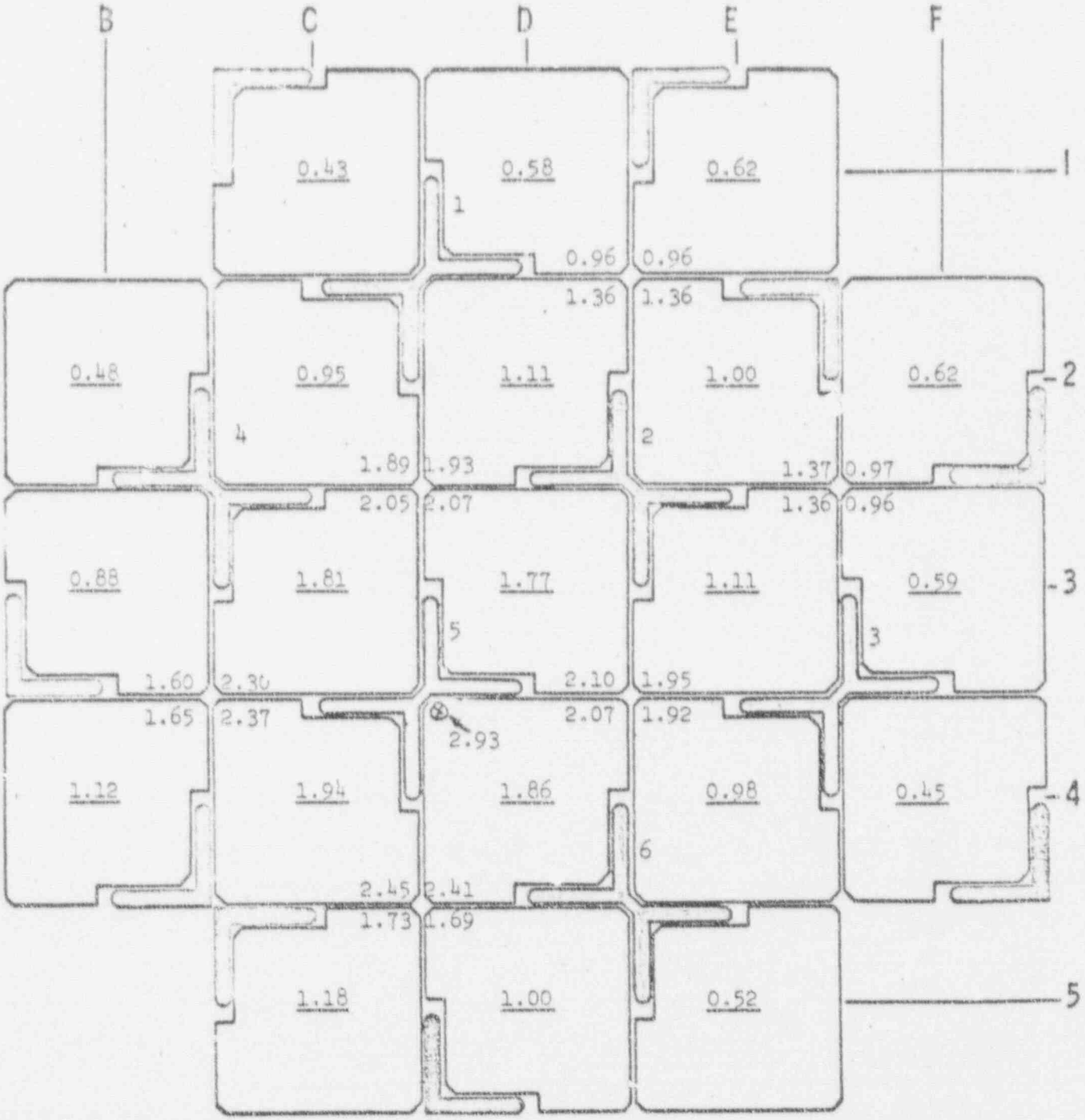

The underlined value in each assembly is the average power in that assembly relative to the average power in the core. The relative power is also shown for individual fuel rods near the uncontrolled corners of assemblies (where hot spots usually occur). The peak power includes a correction for the discrepancy between analysis and experiment from Saxton Core I.

Stuck Rod Power Distribution

FIGURE T-10

PDQ Power Distribution

Configuration: 9 PuO_2-UO_2 Assemblies (6.5 w/o PuO_2) in Center Positions, Rod 6 in, 1000 ppm Boron Depleted Followers and L-Sections

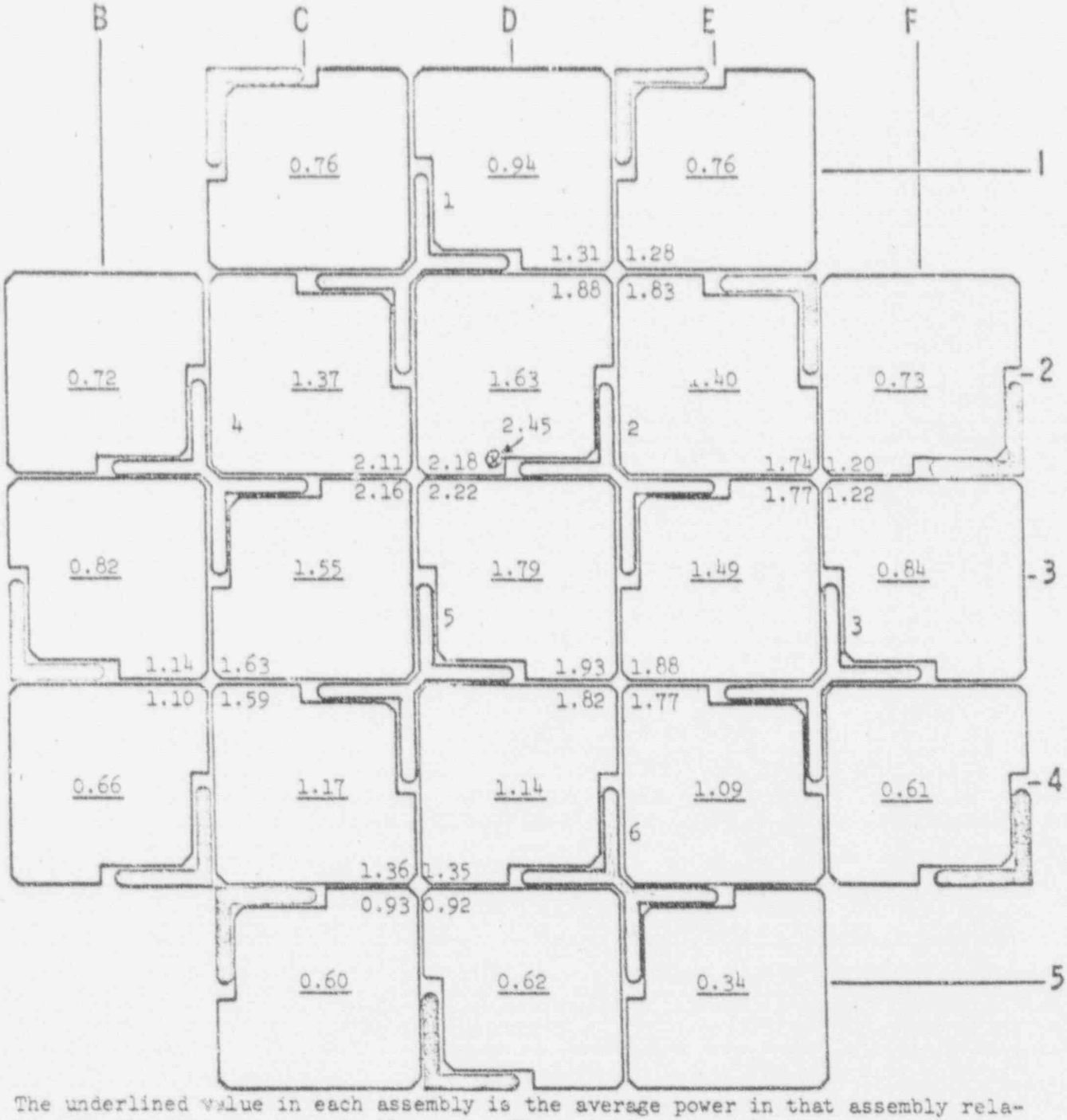

The underlined value in each assembly is the average power in that assembly relative to the average power in the core. The relative power is also shown for individual fuel rods near the uncontrolled corners of assemblies (where hot spots usually occur). The peak power includes a correction for the discrepancy between analysis and experiment from Saxton Core I.

FIGURE II-11

Dropped Rod Power Distribution

III. CORE HYDRAULIC AND THERMAL DESIGN

A. GENERAL

Introduction

The power level at which the reactor may be operated without core damage depends on the ability to remove heat from the core without exceeding limiting clad and fuel temperatures.

The hydraulic and thermal design of the core must provide sufficient margin so that the appropriate safety limits as defined below are not exceeded during steady state operation and reactor transients.

The maximum temperatures are evaluated by using the concept of hot channel factor, i.e., the ratio of maximum to average conditions within the core. For the evaluation of this ratio, neutron flux distribution, coolant flow distribution and the core fabrication tolerances are considered.

Thermal Design Safety Criteria

The thermal output of Core II has been established on the basis of the following ground rules:

No bulk boiling is allowed in the hot channel during normal steady state operation even with the core inlet temperature at the upper limit of the control deadband with maximum nuclear instrumentation error, and with the primary system pressure at steady state minimum.

The reactor is not permitted to reach a condition corresponding to a calculated departure from nucleate boiling ratio (DNB ratio) lower

than 1.25 without actuation of an automatic scram. Departure from nucleate boiling is defined in Section III-E.

Center melting of the fuel is not permitted to occur during normal operation or normal transient conditions.

During core life, the core power rating may be increased as the maximum to average power density decreases. In no event will the maximum heat flux and linear power density conditions, as given for ≤ 22.1 MWt power rating, be exceeded.

B. COOLANT FLOW

Coolant Flow Rate

The total primary coolant flow rate at operating temperature and pressure with one pump operating is 2.94×10^6 lb/hr.

Eighty-five percent (85%) of the flow entering the vessel is effective for heat removal which is the same as Core I.

Pressure Drop

Core II pressure drop is calculated to be approximately 0.1 psia greater than Core I even though the spring clip grid design has been modified.

C. VARIATION OF PRIMARY SYSTEM TEMPERATURE AND PRESSURE

Pressure

The maximum steady state primary system pressure variation including instrument errors and deadband, is +50 and -50 psi. The minimum

steady state pressure is used to calculate the conditions in the hot channel under the worst steady state conditions.

Temperature

The maximum steady state temperature variation, including secondary steam pressure control system errors and deadband, is 5.0°F. The maximum inlet temperature is used in the calculation of the departure from nucleate boiling ratio (DNBR).

D. ENGINEERING HOT CHANNEL FACTORS

The engineering hot channel factors used in the Core II design are 1.045 for F_q and 1.22 for $F_{\Delta H}$. The subfactors used in obtaining these values are described below.

Definition of Engineering Hot Channel Factors

The total hot channel factors for heat flux and enthalpy rise are defined as the maximum-to-average ratios of these quantities. The first considers the local maximum at a point (the "hot spot"), and the latter involves the maximum integrated value along a channel (the "hot channel").

Each of the total hot channel factors is the product of a nuclear hot channel factor describing the nuclear flux distribution and an engineering hot channel factor to allow for variations from nominal design conditions. The engineering hot channel factors account for the effects of flow conditions and fabrication tolerances and are made up of subfactors accounting for the influence of the variations of fuel pellet diameter, fuel density, enrichment and eccentricity;

fuel rod diameter, pitch and bowing; inlet flow distribution; flow redistribution; and flow mixing. Table III-1 is a list of the subfactors comprising the engineering factors.

Basis for Confidence

The engineering hot channel factors are estimated[1] using the maximum allowable manufacturing deviations to determine each engineering hot channel subfactor. These subfactors are combined by multiplication which gives a resulting engineering hot channel factor with the maximum deviations occurring simultaneously at the hot spot or hot channel. These estimated engineering hot channel factors are combined with the nuclear hot channel factors to establish the design. The total engineering hot channel factors listed below apply to both the pelletized and vibratory compacted fuel.

TABLE III-1

ENGINEERING HOT CHANNEL FACTORS

F_q^E Subfactor	Sexton Core II
Pellet Diameter, Density Enrichment, and Eccentricity	1.041
Rod Diameter, Pitch and Bowing	1.004
Resulting F_q^E	1.045

(1) Nucleonics, Vol. 20, No. 9, September 1962, "Engineering Hot Channel Factors for Open-Lattice Cores," H. Chelemer, L. S. Tong.

$F^E_{\Delta H}$ Subfactor	Saxton Core II
Pellet Diameter, Density, Enrichment, and Eccentricity	1.037
Rod Diameter, Pitch and Bowing	1.10
Inlet Flow Maldistribution	1.07
Flow Redistribution	1.05
Flow Mixing	0.95
Resulting $F^E_{\Delta H}$	1.22

E. DEPARTURE FROM NUCLEATE BOILING

General

Westinghouse has developed correlations to predict the conditions at which DNB will occur. These are the W-2 DNB correlations[1], which are based upon an extension of a dimensional analysis performed by Griffith[2] and verified by a parametric study of about 3000 published DNB data points. Since the data points were obtained by various independent investigators, the correlations include both systematic and random uncertainties. The data points used to develop the W-2 DNB correlations cover the full range of points for PWR cores. Therefore, this correlation may be confidently used in the design of PWR cores.

(1) Tong, L. S., Currin, H. B., and Thorp, A. G. II, "New Correlations Predict DNB Conditions," Nucleonics, Vol. 21, No. 5, May 1963.

(2) Griffith, P., "A Dimensional Analysis of the Departure from Nucleate Boiling Heat Flux in Forced Convection," WAPD-TM-210, 1959.

Development of the W-2 Correlation

The correlations of DNB data obtained from various investigators are not in agreement.[1] Jens and Lottes[2] and Zenkevich and Subotin[3] reported that DNB is strongly influenced by local subcooling and local heat flux. Cook,[4] however, found DNB to be independent of local peak heat flux because, for a given inlet enthalpy and flow rate, DNB occurred at a same power input for both a uniform and cosine power distribution. These apparently conflicting results are explained by the hypothesis that there can be two types of DNB: namely, a q"-DNB due to excessive local heat flux and H-DNB due to the high enthalpy at the vicinity of heated surface.

The following nomenclature will be used in the discussion of the W-2 correlation:

A_c Cross-sectional area for flow, ft^2

A_h Heat transfer surface area, ft^2

β The bubble angle between liquid and solid surfaces

---

(1) Tong, L. S., Currin, H. B., and Thorp, A. G. II, "New Correlations Predict DNB Conditions," Nucleonics, Vol. 21, No. 5, May 1963.

(2) Jens, W. H., and Lottes, P. A., "Analysis of Heat Transfer Burnout Pressure Drop and Density Data for High Pressure Water," ANL-4627, 1951.

(3) Zenkevich, B., and Subotin, V., "Critical Heat Flux in Forced Circulation of Water; Subcooled to Boiling," Atomic Energy No. 8, USSR, 1957.

(4) Cook, W. H., "Fuel Cycle Program - First Quarterly Report," GEAP-3558, p. 35, September 1960.

D_e	Equivalent diameter, ft.
G	Local mass velocity, $lb/hr\text{-}ft^2$
H	Local enthalpy, Btu/lb
H_{in}	Inlet enthalpy, Btu/lb
H_f	Saturated liquid enthalpy, Btu/lb
H_{fg}	Heat of evaporation, Btu/lb
ΔH_{DNB}	$(H_{DNB} - H_{in})$, Btu/lb
L	Length in heated channel from inlet to local point, ft.
P_h	heated periphery, ft.
p	Pressure, psia
$q"_{DNB}$	Heat flux at DNB, $Btu/hr\text{-}ft^2$
$\bar{q}"$	Average heat flux of test section, $\bar{q}" = \frac{1}{L}\int_o^L q"dz$. Btu $hr\text{-}ft^2$
T	Temperature, F
ΔT_{sc}	Subcooling $(T_f - T_{local})$, F
T_f	Saturation temperature, F
ρ_f	Weight density of saturated liquid, lb/ft^3
ρ_g	Weight density of saturated vapor, lb/ft^3
x	Steam quality, percent by weight
z	Axial length, ft.
v_i	Inlet velocity, ft/sec.
μ_g	Viscosity of saturated vapor, lb/hr-ft
μ_f	Viscosity of saturated liquid, lb/hr-ft
σ	Surface tension, lb/ft

DNB Correlation in the Quality Region

DNB in the quality region is due to excessive enthalpy in the vicinity of the heated surface. The W-2 correlation for this type of DNB (H-DNB) is given by:

$$\Delta H_{DNB} = 0.529\ (H_f - H_{in}) + \left[0.825 + 2.36 \exp\ (-204\ D_e)\right] H_{fg}$$

$$\exp\ (-1.5\ G/10^6) - 0.41\ H_{fg} \exp\ (-0.0048\ L/D_e) - 1.12\ H_{fg} \rho_g / \rho_f$$

$$+0.548\ H_{fg}$$

The above equation represents the best fit to the existing data from 800 to 2750 psia. Figures III-1 and III-2 show how well the equation predicts the ΔH_{DNB} actually measured in tests. Figure III-1 is a comparison of the measured and predicted ΔH_{DNB} for the existing data from 800 to 2750 psia. The locus of points where the measured and predicted ΔH_{DNB} are equal is shown as a 45 degree line. An analysis of the deviations of experimental data from this line shows that measured DNB points fall within a range $\pm$ 25 percent of the ΔH_{DNB} predicted by the W-2 correlation with a probability of 90 percent. A statistical analysis showed that at a 95% confidence level there is a 91 percent probability that DNB will not occur if ΔH is 25 percent less than ΔH_{DNB} ($\Delta H = 0.75\ \Delta H_{DNB}$) as predicted by the W-2 correlation.

Figure III-2 shows the comparison of measured and predicted ΔH_{DNB} using the W-2 correlation for only those data points of a pressure 2000 psia. An analysis of the deviation of these data points from the locus of points where the measured and predicted ΔH_{DNB} are equal (again at 45 degree line) shows a narrower distribution than that obtained when all data points were included. For a confidence level

of 95 percent, the measured DNB points in this range of pressure falls above 80 percent of the ΔH_{DNB} predicted by the W-2 correlation with a probability of 94 percent.

The effect of axial flux distribution was investigated using data reported by De Bortoli[1] and was found to be insignificant. The ranges of parameters of the correlated experimental data for ΔH_{DNB} are as follows:

Geometries: Circular tube, rectangular channel and rod bundle
Axial Heat Flux Distribution: Uniform and non-uniform
Mass Velocity = 0.2 to 4.0 x 10^6 lb/hr-ft^2
Pressure = 800 to 2750 psia
L/D_e = 21 to 656
Inlet Enthalpy: $H_{in} \geq 400$ Btu/lb
Local Heat Flux = 0.1 to 1.8 x 10^6 Btu/hr-ft^2
Exit Quality = 0 to 0.90 by weight

DNB Correlation in the Subcooled Region

DNB in the subcooled region is due to excessive local heat flux and can be attributed to the interference of the liquid and bubble flows normal to the heated surface with influences from the convection effect of the mass flow rate. The W-2 correlation for this type of DNB (q"-DNB) is given by:

---

(1) De Bortoli, B. A., et al, "Forced Convection Heat Transfer Burnout Studies for Water in Rectangular Channels and Round Tubes at Pressure above 500 psia," WAPD-188, 1958.

$$q''_{DNB} = (0.23 \times 10^6 + 0.094G)\ (3.0 + 0.01\ \Delta T_{sc})$$
$$\left[0.435 + 1.23 \exp\ (-0.0093 L/D_e)\right]$$
$$\left[1.7 - 1.4 \exp\ \left\{-0.532\ \left[(H_f - H_{in})/H_{fg}\right]^{0.75}\ (\rho_g/\rho_f)^{-0.33}\right\}\right] \quad (10)$$

This equation represents the best fit to the existing uniform heat flux data. Figure III-3 shows how well the equation predicts the q''_{DNB} actually measured in tests. It is a comparison of the measured and predicted q''_{DNB} for all the existing uniform heat flux data. An analysis of the deviation of the data points from the locus of points where the measured and predicted q''_{DNB} are equal (45 degree line) shows that the measured DNB points fall within $\pm$ 20 percent of the q''_{DNB} predicted by the W-2 correlation with a probability of 90 percent at a confidence level of 95 percent. This means that, for the entire range of the data correlated, there is 86 percent probability that q"-DNB will not occur if q" is 20 percent less than q''_{DNB} ($q'' = 0.8\ q''_{DNB}$) as predicted by the W-2 correlation. The following parameters are covered by this correlation:

Geometries: Circular tube, rectangular channel and rod bundle
Axial Heat Flux Distribution: Uniform
Mass Velocity: 0.2 to 8.0 x 10^6 lb/hr-ft^2
Pressure: 800 to 2750 psia
L/D_e: 21 to 365
Inlet Subcooling ($H_f - H_{in}$): 0 to 700 Btu/lb
Local Heat Flux: 0.4 to 4.0 x 10^6 Btu/hr-ft^2
Subcooling at DNB: 0 to 228°F

Application of DNB Correlations in Design

Definition of DNB Ratio

H-DNB ratio is the ratio of the predicted enthalpy rise at DNB to the enthalpy rise from inlet to the corresponding point in hot channel.

Local q"-DNB ratio is the ratio of the predicted DNB heat flux to the local heat flux at the corresponding point in the hot channel.

Statistical Combination of DNB Correlation and Engineering Hot Channel Factors

The occurrence of DNB depends upon the statistical nature of the hot channel factors and the DNB correlation. The nuclear hot channel factors are not treated statistically because of the complicated treatment involved. Instead, the maximum calculated values are used with an added 10 percent margin to account for uncertainties. Engineering hot channel factors are calculated on the basis of the worst tolerances permitted in fabrication. However, as was discussed earlier, due to the statistical nature of deviations in fabrication, the engineering hot channel factors can be treated statistically.

The statistical convolution of the probability functions for the W-2 correlation for ΔH_{DNB} and the engineering hot channel factor for $F_{\Delta H}$ results in Figure III-4 showing the probability of not reaching DNB as a function of the minimum ΔH-DNB ratio calculated from the W-2 correlation using design hot channel factors. It can be seen that using a design ΔH-DNB ratio of 1.25 results in a probability of over 99 percent of not reaching DNB.

Because the engineering hot channel factor F_q is very nearly 1.0, there is not very much to be gained by convoluting the probability functions for F_q and q"-DNB. Here the probability of DNB not being

exceeded is 96 percent when the design engineering hot channel factor for F_q is used together with a minimum DNB ratio of 1.25 as shown by Figure III-5 giving the probability function of q"-DNB.

Film Boiling Heat Transfer Coefficient

Heat transfer immediately after departure from nucleate boiling is conservatively assumed to be limited by film boiling. A period of transition boiling is neglected. The heat transfer coefficient in film boiling was obtained by correlating the existing data as shown in Figure III-6.

F. HYDRAULIC AND THERMAL DESIGN PARAMETERS

The hydraulic and thermal design parameters for Core II are given in Table III-2.

TABLE III-2

HYDRAULIC AND THERMAL DESIGN PARAMETERS*

TOTAL CORE

Total Heat Output (Initial)	22.1 MWt
Total Heat Output (Initial)	75.4×10^6 Btu/hr
Heat Generated in Fuel	97.4%
System Pressure, Nominal	2000 psig
System Pressure, Minimum Steady State	1950 psig

*Based on a radial peak rod to core average factor of 2.30 and a linear power density of 16 KW/ft.

Coolant Flow	
Total Flow Rate	2.94×10^6 lb/hr
Effective Flow Rate for Heat Transfer	2.5×10^6 lb/hr
Flow Area for Heat Transfer Flow (Unit Cells)	2.51 ft^2
Average Velocity along Fuel Rods	5.8 ft/sec
Coolant Temperatures	
Nominal Inlet	520.0 F
Maximum Inlet, including Instrumentation Errors and Deadband	525.0 F
Average Rise in Vessel	20.7 F
Average Rise in Core	24.8 F
Average in Vessel	530.7 F
Average in Core	532.5 F
Average Film Coefficient	2540 Btu/hr-ft^2-F
Average Film Temperature Difference	58.0 F
Heat Transfer	
Active Heat Transfer Surface Area of Fuel Rods	498 ft^2
Average Heat Flux	147,200 Btu/hr-ft^2
Average Thermal Output	4.4 Kw/ft
Maximum Clad Surface Temperature at Nominal Pressure	642 F
Pressure Drop	
Across Core	4.1 psi
Across Vessel, including Nozzles	11.3 psi

CENTRAL CORE REGION (UO_2-PuO_2 Fuel)

F_q Heat Flux Hot Channel Factor	3.61
$F_{\Delta H}$ Enthalpy Rise Hot Channel Factor	2.81
Nominal Outlet Temperature of Hot Channel	586.7°F
Maximum Outlet Temperature of Hot Channel	591.7°F
Maximum Outlet Enthalpy of Hot Channel	595.8 Btu/lb
Saturation Enthalpy at Minimum Steady State Pressure	665.9 Btu/lb
Maximum Heat Flux	553,700 Btu/hr-ft^2
Maximum Thermal Output	16.0 Kw/ft

DNB Ratios

Local q"-DNBR at 100% Power, Nominal Conditions	2.62
Local q"-DNBR at 120% Power, 1800 psia, Max. T_{in}	1.87
ΔH-DNBR at 100% Power, Nominal Conditions	N.A.(1)
ΔH-DNBR at 120% Power, 1800 or 2200 psia, Max. T_{in}	N.A.(1)

OUTER CORE REGION (UO_2 Fuel)

F_q Heat Flux Hot Channel Factor	2.04
$F_{\Delta H}$ Enthalpy Rise Hot Channel Factor	1.59
Nominal Outlet Temperature of Hot Channel	558.9°F
Maximum Outlet Temperature of Hot Channel	563.9°F
Maximum Outlet Enthalpy of Hot Channel	558.9 Btu/lb
Saturation Enthalpy of Hot Channel	665.9 Btu/lb
Maximum Heat Flux	301,600 Btu/hr-ft^2
Maximum Thermal Output	9.05 Kw/ft

DNB Ratios

Local q"-DNBR at 100% Power, Nominal Conditions	4.86
Local q"-DNBR at 120% Power, 1800 psia, Max. T_{in}	3.47

DNB Ratios (cont'd)

ΔH-DNBR at 100% Power, Nominal Conditions	N.A.(1)
ΔH-DNBR at 120% Power, 1800 or 2200 psia, Max. T_{in}	N.A.(1)

G. CENTRAL TEMPERATURE OF THE HOT PELLET

1. Uranium Dioxide Fuel

The temperature distribution in the pellet is mainly a function of the uranium dioxide thermal conductivity and the local power density. The absolute value of the temperature distribution is affected by the cladding temperature and the thermal conductance of the gap between the pellet and the cladding.

The occurrence of nucleate boiling maintains maximum cladding surface temperature below about 647 F. The cold gap between pellet and cladding is specified to obtain contact during full power operation at the core hot spot. A contact conductance of 1000 Btu/hr-ft^2-F at the hot spot was estimated for stainless steel cladding.(2) For Zircaloy clad a contact conductance of 1200 Btu/hr-ft^2 was used.(3)

---

(1) Not applicable - no bulk boiling in channel.

(2) E. A. McCabe, Jr., "Thermal Design Aspects of the Yankee First Core Fuel Rod," YAEC-106, November 1960.

(3) R. A. Dean, "Thermal Contact Conductance Between UO_2 and Zircaloy-2," CVNA-127, May 1962.

The thermal conductivity of uranium dioxide was evaluated from published results of recent work at ORNL[1], Chalk River[2], and WAPD[3][4]. The recommended curve (Curve B) for thermal conductivity is given in Figure III-7. The section of the curve at temperatures between 0°F and 3000°F is based on the data of Godfrey, et al[1].

The section of the curve between 3000 F and 5000 F was based on two factors:

a) In-pile observations of fuel melting dictate a positive temperature coefficient for conductivity above approximately 3000 F. The temperature dependence in this range should conform to an exponential curve since this reflects the most credible physical interpretation of the high temperature conductivity increase.

---

(1) T. G. Godfrey, et al, "Thermal Conductivity of Uranium Dioxide and Armco Iron by an Improved Radial Heat Flow Technique," ORNL-3556, June 1964.

(2) J. A. L. Robertson, et al, "Temperature Distribution in UO_2 Fuel Elements," Journal of Nuclear Materials 7, No. 3, 1962, pp. 225-262.

(3) R. N. Duncan, "Rabbitt Irradiation of UO_2," CVNA-142, June 1962.

(4) J. A. Christensen, "Thermal Conductivity of Nearly Stoichiometric UO_2 - Temperature and Composition Effects," WCAP-2531, November 1963.

(5) G. R. Horn and J. A. Christensen, "Identification of the Molten Zone Irradiated UO_2," ANS Winter Meeting Transactions, 1963, p. 348, No. 5.

b) The area under the recommended curve is such that the integral $\int k \, dt$ is equal to approximately 97 w/cm as given by Robertson, et al[1] and Duncan[2]. This value is based upon the interpretation of fuel melt radius as determined at Hanford[3] and Chalk River[1].

The thermal conductivity curve can best be represented by the following equations:

a) Temperature Range - $0 \leq T \leq 1650$ C

$$k = \frac{40.4}{464 + T} + 1.32 \times 10^{-4} \exp (1.88 \times 10^{-3} T)$$

b) Temperature Range - $1650 \leq T \leq 2800$ C

$$k_2 = 0.019 + 1.32 \times 10^{-4} \exp (1.88 \times 10^{-3} T)$$

with k in w/cm $^{\circ}$C for 94 percent dense fuel and T in $^{\circ}$C

2. Uranium Dioxide - Plutonium Dioxide Fuel

Pelletized Fuel

The thermal conductivity of the UO_2-PuO_2 sintered pellets was taken to be the same as that for UO_2 fuel as given above. The hot rod in Saxton Core II will be of this type with either

---

(1) J. A. L. Robertson, et al, "Temperature Distribution in UO_2 Fuel Elements," Journal of Nuclear Materials 7, No. 3, 1962, pp. 225-262.

(2) R. N. Duncan, "Rabbitt Irradiation of UO_2," CVNA-142, June 1962.

(3) G. R. Horn and J. A. Christensen, "Identification of the Molten Zone in Irradiated UO_2," ANS Winter Meeting Transactions, 1963, p. 348, No. 5.

Zircaloy or stainless steel clad. The maximum central temperature of the hot pellet at steady state for each type of clad is:

a) Zircaloy, PuO_2-UO_2	3400°F
b) Stainless Steel, PuO_2-UO_2	3440°F
c) Stainless Steel, UO_2	2550°F

Flux depression compatible with enrichment and density was included.

All temperatures are well below the irradiated PuO_2 fuel melting point of 5050°F and the irradiated UO_2 melting point of 5000°F. During a maximum overpower transient the centerline temperatures are:

a) Zircaloy, PuO_2-UO_2	4000°F
b) Stainless Steel, PuO_2-UO_2	4060°F
c) Stainless Steel, UO_2	2930°F

Vibratory Compacted Fuel

The present core loading plans are such that the vibratory compacted fuel assemblies will not contain the highest power density rod. However, a maximum central fuel temperature was determined assuming maximum power density conditions. The curve of thermal conductivity is shown on Figure III-8. The maximum steady state centerline temperature was 4060°F. Again, a flux depression compatible with theoretical density and enrichment was included. For maximum overpower transient the centerline temperature was 4600°F.

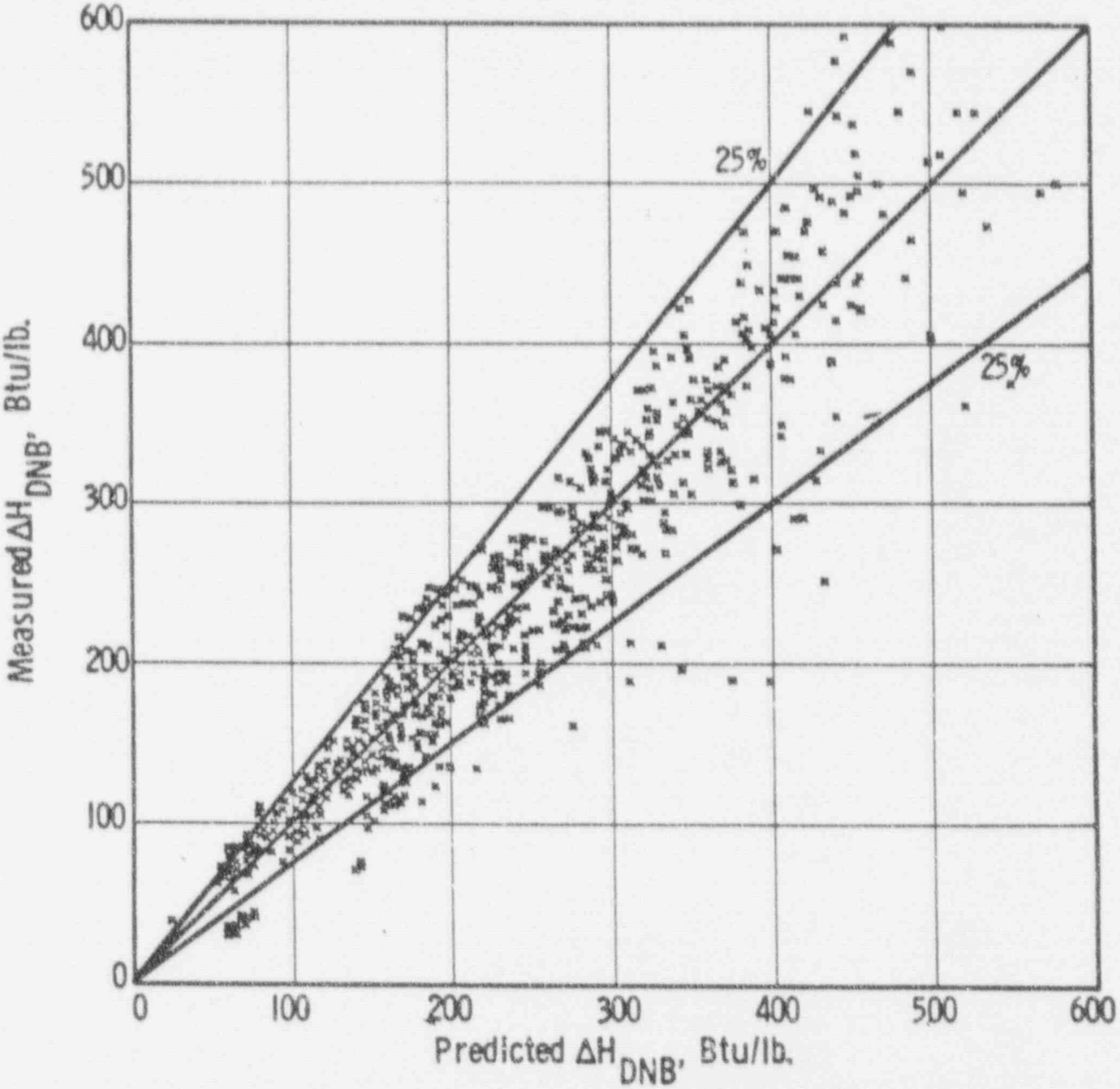

COMPARISON OF H-DNB CORRELATION
WITH MEASURED DATA IN QUALITY REGION

(p = 800 to 2750 psia)

FIGURE III-1

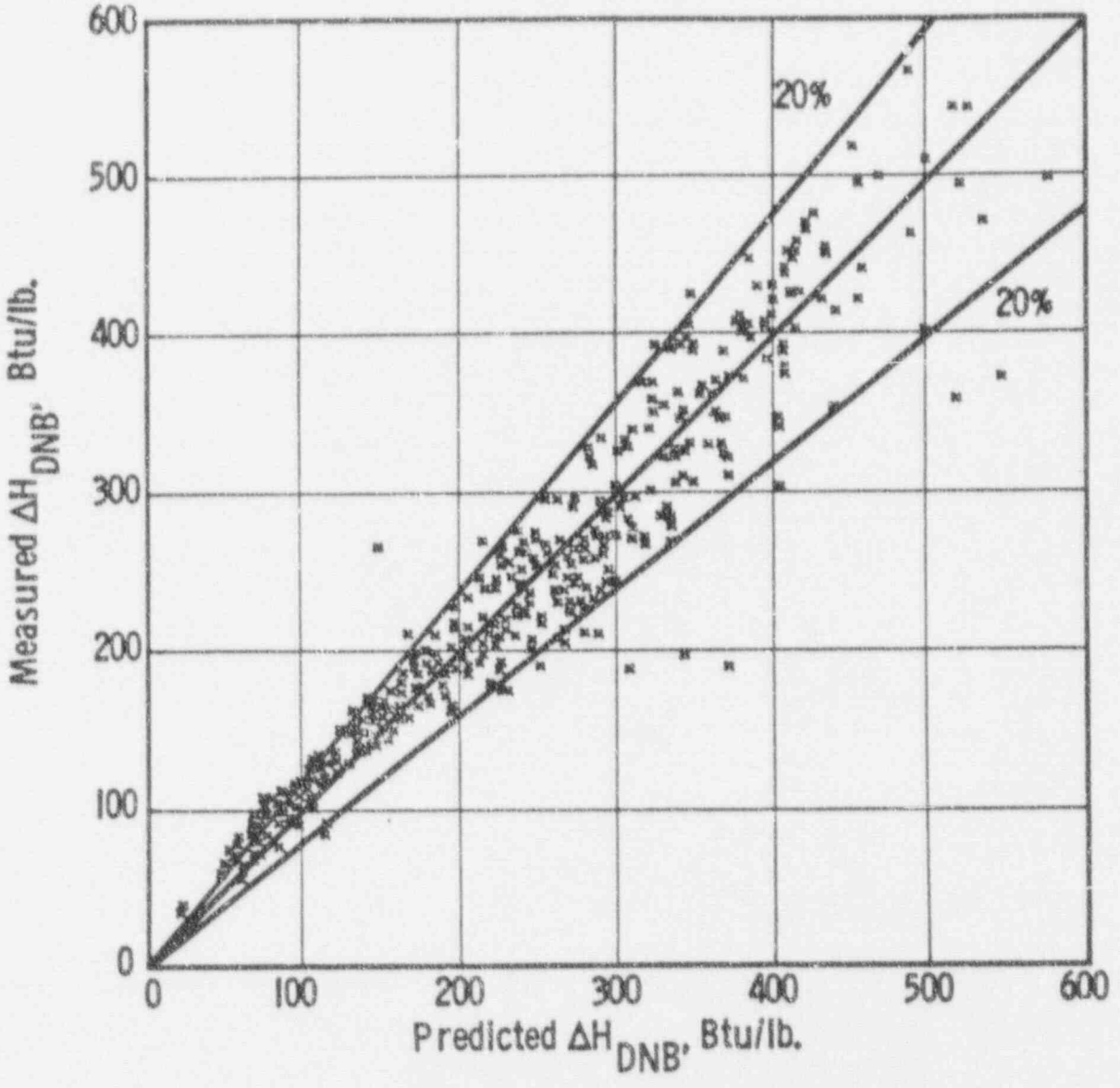

COMPARISON OF H-DNB CORRELATION
WITH MEASURED DATA IN QUALITY REGION

(p = 2000 psi)

FIGURE III -2

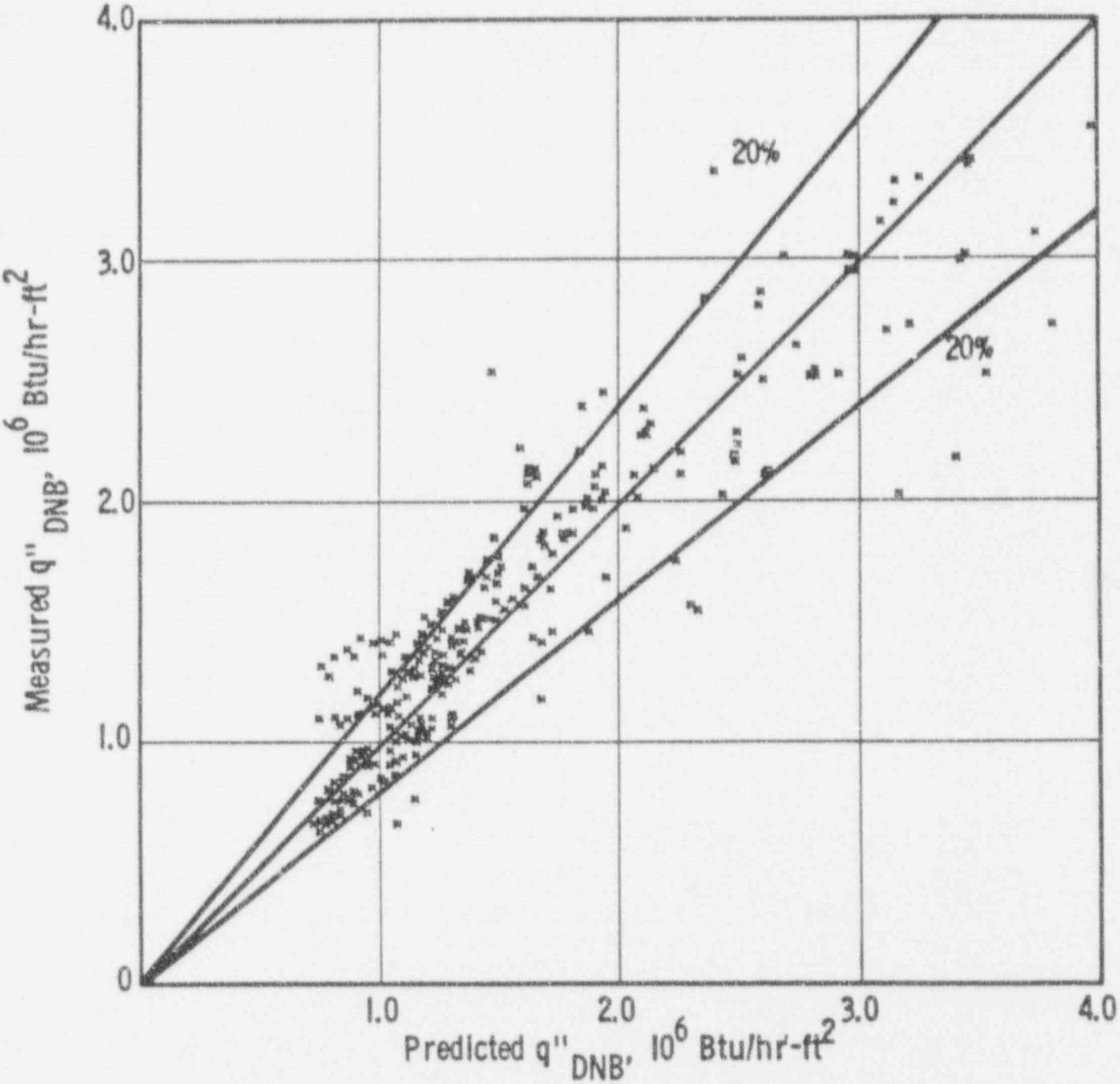

COMPARISON OF q'' - DNB CORRELATION
WITH MEASURED DATA IN SUBCOOLED REGION

(P = 800 to 2750 psia)

FIGURE III - 3

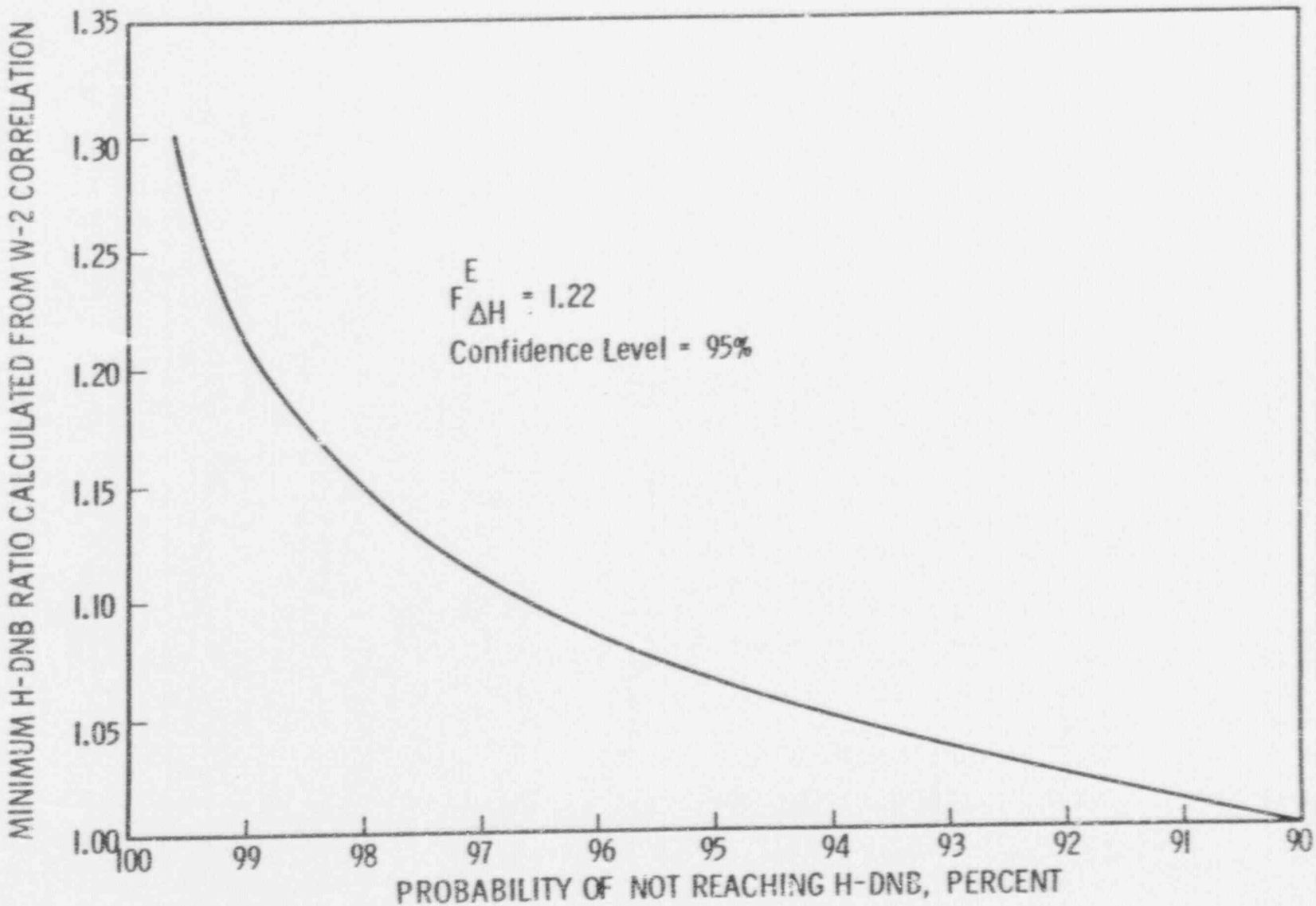

H-DNB PROBABILITY CURVE AT 2000 PSIA

FIGURE III - 4

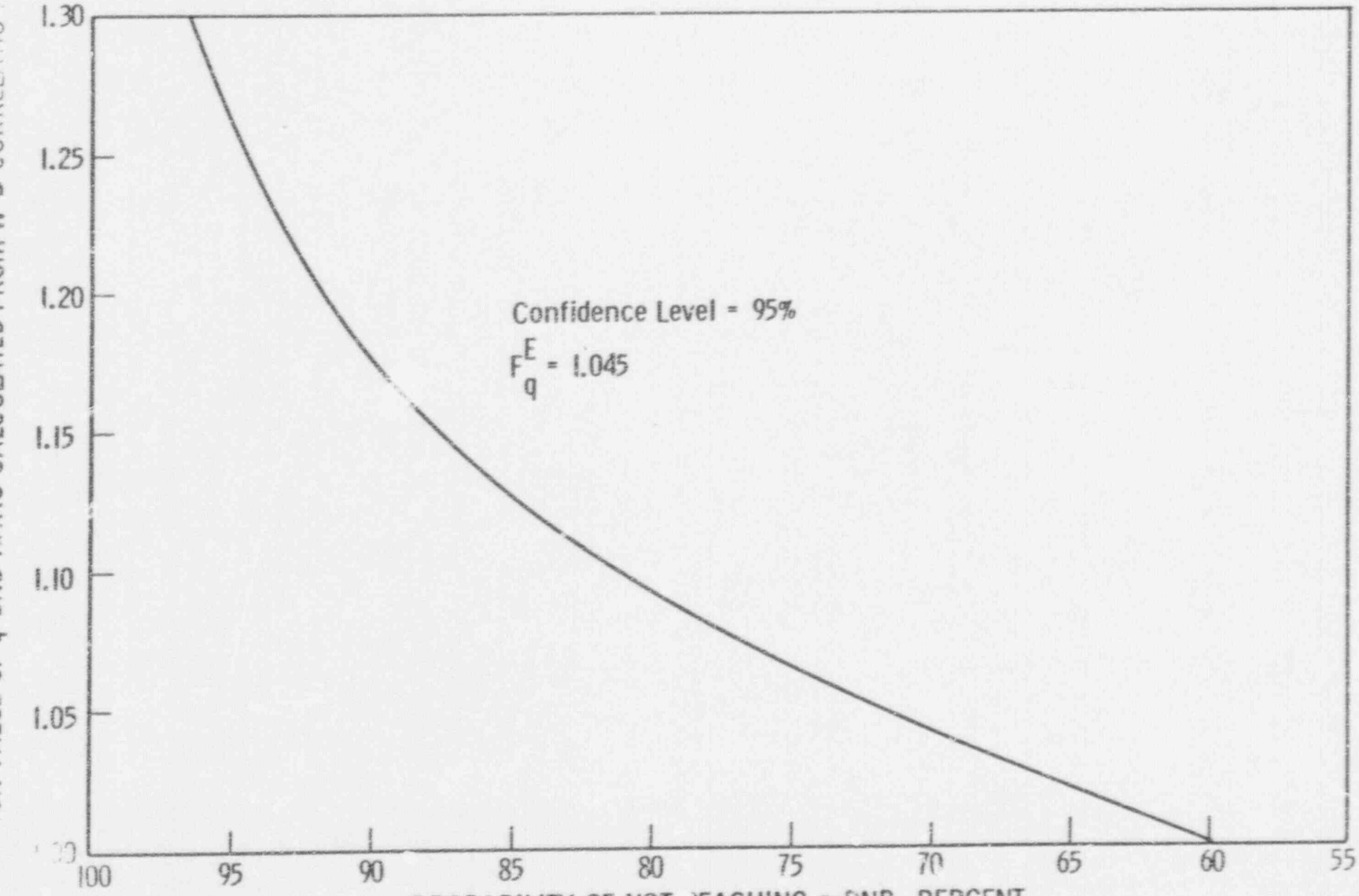

q-DNB PROBABILITY CURVE AT 2000 PSIA

FIGURE III-5

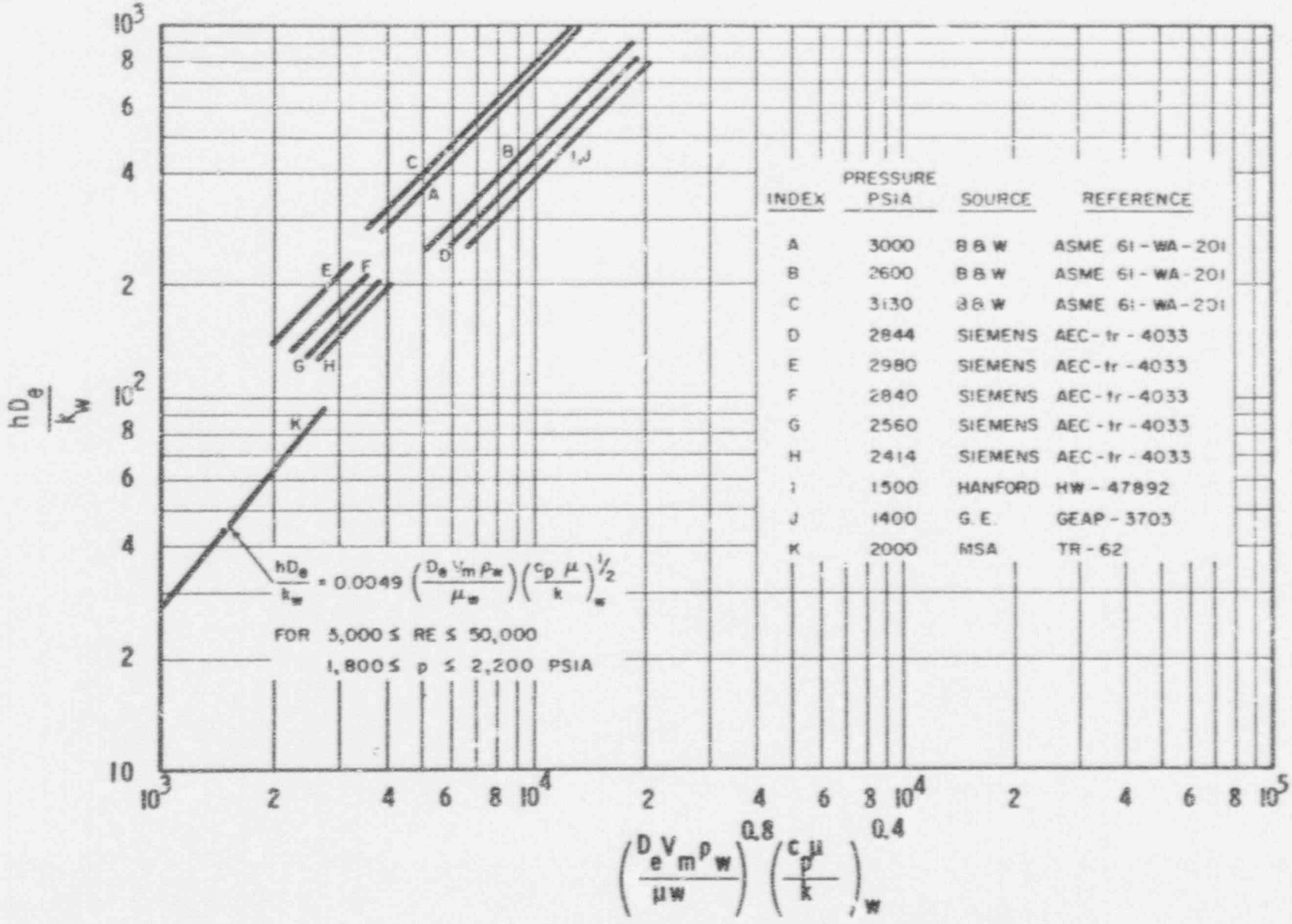

STABLE FILM BOILING HEAT TRANSFER DATA AND CORRELATION

FIGURE III - 6

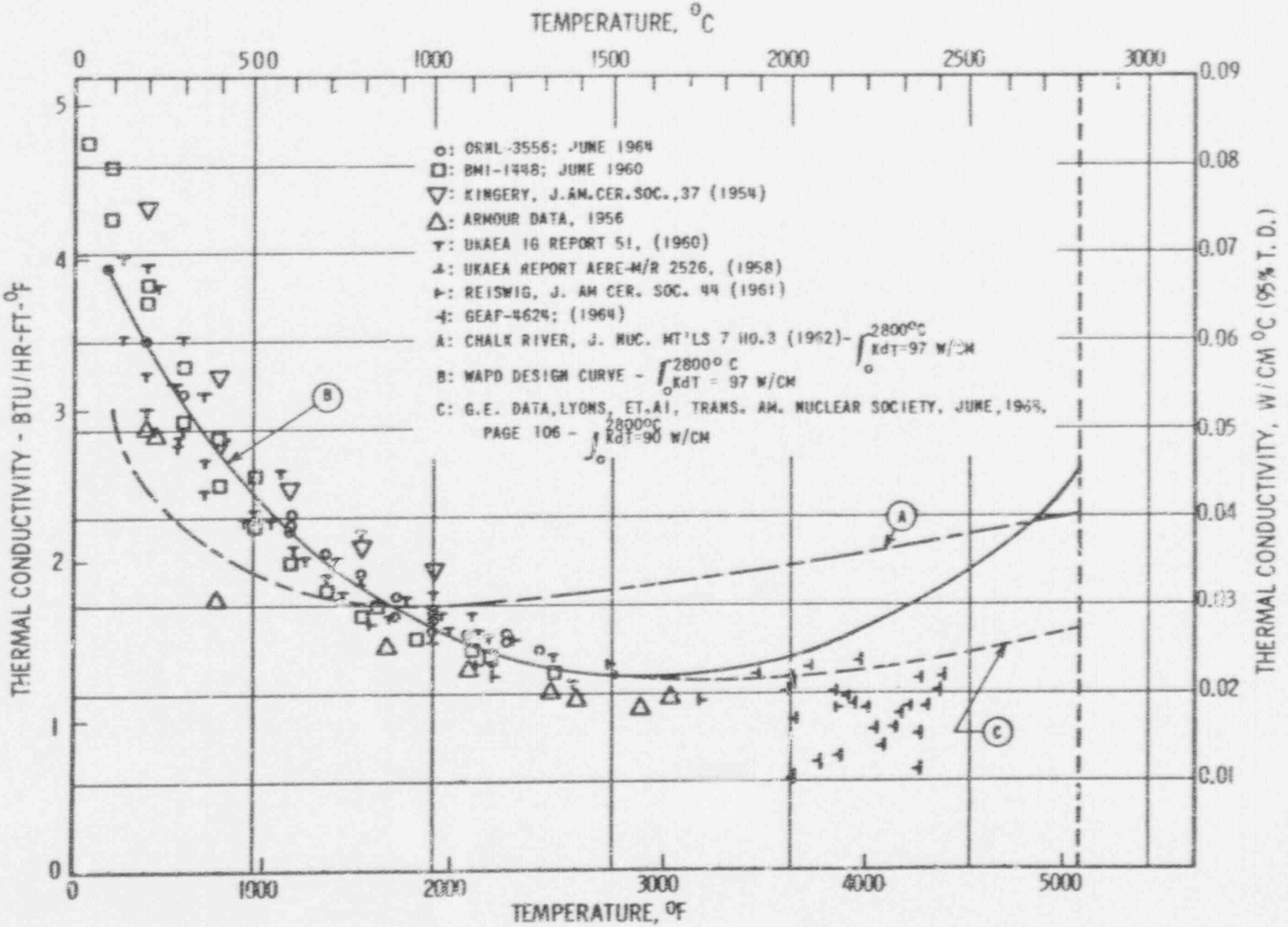

THERMAL CONDUCTIVITY OF URANIUM DIOXIDE

FIGURE III - 7

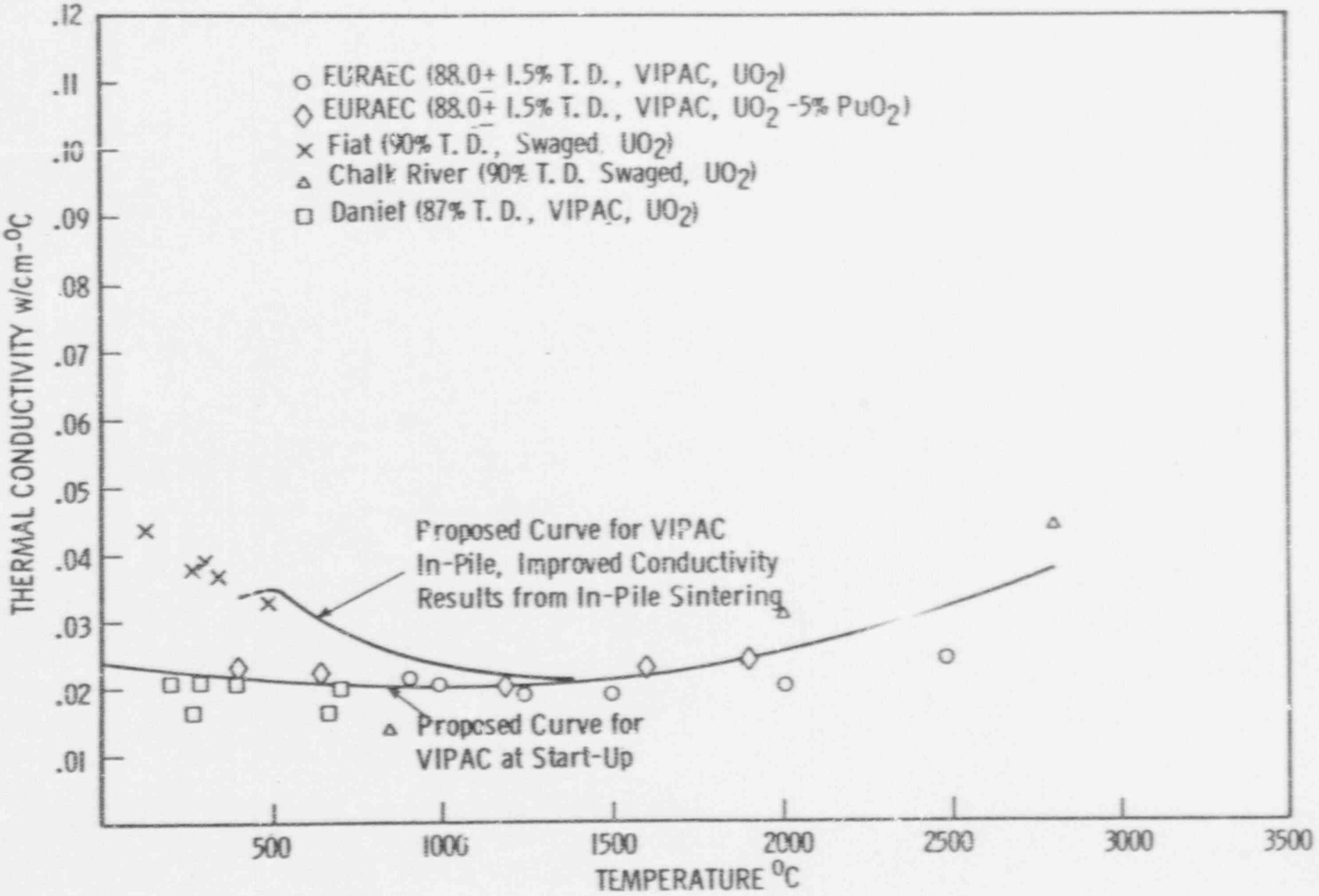

THERMAL CONDUCTIVITY OF VIBRATIONALLY COMPACTED FUEL

FIGURE III-8

IV. MECHANICAL DESIGN

A. CORE LOADING

The 21 main fuel assemblies (9 x 9 array) in the Saxton Core II fuel loading will be made up of 9 plutonium fuel assemblies, 11 new UO_2 fuel assemblies, and the special hollow 51 rod UO_2 assembly presently installed in the reactor for the supercritical program. The 11 new UO_2 assemblies will further consist of four assemblies of the existing Core I design and seven assemblies of the new Core II design.

As with the Core I fuel assemblies both the plutonium and new UO_2 assemblies will be comprised of two groups; one group of the 72 rod design, and a second group of the hollow 63 rod design to accommodate 9 rod removable subassembly. A breakdown of the number of plutonium and UO_2 fuel assemblies in each group is given in Table IV-1.

As with the present core in Saxton, two rod positions in each of the main fuel assemblies in Core II will be used for either in-core instrumentation as indicated in Section V, source rods, or removable fuel rods, depending on the location of the fuel assembly in the core. In addition, the special L-shaped assemblies presently installed in the control rod slots in the peripheral fuel assemblies will be reused with the fuel assemblies in Core II.

The remaining fuel loading for Core II will be made up of the six control rod followers presently in the reactor, the supercritical assembly, and four of the removable 3 x 3 type fuel subassemblies to be used in conjunction with the hollow 63 rod design fuel assembly.

TABLE IV-1

FUEL ASSEMBLY TYPES

	Number of Assemblies	
	72 Rod Assembly	63 Rod Assembly
Plutonium Assemblies	8	1
Core I Design UO_2 Assemblies	3	1
Core II Design UO_2 Assemblies	5	2
Supercritical Assembly	(51 rod design)	1

B. FUEL ASSEMBLY DESIGN

1. Overall Construction

The construction of the plutonium and uranium fuel assemblies remains essentially the same as that for the Core I fuel assemblies. No change has been made in the overall fuel assembly dimensions or fuel rod pitch and the fuel assembly cross-section remains identical to that shown in Figure 203.1 of the original Saxton Final Safeguards Report. The only change in the basic Core I fuel assembly design made for the Core II assemblies is in the type spring clip grids used for radial support of the fuel rods in the fuel assembly.

2. Core II Grid Design

The improved design spring clip used with the Core II fuel assemblies consists of interlocking sheet metal grid straps brazed together in an egg crate type construction similar to the Core I grids. With the improved grid design, however, the fuel rods are supported with a six point support instead of a four point support as in the previous design.

In the old design, the fuel rods were supported laterally on all four sides at each grid location by spring fingers which extended out, in the form of cantilevers, from the main body of the straps. This arrangement provided ample lateral support for the rods but offered no moment to restrain bending of the rods between the grids.

In the new grid design, the fuel rods are supported within each grid lattice by a combination of spring fingers and pairs of stiff formed dimples. In this case the spring fingers are

located on only two sides of each fuel rod, at 90° from each other, and are formed within the main body of the grid straps. The pair of dimples associated with each spring are formed in the parallel grid strap on the opposite side of the fuel rod from the spring and are spaced evenly above and below the spring.

Insertion of a fuel rod between each spring and its associated dimples preloads the spring, which, in conjunction with the dimples, produces both a force and a couple to restrain the rod against motion. The magnitude of the force and couple is sufficient to maintain contact between the fuel rod and the support surfaces under all anticipated combinations of assembly misalignment and reactor operating conditions. This built-in condition of the fuel rods at the grid locations will minimize any possible fretting between the fuel rods and supporting grid straps. A comparative sketch of the old and new spring clip designs is given in Figure IV-1.

C. FUEL ROD DESIGN

1. Overall Designs

The Core II plutonium fuel rods are composed of either pelletized or vibratory compacted fuel encased in either cold worked 304 stainless steel or Zircaloy-4 cladding (all four combinations are utilized). The fuel rods are of the same overall size as the Core I fuel rods (nominally 0.391 inch in outside diameter and 39.051 inches long). Table IV-2 lists the number of rods, type of clad and fuel configuration.

TABLE IV-2

UTILIZATION OF PLUTONIUM FUEL ROD LOCATIONS IN CORE II

Fuel Configuration	Cladding	Number of Rods
Pelletized	Zr-4	473
Pelletized	304 SS	20
Vibratory Compacted	Zr-4	136
Vibratory Compacted	304 SS	10
Instrumentation Locations	-	7
Source Rods		2
	Total	651

The Core II uranium fuel rods consist of UO_2 pellets encased in cold worked 304 stainless steel and, like the plutonium rods, are of the same overall size as the Core I fuel rods. A total of 483 of these fuel rods are used in the Core II design fuel assemblies. The remaining fuel rods will be of the Core I design.

All of the fuel rods are provided with end gaps to allow for differential axial growth between the fuel and clad and to provide void space for fission gases, moisture and other gases contained within the fuel.

To compensate for radial growth resulting from thermal expansion and swelling of the fuel under the high burnups, the pelletized fuel rods are also provided with diametral gaps between the fuel and cladding. However, because of the lower density of the vibratory compacted fuel, no diametral gap is required. The cladding dimensions, pellet sizes, and radial and end gaps required for the Core II fuel rods are given in Table IV-3.

TABLE IV-3

CORE II FUEL ROD DIMENSIONS

	PuO_2 Fuel		UO_2 Fuel
Clad Type	Zircaloy-4	304 SS	304 SS
Clad inside diameter, in.	0.3445	0.361	0.361
Clad wall thickness, in.	0.0233	0.015	0.015
Rod overall length, in.	39.051	39.051	39.051
Pelletized fuel rod			
Pellet diameter, in.	0.3374	0.3558	0.357
Pellet length, in.	0.366	0.366	0.600
Diametral gap, in.	0.0071	0.0052	0.004
Pellet stack height, in.	36.6	36.6	36.6
End gap, in. (minimum)	0.726	0.609	0.612
Vipac fuel rod			
Fuel column height	36.6	36.6	-
End gap (minimum)	0.784	0.784	-

In order to ensure that the fuel remains solidly packed in the fuel rods, a retaining device is used at the upper end of all pelletized plutonium and uranium fuel columns. The retainer is designed to prevent axial motion of the fuel under the loads expected during handling and shipping of the rods, but permits free axial expansion of the fuel relative to the cladding during reactor operation.

2. Fuel Design and Characteristics

The fuel for both the pelletized and vibratory compacted plutonium fuel rods is composed of a mixture of natural uranium dioxide and plutonium dioxide powders. The enrichment for both types of fuel rods has been set at 6.6 w/o PuO_2. The mixed oxide will have an initial melting point of 5170°F.

The fuel pellets are produced by sintering compacted powder to obtain a final density of 94 ± 2% of the theoretical solid fuel density. The pellets are centerless ground to the required diameter after sintering. In order to provide axial space within the pellet stack for differential expansion resulting from the radial thermal gradient in the fuel, one end of each pellet is dished. The pellets are then stacked with the dished ends oriented in one direction to a stack height of 36.6 ± 0.183 inches (one half a pellet height). Although the tolerance on the pellet stack is fairly large, the end gaps in the fuel rods are controlled to a minimum of 0.609 inches by the addition of thin aluminum oxide spacers at the top end of the stack.

The vibratory compacted fuel is compacted within the clad to a density of 87 ± 1% of the theoretical solid fuel density. The fuel columns for the vipac fuel will be 36.6 ± 0.188 in., and the end gaps will be controlled, as in the pelletized rods, to a minimum of 0.784 inches by the addition of the aluminum oxide spacers.

The uranium fuel for the core II design fuel rods is composed of 5.69 w/o enriched UO_2 pellets. As with the plutonium pellets, these pellets are produced by sintering and are centerless ground to size. Because of the longer length of the UO_2 pellets, however, the pellets are dished at both ends and the tolerance on the 36.6 inch stack height is $\pm$ .300 inch. The tolerance on the end gap in this case is held to $\pm$ .068 inch with the aluminum oxide spacers.

The moisture content and allowable gas volumes specified for the Core II fuel are as listed in Table IV-4.

3. Cladding Design

The fuel cladding consists of either 10% cold worked type 304 stainless steel or cold drawn Zircaloy-4 tubing. The fuel rod design for the stainless steel clad rods was established with the criteria that the cladding be free standing under design pressure and temperature conditions, that diametral contact between the pellets and cladding occurs only under the worst expected tolerance, power and burnup combinations, and that the internal gas pressure at the end of life is less than the reactor operating pressure. The fuel rod design with the Zircaloy-4 cladding was established using a criteria similar to that used for the stainless steel with the exception that diametral contact between the pellets and clad is not limited entirely to the worst tolerance, power, and burnup combinations. Because of the creep properties of Zircaloy-4 at high temperatures, it is expected that some reduction in clad diameter may occur in the hot zone of the fuel rod. However, since this creep will be limited to the high temperature region of the rod and will cease upon contact between the fuel and the clad, it will not affect the integrity of the clad nor will it introduce any undue hazard into the operation of the reactor. The clad thickness, diametral clearance between the pellets and cladding, and the fuel rod internal void volume for both the stainless steel and Zircaloy-4 clad were established consistent with the foregoing criteria.

The maximum clad stresses calculated for the pelleted Plutonium fuel are compressive and occur at the beginning of core life when the internal pressure is taken to be zero. These stresses are calculated on the assumption that the clad cross section is oval, and the external pressure then induces bending stresses at the major and minor clad axes. Table IV-5 lists the values of these stresses for both the stainless steel and Zircaloy-4 cladding. The values listed in Table IV-5 are maximum values and will be reduced after a short period of operation at power because of internal pressure generated by the water vapor and gases that are left in the fuel during manufacture as shown in Table IV-4.

The maximum internal fission gas pressure at the end of life has been calculated to be less than the external coolant pressure for both the stainless steel and Zircaloy-4 clad fuel rods.

Thus the net pressure acting on the clad will induce no tensile stresses, and the maximum tensile stress will be due to thermal stresses only. The maximum tensile thermal stresses calculated at the hot spot for both clad materials are:

1) Stainless steel clad - Thermal stress at outer surface = 7780 psi
2) Zircaloy-4 clad - Thermal stress at outer surface = 2380 psi

The stresses for the UO_2 stainless steel clad fuel rods for Core II are lower than the stresses for the Plutonium stainless steel clad fuel rods, and thus have not been included in Table IV-5.

As a further safeguard against clad failure, the end plug weld procedures have been established to obtain a weld penetration equal to 90% or more of the minimum wall thickness of the cladding.

The end plug welds for the UO_2 rods will be 100% radiographed and the pelletized PuO_2 rod end plug welds will be 100% dye penetrant inspected. The welds for the Vipac PuO_2 rods will be ultrasonically inspected. Other procedures that will be used to ensure the integrity of the end plug welds include sectioning and inspection of sample welds and as a final check, the finished fuel rods will be helium leak tested.

D. JUSTIFICATION FOR THE RE-USE OF THE CONTROL ROD FOLLOWERS AND L ASSEMBLIES

Because it is planned to continue to use the L assemblies and control rod followers presently in the core for operation with Core II, our analysis was performed which indicated that such continued operation was safe.

The analysis was based upon the worst combination of burnup, pellet and cladding tolerances and fuel swelling based on a fuel density of 93% of theoretical. The basic criterion used to establish acceptability of the re-use of the followers and L assemblies was that the end of life internal gas pressure should not greatly exceed external coolant pressure at operating conditions. The results of the analysis are presented in Table IV-6. The results show that in order to meet the above criterion the two center followers (central rods #2 and #5) would have to be moved to peripheral locations during the operation of Core II. In addition to limiting the increase in internal gas pressure, the shift of the followers also limits the peak pellet to clad pressure due to fuel swelling to very low levels.

TABLE IV-4

MAXIMUM ALLOWABLE GAS AND VAPOR
CONTENT FOR PLUTONIUM FUEL MIXTURES

	Plutonium Pelletized Fuel	Plutonium Vipac Fuel	Uranium Pelletized Fuel
H_2O, ppm	30	100	30
N_2, ppm	100	100	75
H_2, from hydrocarbon impurities ppm	15	5	-
Total gas release at 1000°C (Exclusive of water)SCC/gm	.05	.067	-

TABLE IV-5

MAXIMUM PRESSURE STRESS PLUS THERMAL STRESS
IN FUEL CLAD AT BEGINNING OF CORE LIFE

Cladding Material	Condition	Avg. Clad Temp. (°F)	0.2% Yield Strength at Clad Temp. (psi)	Circumferential Stress (Psi)			
				Minor Axis		Major Axis	
				Inside	Outside	Inside	Outside
Stainless Steel	Avg. Rod	600	65000	- 9130	-47490	-53500	- 3120
	Hot Spot	672	62000	-37980	-18640	-41040	-15580
Zircaloy-4	Avg. Rod	605	55000*	-13150	-25030	-28700	- 9500
	Hot Spot	692	51000*	-23750	-14580	-24710	-13620

* 0.2% yield strength in circumferential direction where (yield strength circumferential) = 1.475 (yield strength longitudinal - 2000).

TABLE IV-6

CONTROL ROD FOLLOWER AND L ASSEMBLY BURNUP ANALYSIS

Fuel Rod	Peak Burnup (MWD/MTU)	Peak Power Density (KW/ft)	Fission Gas Pressure (psi)	Pellet-Clad Contact Pressure (psi)
L-Assembly Rod	43,900	7.44	689	0
Control Rod Follower Rod				
Same Locations as Core I	55,000	10.82	2993	2900
Moved to Periphery in Core II	49,700	8.22	2070	20

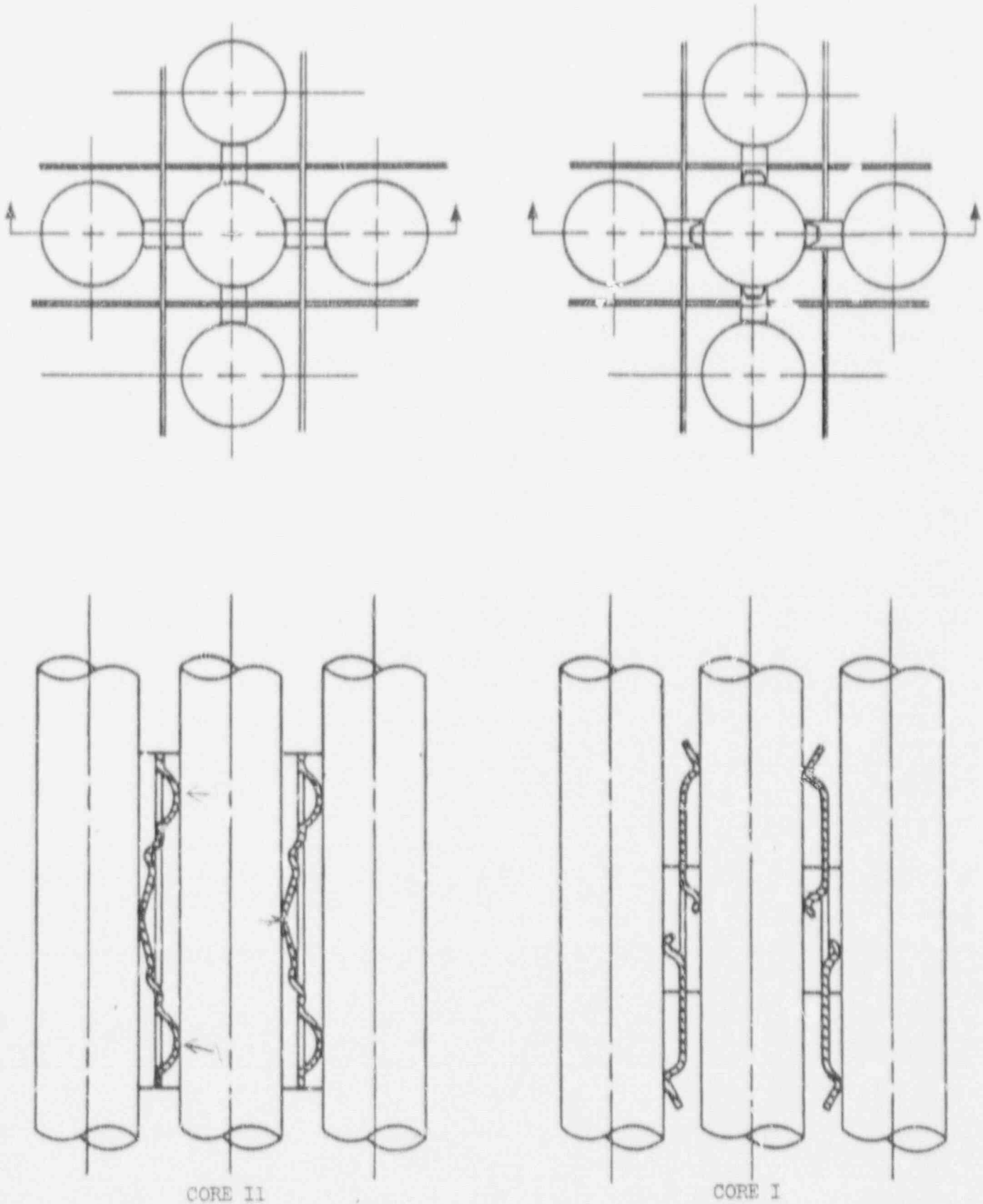

SAXTON GRID DESIGN

FIGURE IV-1

V. INSTRUMENTATION

A. IN-CORE INSTRUMENTATION

In order to provide experimental measurements and continuous monitoring of conditions in the core, the Saxton Reactor was provided with a relatively extensive in-core instrumentation system. The system is capable of measuring outlet temperature, flow rate, pressure drop and the magnitude and axial distribution of the neutron flux. No modifications of the system are required or planned because of the installation of a partial plutonium core.

The in-core instrumentation system consists of the following components:

Pitot Tubes

Inlet and outlet flow rates may be monitored at positions 2E, 2F, 3E, 4B, 4C, 4D, 4E, 4F, 5D, and 5E and inlet flow rates only may be monitored at positions 3D, 3B, and 5C. In addition, coolant pressure drop across the core may be measured at positions 3D, 4F and 5C.

Thermocouples

Fuel assembly outlet temperatures are measured over the central position of the following assemblies: 2E, 2F, 3E, 4B, 4C, 4D, 4E, 4F, 5C, 5D, and 5E. In addition several thermocouples are provided over the area of assembly 2E in order to monitor the outlet temperature distribution.

Flux Wires

Activation of manganese in carbon steel wires is used to determine the magnitude and axial distribution of power in the fuel rods adjacent to the flux wire thimbles. The wires are moved by remote operation from a storage position into the core for activation and thence into a scanning position for scanning with a sodium iodide crystal to determine flux data. It is probable that this system may be equipped with small, moveable detectors in the place of one or two flux wires in order to get more rapid results and interpretations on flux levels and responses to system changes (e.g. control rod motion).

Figure V-1 shows the location of the in-core instruments in relation to the Saxton core. The central nine assemblies (C, D, E - 2, 3, 4) will contain the plutonium fuel.

B. PLANT SITE MONITORING

In order to provide a complete radiation detection capability at Saxton, an alpha monitoring system will be added to the plant site monitoring procedures presently being used at Saxton. The alpha monitoring system will be capable of detecting and indicating alpha contamination levels throughout the Saxton plant.

The alpha monitoring system will be capable of detecting surface contamination and air particulate contamination. Surface contamination will be monitored using two separate systems. One system consists of portable (battery powered hand held) survey meters that have a detection sensitivity range of 2 to 2000 alphas per square centimeter per minute. The second system that will have a more sensitive detection limit for surface contamination is a portable smear sample kit. The kits are equipped with the necessary laboratory analysis instrumentation to detect alpha activity levels of 0.2 alphas per square centimeter per minute.

Air particulate contamination will also be monitored using two separate systems. The alpha contamination of the vapor container will be monitored by an on-line air sampling system. This system takes an air sample from the container through a closed, sealed system, passes it through a scintillation detector, filter paper assembly and then returns it to the vapor container. Particles greater than 1 micron in diameter are collected by the filter paper. The paper is then viewed by a photomultiplier-scintillation crystal combination and monitored for alpha activity. The system contains sufficient delay time between collection and monitoring to permit the decay of the masking Radon-Thoron activities. The overall sensitivity of this system is of 1×10^{-12} μc/cc for Pu-239.

In order to provide a flexible air monitoring system that can be used to monitor specific areas of the containment or areas not covered by the installed air sampling system, portable air sampling collectors and associated laboratory analysis instrumentation are also included in the alpha monitoring system. This portable air monitoring system will have a detection sensitivity of 2×10^{-12} μc/cc for Pu-239. These portable detectors will be used in conjunction with the routine radiation protection program at Saxton or in specific instances such as sampling and analysis of the reactor coolant.

FIGURE V - 1

BAXTON IN-CORE INSTRUMENTATION

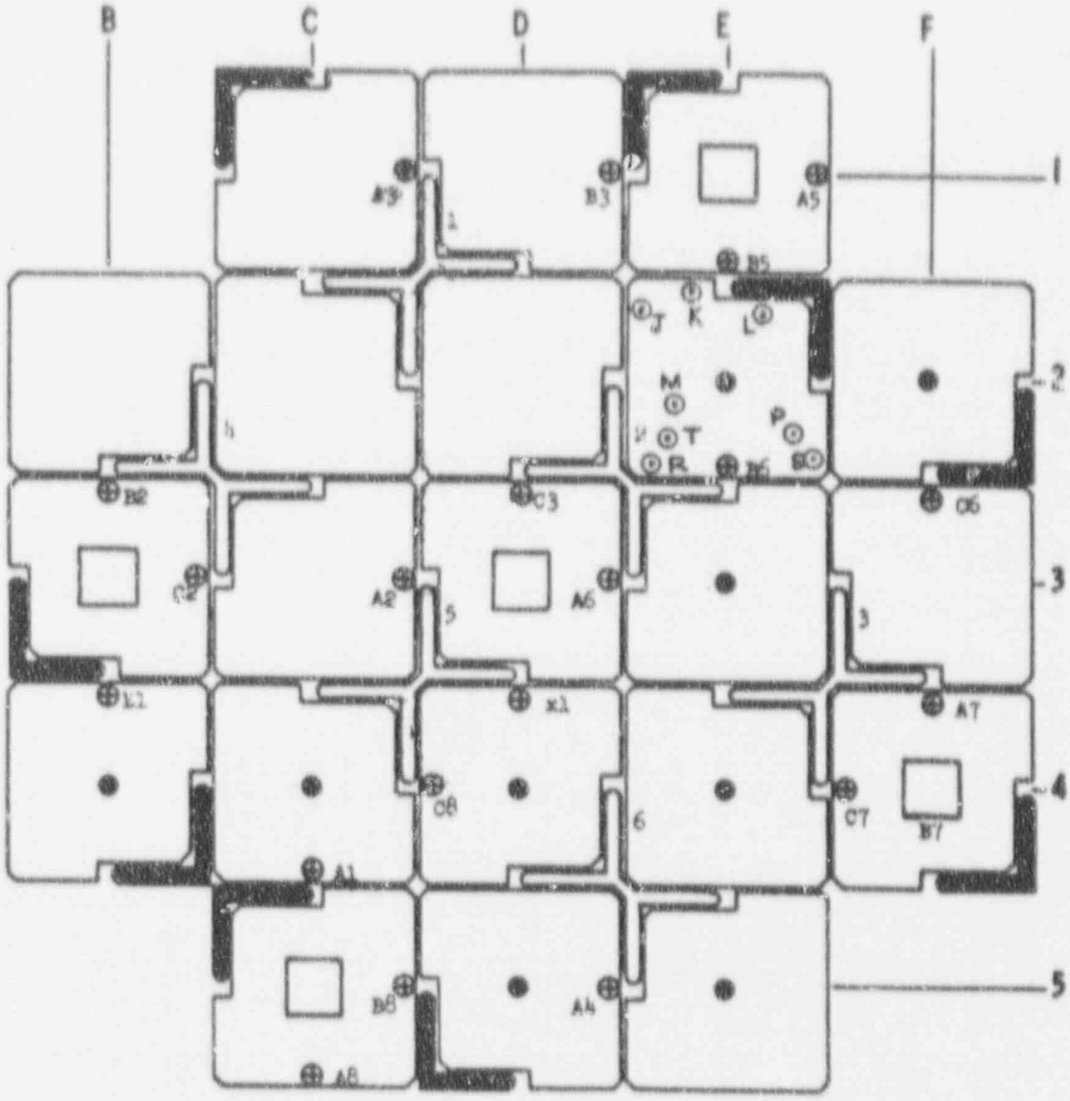

● PITOT TUBE AND THERMOCOUPLE

⊙ THERMOCOUPLE

⊕ FLUX WIRE THIMBLE

VI. ACCIDENT ANALYSIS

A. GENERAL

The use of a partial loading of plutonium in the second core of the Saxton reactor requires a re-evaluation of some of the accidents previously analyzed and reported in the Saxton Final Safeguards Report and in the Safeguards Report for Phase I of the Saxton Five-Year Research and Development Program. The information in Section 502 of the Final Safeguards Report relating to the possible causes of accidents and the safeguards provided applies to the accidents analyzed for this report and will not be repeated.

The magnitude and rate of potential power excursions in the Saxton reactor are reduced by three inherent negative reactivity effects associated with low-enriched pressurized water reactors.

The negative moderator temperature coefficient brings about a reactivity reduction with increases in moderator temperature. The time lag associated with the diffusion of heat through the oxide pellet and cladding makes this comparatively large coefficient important primarily in limiting slow power excursions.

The negative Doppler coefficient reduces reactivity with an increase in fuel temperature as a result of increased resonance absorption of neutrons in plutonium and uranium. This reactivity effect is prompt since fuel heating begins immediately with an increase in reactor power. Thus the Doppler coefficient is particularly important in limiting rapid power transients.

Formation of steam bubbles in the core due to net boiling of water also reduces reactor power. The reactivity reduction associated with the formation of steam bubbles is the "void coefficient" which, since net boiling does not normally occur in the core, is important only in accidents that result in a low primary system pressure (i.e. loss of coolant or steam break).

The reactor safety system monitors reactor operation and prevents core damage by causing a reactor shutdown when necessary to keep the fuel element cladding in the hottest channel from melting. The safety system functions primarily in the event of equipment failures or operational errors.

Additional protection against a contamination hazard is provided by the containment vessel, which houses the entire primary system. In the event of a maximum credible incident, the containment vessel and associated shielding protect the area surrounding the plant from contamination and radiation.

To give assurance that safeguards incorporated in the plant are adequate, it is necessary to analyze and evaluate their effectiveness under a number of postulated accident situations. The most adverse combination of system parameters for each particular accident was analyzed. Therefore, it was not necessary to analyze each accident for all possible combinations of system parameters that may occur during core life. The probability of obtaining this most adverse combination of system parameters simultaneously with the corresponding accident is, of course, very small. Therefore, the results of the accident analyses must be considered as a limiting case for each accident considered. In the same way, reported DNB ratios for accident conditions actually represent the lower bounds of all possible DNB ratios that may occur for a given accident condition.

The accident analyses performed for Core II have been based on the assumption of chemical shim operation at the beginning of life as the worst hot channel factors occur under these conditions for the partial plutonium Core II. The accident analysis for non-chemical shim (rodded) operation of this core would yield less severe results. The use of control rods for some control of the core reduces the peak rod to core average radial power ratio as listed in Section II so that for a given power level the maximum linear power density will be below 16 Kw/ft which is the design limit.

B. REACTIVITY ACCIDENTS

Reactivity accidents are those which result in the addition of more reactivity at a faster rate than is required for normal changes in core power level.

Such reactivity additions might be caused by control rod motion, by moderator temperature changes or by soluble poison removal. As a result of such addition, the reactor power level will increase at a rate and with a magnitude that depends on the rate and magnitude of the reactivity addition. The inherent negative reactivity effects in the core under these conditions will compensate to some extent for the reactivity addition. In addition, the reactor safety and protection systems are designed to protect against conditions which might endanger the integrity of the core. However, as in any reactor, continued reactivity addition accompanied by failure of the safety systems and operator errors can result in damage to the core and release of fission products to the reactor coolant.

1. Uncontrolled Rod Withdrawal at Cold Startup

The condition for uncontrolled rod withdrawal during startup procedures requires a series of multiple failures in the nuclear instrumentation and control systems coupled with simultaneous operator error and violation of procedure.

The continuous withdrawal of the most reactive control rod group at the maximum rate in its most effective region would result in a maximum reactivity addition rate of 7.2×10^{-5} Δ k/sec. The reactor control system is designed to prevent movement of the two control rod groups (the inner two or the outer four) simultaneously so that large insertion rates are not possible. However, for this accident study, a conservative insertion rate of 2.5×10^{-4} Δ k/sec was assumed. In addition, the following assumptions were also used.

a) Maximum expected value of the moderator temperature coefficient: $+ 0.3 \times 10^{-4} \Delta k/k/F°$

b) Minimum expected absolute value of the negative fuel temperature (Doppler) coefficient: $-1.1 \times 10^{-5} \Delta k/k/F°$

c) Initial average core moderator temperature of 70°F

d) The reactor is subcritical by 2% Δk at the initiation of the accident.

e) Overpower set point initiates scram at 122% of nominal power (7% above scram set point of 115%)

f) Scram initiation delay of 1.1 sec (0.5 sec instrumentation and 0.6 sec for control rod motion in region of little effectiveness)

g) Scram insertion worth of 2% $\Delta k/k$ at a linear rate during a 0.9 sec period. (A total delay of 2.0 sec from signal to completion of scram)

h) Nominal power level is 103% of the initial design limit of 21.6 MWt

The results of the cold startup accident transient are shown in Figures VI-B-1, 2, 3 and 4. The reactor power transient shown in Figures VI-B-1 and 2 is terminated at the first peak by the Doppler coefficient of the fuel. The peak is at 115% of nominal power which would normally initiate a reactor scram signal but the accident analyses assumes no scram until a power level of 122% to account for errors and deadband. The power then decreases slightly and then increases again until the high power level scram is initiated at approximately 137 sec. Figure VI-B-3 shows the average fuel, average clad and core water temperature during the transient. The maximum values attained by each of these variables is much less than normal operating conditions so that the scram occurs well before clad damage could occur. The core water temperature rises only slightly above its initial ambient value so that

it is subcooled to such a degree that DNB ratios are well above those for normal operating conditions. The reactor hot spot heat flux, as shown in Figure VI-B-4, reaches a maximum value of about 108% of normal steady state conditions.

The analysis shows that the reactor and control system can safely withstand a rod withdrawal accident from a cold shutdown condition.

2. Uncontrolled Rod Withdrawal - Hot Shutdown

The uncontrolled rod withdrawal at startup with the reactor coolant at operating temperature was also analyzed. The same assumptions used for the cold startup analysis apply except for the following:

a) Moderator temperature coefficient of $-2.7 \times 10^{-4} \Delta k/k/F°$

b) Fuel temperature (Doppler) coefficient of $-1.0 \times 10^{-5} \Delta k/k/F°$

c) Core water average temperature of 530°F

The results of the analyses are shown in Figures VI-B-5, 6, 7 and 8. The reactor power level during the transient is shown in Figures VI-B-5 and 6. The power transient is terminated after approximately 100 seconds because of the overpower scram circuitry. The power level rose to 122% of the nominal setting before the Doppler effect of the fuel could become effective. The average fuel, average clad and core water temperatures are shown in Figure VI-B-7. The clad and fuel temperatures are well below normal operating conditions at their peak values during this transient. The core water temperature rises only slightly above the initial value of 530°F so that it is still subcooled. The heat flux response during the transient is shown in Figure VI-B-8. The peak of the heat flux reaches only 17% of the nominal steady state condition before scram is initiated. As in the cold startup analysis in the previous section, the DNB ratios during this transient are very much greater than those at normal operating conditions.

As the analysis shows, the reactor core is protected from damage by the control system during a rod withdrawal at hot startup. Only simultaneous system failure and operator error could cause circumstances that would lead to core damage and release of fission products to the coolant.

3. Uncontrolled Rod Withdrawal at Power

Requirements for manual rod motion when the reactor is at power may arise due to the need to adjust control rod positions to account for xenon changes or fuel burnup. These changes are slowly varying effects and therefore the requirements for manual control rod movements are infrequent and rod movements are small.

In the unlikely event of an uncontrolled rod withdrawal at power, the maximum possible reactivity insertion rate of the most reactive control rod group is calculated to be $7.2 \times 10^{-5} \Delta k/sec$. This rate assumes that the most reactive group is moving through the region of most effectiveness at its maximum withdrawal rate. However, in order to study a worst possible condition (not credible) a reactivity insertion rate of $2.5 \times 10^{-4} \Delta k/sec$ was assumed for the purposes of the accident study. In addition, the following assumptions were made for the study:

a) Initial power level is 103% of nominal power setting because of calorimetric errors (100% = 21.6 MWt).

b) Primary coolant pressure is at its maximum nominal value of 2050 psia because of instrument errors.

c) Minimum expected absolute value of the negative fuel temperature (Doppler) coefficient: $-1.0 \times 10^{-5} \Delta k/k/F°$

d) Minimum expected absolute value of the negative moderator temperature coefficient: -2.7×10^{-4} Δ k/k/F°

e) Scram initiation due to overpower scram at 122% of nominal power (7% over 115% scram set point due to instrumentation errors)

f) Delay of scram initiation for 1.1 sec (0.5 sec due to instrumentation and 0.6 due to rod motion in a region of small effectiveness)

g) Scram insertion worth of 2% Δ k/k at a linear rate during 0.9 sec period (total delay of 2.0 sec from signal to completion of scram)

Figure IV-B-9 presents the nuclear power response, hot spot heat flux response and moderator pressure response as a function of time after initiation of the accident. The minimum DNB ratio calculated by the W-2 correlation that will occur during the rod withdrawal transient is 2.05 (Δ H-DNB). This minimum DNB ratio condition occurs at 5.2 sec. This minimum ratio is well above the minimum design DNB ratio of 1.25 and indicates that under the most conservative conditions that the power level scram protection system will be able to protect the core.

Additional safety factors which would preclude core damage due to an uncontrolled rod withdrawal accident at power are

a) Control rod circuitry restricts rod motion so that maximum reactivity insertion rate could only be a fraction of the value used in this study.

b) There are three separate power level scram circuits and operation of any two of the three will initiate the scram.

It may be concluded from the above analysis that the uncontrolled rod withdrawal at power accident is highly improbable and would not result in core damage unless there were a simultaneous failure of the power level scram circuitry and operator error.

4. Boron Release Accident

The results of extensive chemical shim experiments and operations both out-of-pile and in-pile at the Saxton and Yankee reactors as well as detailed crud behavior follow and surveillance in these and other reactors have not revealed any credible mechanisms for the boron release accident as postulated in the Safeguards Report for Phase I of the Saxton Five-Year Research and Development Program. In addition, the large amount of data that has been analyzed has shown that even if such an accident were credible, the maximum reactivity release rates that could be associated with this accident are less than those that could be experienced in the worst rod withdrawal accident and are therefore well within the control capabilities of the reactor. For these reasons, the boron release accident has not been re-analyzed for the chemical shim operation of Core II.

The basic objectives of the chemical shim control program and experiment as outlined in the Safeguards Report for Phase I have been the accumulation of reactor operating experience to demonstrate the feasibility of the concept and the determination that no operating problems exist with chemical shim control. The major concern in the use of chemical shim control of a reactor was the possibility that boron might accumulate in some manner on the core surfaces and subsequently be released rapidly causing a large reactivity transient. It was this concern that led to the postulation and analysis of the boron release accident. A secondary concern of the program was that boron accumulation on the core surfaces might occur in an irreversible manner (that is, the accumulation is not reduced as the coolant concentration is reduced) and therefore lead to a significant reduction in core lifetime.

Extensive out-of-pile tests have disclosed only two mechanisms by which significant boron accumulation could occur.(1) The first possibility

(1) WCAP-3731, "Radiotracer Studies of Hideout at High Temperatures and Pressure," (June 1963), L. Picone, D. Whyte, and G. R. Taylor.

was indicated by the study of solutions during nucleate boiling on the surfaces of electrically heated rods. By means of a sodium tracer, it was demonstrated that, under nucleate boiling conditions in the presence of unusually heavy crud deposits, a significant concentration of the sodium occurred in the crud on the surface of the rods. The accumulation disappeared rapidly when boiling on the surface of the rod was terminated. This concentration effect was observed only in the presence of crud deposits far heavier than those expected or experienced in normal reactor operation.

The second possibility indicated was the deposition of alkali borate salts on the surfaces of rods under nucleate boiling conditions. It has been observed that crud levels in pressurized water reactors are reduced when the reactor coolant is maintained at an alkaline pH. Since boric acid is essentially un-ionized at normal reactor operating conditions, these benefits of high pH can be obtained with the addition of relatively small amounts of alkali in the borated coolant. Out-of pile evidence indicates that if the alkali borate salt deposition were to occur with a lithium additive, re-solution of the salt might not occur.

A third, less extensive mechanism, one of simple "exchange absorption" of borate by the crud deposits, is also known. The extent of boron accumulation in the crud is dependent on the boric acid concentration in the coolant and the amount of crud. However, the small amounts of borate that can be absorbed by this process make it insignificant from a reactivity point of view.

Three major techniques have been used to demonstrate the absence of boron accumulation in the crud during the chemical shim experiment. The first of these has been to conduct a careful reactivity follow throughout core life and compare the predicted and observed activity. Particular attention was paid to the transition from nucleate boiling to non-nucleate boiling conditions. If boron hideout did occur with

the reactor in nucleate boiling conditions, it would be observed as a reactivity loss, and in particular, as an abrupt change in the power coefficient with the onset of nucleate boiling. The reactivity loss would then reverse itself once nucleate boiling operation ceased.

The second technique was to conduct a careful follow of the alkali to boron ratio during the chemical shim experiment. Demonstration that this ratio did not change throughout the test would indicate the absence of metaborate precipitation.

The third technique used was that of hot cell examination of a test 3x3 subassembly after appreciable operation under chemical shim conditions. Crud samples from the surfaces of the fuel rods are weighed, analyzed and the reactivity worth of the total deposit estimated.

Prior to the beginning of chemical shim operation, an extensive series of low power physics tests were conducted followed by a period of rodded operation at power. These operations provided the information required to get a base point to conduct the reactivity follow during the chemical shim operation.

The chemical shim operation of the Saxton reactor began in May 1963 and has continued, almost without interruption, since then. A short period of non-chemical shim operation took place from January 30, 1964 to March 6, 1964 to provide additional information on the effect of burnup on the reactivity in an unborated reactor.

This chemical shim test program has successfully demonstrated the feasibility of chemical shim control for pressurized water reactors.(2) No significant operating problems have been encountered during the program. Under the normal operating conditions of the Saxton reactor, the test program data indicate that:

---

(2) WCAP-2599, "The Chemical Shim Experiment," (August 1964), J. Weisman and S. Bartnoff

a) There is no significant accumulation of boron-containing material on the core surface during normal plant operation. The deviation from the reactivity predictions were well within the estimated error and no deleterious trends could be observed.

b) There is no decrease in core lifetime because of chemical shim operation. The hot cell examination and analysis of the central 3x3 subassembly showed no significant accumulation of high cross section materials on the core surfaces.

c) Successful pH control of the coolant can be accomplished and there is no problem with alkali stability in the coolant.

d) The hot channel factors were in reasonable agreement with the calculated values.

e) Chemical shim control, under normal conditions, causes no hazardous situations to arise that could affect plant operation.

As a supplement to the Saxton chemical shim experiment and results as described above, further experiments have been conducted in the Saxton reactor which demonstrate that the hideout problem does not exist even under the conditions of abnormal amounts of crud deposits on the core surfaces. This experimental program is described in detail in Addendum No. 4 to the Phase I Safeguards Report. The experiment consisted basically of two phases. The first was the deposition of artificial crud on the core surfaces by injection of ferrous hydroxide into the reactor coolant while operating at essentially zero boron concentrations and maximum rodded power level. Following the deposition of sufficient amounts of crud as determined by calculations and visual examination of the central 3x3 subassembly, the second phase was to observe the reactivity behavior of the reactor during chemical shim operation at various power levels. The results of this experiment are available and provide additional assurance that hideout would not occur even if the careful chemistry control of the coolant as used in Saxton were not followed.

The results of the chemical shim experimental program at Saxton have demonstrated that the boron release accident as originally postulated at the beginning of the program is not credible even under the extreme operating conditions of the crud test. It may therefore be concluded that the requirements of an unexplained reactivity limit and a detailed reactivity follow program as applied to the chemical shim operation of Core I are no longer necessary for the normal chemical shim operation of the Saxton reactor.

5. Steam Break Accident

Introduction

The rupture of a secondary plant steam line is reflected into the primary system as a step load increase. For small break sizes resulting in a step load increase within the transient capability of the Saxton plant, reactor power level will increase to match the load increase and the decrease in equilibrium average primary coolant temperature. This condition, as far as the primary plant is concerned, is not different from a design step load change and no protective action is required. Depending on secondary plant conditions, the operator will decide when to initiate a manual plant shutdown and to proceed with necessary repairs. If the step load increase resulting from a steam line rupture exceeds the transient capability of the plant, the reactor protection system will automatically shutdown the reactor by either a low pressure scram or an overpower scram and prevent the core from reaching a DNB condition. Following scram, a large power unbalance exists between heat generation in the core (essentially decay heat) and heat extracted from the primary loop as demanded by the steam flow through the break. As a result, the primary coolant temperature decreases and due to the negative moderator temperature coefficient, a reduction in shutdown margin is to be expected until operator action terminates heat removal.

Analysis

The maximum credible steam break accident (equivalent to an 0.034 sq. ft. ductile rupture of the steam dome) was analyzed for chemical shim operation of Core I at 23.5 MWt with a spiked assembly generating 16 KW/ft in the Safeguards Report for Phase I of the Saxton Five Year Research and Development Program.

The calculated reactivity coeffi...nts for Core I and Core II are listed below:

		Core I	Core II (Worst Case)
Moderator Temperature	$\Delta k/k/^{o}F$	-4.6×10^{-4}	-4.1×10^{-4}
Fuel Temperature	$\Delta k/k/^{o}F$	-0.4×10^{-5}	-1.25×10^{-5}
Moderator Pressure	$\Delta k/k/psi$	$+4.6 \times 10^{-6}$	$+3.5 \times 10^{-6}$

Because it has the largest absolute value, the moderator coefficient is the most important in determining the reactivity transient following the steam break accident. As the above table shows, the partial plutonium Core II has a less negative moderator temperature reactivity coefficient and therefore the steam break accident for Core II will be less severe than for Core I.

In order to assess the upper limit of possible reactor damage, the maximum hypothetical steam break was analyzed for Core II. This steam break accident is the complete severance of the steam pipe at the outlet of the steam generator with an internal diameter of 5.5 inches (0.165 sq. ft. area).

The steam flow through the break as a function of steam pressure was evaluated by the modified Darcy formula (ref. Flow of Fluids, CRANE Technical Paper No. 410). The formula is of the following form:

$$W_S = 0.525\ Y\ d^2 \sqrt{\frac{P}{KV_1}}$$

where

Y = net expansion factor for compressible flow through orifices, nozzles or pipe

d = internal diameter of pipe, inches

ΔP = pressure drop, psi

k = resistance factor for pipe length from steam generator to break, including entrance and exit losses

V_1 = steam specific volume, ft^3/lb

W_S = steam flow, lb/sec

This accident was analyzed for three different cases with the following reactivity coefficients:

		Moderator Temperature	Fuel Temperature
(a)	2000 ppm	-2.7×10^{-4} $\Delta k/k/^oF$	-1.25×10^{-5} $\Delta k/k/^oF$
(b)	1000 ppm	-3.4×10^{-4} $\Delta k/k/^oF$	-1.25×10^{-5} $\Delta k/k/^oF$
(c)	0 ppm	-4.1×10^{-4} $\Delta k/k/^oF$	-1.25×10^{-5} $\Delta k/k/^oF$

For each case, the amount of negative reactivity insertion from control rods required to maintain the core subcritical by an 0.5% Δk shutdown margin during the course of the steam break accident was computed assuming no safety injection flow. The shutdown margin will increase substantially with safety injection flow. Since the steam generator feedwater pumps are steam driven, the steam break accident causes termination of the feedwater flow, and as a result, the steam generator is empty in approximately 78 seconds and the cooldown of the primary system is terminated.

Results

The primary system pressure response after initiation of the accident is shown on Figure VI-B-10. The steam generator flow rate, the neutron flux and hot spot heat flux responses are shown on Figure VI-B-11. The steam generator inlet and outlet temperature and the core inlet and outlet temperature responses are shown in Figure VI-B-12.

The minimum DNB ratio calculated for the three cases analyzed is a q" DNBR of 2.26 for the 0 ppm condition (nominally end of life). The reactivity required in control rods out of the core to prevent return to criticality during the course of the accident without safety injection is shown on Figure VI-B-13. Curve B assumes that all rods scram upon signal and curve A assumes that the most reactive rod (equivalent to 5.2% $\Delta k/k$) does not scram upon signal.

Conclusions

The Saxton reactor safety system will adequately protect the core in the event of the maximum credible steam break accident. The maximum hypothetical steam break accident in conjunction with a stuck control rod and failure of the safety injection system has such a low probability of occurrence that core damage can be accepted. In addition to the above occurrences, the reactor would have to be operating with boron concentrations well below those planned for the normal chemical shim operation of the plant. Even if the core were to return critical at full power, the stuck rod power distribution of Section VI (Figure II-10) shows that the maximum linear power density would be less than 20 KW/ft.

6. Cold Water Introduction

The analysis and results of the cold water introduction accident as presented in the Saxton Final Safeguards Report are unchanged for Saxton Core II.

7. Xenon Burnout

The analysis and results of the xenon burnout reactivity transient as presented in the Final Safeguards Report are unchanged for Saxton Core II.

8. Conclusions

As demonstrated by the preceding accident analyses, the transient behavior of the Saxton reactor is such that negative temperature coefficients of reactivity or the reactor scram circuitry will terminate power excursions well before any core damage could occur. Because of the inclusion of the mixed oxide fuel in Core II, there exists a possibility of some time delay in the effectiveness of the negative Doppler coefficient because of time delay in the heat transfer from the PuO_2 to the UO_2. However, the time delay associated with this core is more than an order of magnitude less than the shortest reactor period calculated for any of the transients and thus it is not effective in altering the Doppler coefficient.

Thus, the accident analyses and results that have been reported are conservative and demonstrate that core damage or hazard to the public from reactivity accidents are highly improbable.

C. MECHANICAL ACCIDENTS

1. Loss of Coolant

A loss of coolant accident for a 0.0375 ft^2 break in the reactor coolant piping during normal operation at 20 MWt was analyzed in the Final Safeguards Report. This analysis was updated in the Safeguards Report for Phase I of the Five-Year Research and Development Program to cover reactor operations at 23.5 MWt. The results of these analyses are applicable to this Core II report and essentially conclude that the core will not be uncovered if the safety injection system functions properly.

2. Loss of Flow Accident

A loss of coolant flow in the reactor coolant system could be caused by either a blockage of the system or by failure of the reactor coolant pump. Since the reactor coolant system of the Saxton reactor contains no valves, complete blockage of the reactor coolant piping is considered incredible and such an accident is not analyzed. Only failure of the coolant pump is analyzed and such failure could be caused by loss of electrical power or by mechanical failure of the coolant pump motor or of the coupling between the motor and the pump. As was assumed in the accident analysis section of the Final Safeguards Report for Saxton, mechanical failure due to sudden seizure of the pump rotor is not considered credible.

In the event of a loss of flow accident, the temperature of the primary coolant in the core will increase because of scram circuit delays which allow the reactor to keep operating at full power while flow coastdown is occurring. Such delays are critical because the DNB ratios are decreasing during this delay period and scram should be completed before possible DNB occurs. If the heat

generation of the core is not terminated rapidly enough to prevent DNB, fuel and clad temperatures may rise to excessive values and clad damage and failure could result.

The first seven seconds of the flow coastdown curve used in the accident analysis is shown in Figure VI-C-1. This curve is the result of measured data taken for the Saxton coolant pump with the reactor at a power level of 14 MWt. The following additional assumptions were used in the evaluation of this accident:

a) Reactor power level is at 103% of nominal power setting because of calorimetric error (100% = 21.6 MWt).

b) Maximum fuel power density is 16.0 kw/ft.

c) Scram delay times of
   (1) Flow decay to set point and error in set point - 0.7 sec
   (2) Instrumentation delay - 0.2 sec
   (3) Rod motion in regions of small effectiveness - 0.6 sec
   Total - 1.5 sec

d) A scram insertion worth of 2% $\Delta k/k$ at a linear rate over a 0.9 sec period.

e) A maximum expected absolute value of the negative fuel temperature (Doppler) coefficient: $-1.15 \times 10^{-5} \Delta k/k/F°$

f) A minimum expected absolute value of the negative moderator temperature coefficient: $-2.7 \times 10^{-4} \Delta k/k/F°$

g) Low flow scram set point is 2.2×10^{6} lb/hr.

The results of the analysis are presented in Figure VI-C-2. This figure shows the transient behavior of the Q and ΔH-DNB ratios (as calculated by the W-2 Correlation) during the loss of flow accident. The ΔH-DNB ratio is the critical parameter in this analysis and it reaches a minimum value of 1.89 at 2.2 seconds. The ΔH-DNB ratio is

decreased at higher pressures and thus a maximum steady state coolant pressure of 2050 psia was used in the ΔH-DNB calculation. If a pressure of 1950 psia is assumed, then the minimum ΔH-DNB is 1.92 at 2.2 seconds. The Q-DNB ratio is also calculated for the transient and reaches a minimum of 2.08 in 1.6 seconds. The Q-DNB ratio is decreased at lower pressures and thus a minimum steady state coolant pressure of 1950 psia is assumed for the Q-DNB calculation.

From the above analysis, it may be concluded that there is an ample margin of safety to prevent clad damage as a result of a loss of flow accident. Clad damage could only result from coincident failure of the low flow scram circuitry and operator error.

D. MAXIMUM HYPOTHETICAL ACCIDENT

The maximum hypothetical accident for the Saxton reactor is defined in Section 508 of the Saxton Final Safeguards Report. The assumption and condition for the accident are as follows:

1. Instantaneous release of the primary coolant along with the associated heat sources and sinks as described in Section 506 of the Final Safeguards Report.

2. Failure of the engineered safeguards to prevent core damage by recovering the core with borated water.

3. Complete core meltdown and the associated fission product releases as calculated in Section 603 of the Saxton Final Safeguards Report.

The energy release associated with this accident is assumed to cause an instantaneous pressurization of the vapor container. The resultant pressure is approximately 30 psig. The vapor container pressure transient for this accident is represented in Figure VI-D-1 taken from the Saxton Final Safeguards Report. The initial pressure peak falls rapidly to approximately 10 psig followed by a slight rise and than a gradual reduction and leveling off at approximately 5 psig. The rise following the initial peak assumes that decay heat is released from the core into the containment. Complete core meltdown is also assumed to occur with this accident because of malfunction of the engineered safeguards designed to prevent core damage.

Because of the substantial fraction of the Saxton second core that is clad with zirconium, the consequences of a metal-water reaction must be considered in conjunction with the maximum hypothetical accident as described above.

The plutonium region will consist of a maximum of nine standard Saxton assemblies of 72 rod spaces per assembly. Two of these spaces are normally left empty to accommodate in-core instrumentation. In addition,

not all of the plutonium fueled rods will be clad with Zircaloy as is indicated in Table IV-2 in Section IV. However, as a conservative upper limit of nine 72-rod assemblies clad with Zircaloy are assumed for this analysis.

Using the nominal Zircaloy clad dimensions of Table II-2, and assuming a total of 648 rods, the total mass of Zircaloy in the core can be calculated as follows:

$$M_{total} = 410 \text{ lb/ft}^3 \left[\frac{648 \times \frac{\pi}{4} \times (0.3911^2 - 0.3445^2) \times 39.051}{1728} \right]$$

$$M_{total} = 161.6 \text{ lbs or } 1.77 \text{ lb moles}$$

For the Zircaloy-water reaction, the energy release is assumed to be approximately 250,000 Btu/lb mole of Zr reacted due directly to the reaction. Additional energy may be obtained from the recombination of the hydrogen gas liberated during the reaction. This recombination energy is approximately 213,000 Btu/lb mole of Zr reacted. Thus, the maximum total energy release from such a reaction is approximately 820,000 Btu for 1.77 lb moles.

If this amount of energy were added to the steam-air mixture of the vapor container that would exist following the hypothetical accident, the pressure would be raised by approximately 2 psi. Such a postulated instantaneous release is not physically possible because the core would require some time to heat up and finally react following the loss of coolant. Because of the rapid decrease of the containment pressure following this accident, the added pressure rise due to the metal-water reaction could not cause the containment design pressure to be exceeded during the hypothetical accident.

The hydrogen recombination reaction can be violent if it occurs in a confined space and the concentration is at the explosive mixture li . The total amount of hydrogen released from the 100% metal-water reaction

is 3.54 lb moles of H_2 gas or 7.1 lb of H_2. The dissolved hydrogen in the reactor coolant is specified as a maximum of 90 cc at STP for each kilogram of reactor coolant. At ambient conditions, the primary coolant system volume contains approximately 21,100 lb (9,600 kg) of water which would yield a maximum of 0.865 M^3 of gas or approximately 77.6 gms at STP which is insignificant when compared to the amount released by the metal-water reaction. Some additional hydrogen is also available from the pressurizer steam bubble. Under normal operating conditions the maximum hydrogen content of the pressurizer steam bubble is approximately 500 cc/kg of steam condensed to atmospheric conditions which yields a hydrogen mass of approximately 7.6 gms.

The vapor container has a free volume of approximately 141,000 ft^3 which would hold about 11,400 lbs of air at STP which is approximately 393 lb moles of air. Thus the ratio of lb moles of air in the containment to lb moles of hydrogen released is approximately 110 so that the average concentration of hydrogen in the vapor container would be about 1% by volume. This hydrogen concentration is approximately 1/4 of the lower flame limit and 1/7 of the lower limit of mixtures that could explode. The rapid dispersal characteristics of hydrogen gas plus the large amount of turbulence that will be associated with the rapidly cooling steam-air mixture in the containment will most assuredly prevent any concentrated pockets of hydrogen.

The fission product activities that might be released to the containment as a result of the maximum hypothetical accident have also been re-evaluated. The inclusion of a partial core of plutonium does not appreciably alter the radiation sources used for the calculation of off-site doses in the Final Safeguards Report for Core I. As a result, the off-site direct whole body and inhalation doses for the maximum hypothetical accident will be the same as presented in Section 600 of the Saxton Final Safeguards Report.

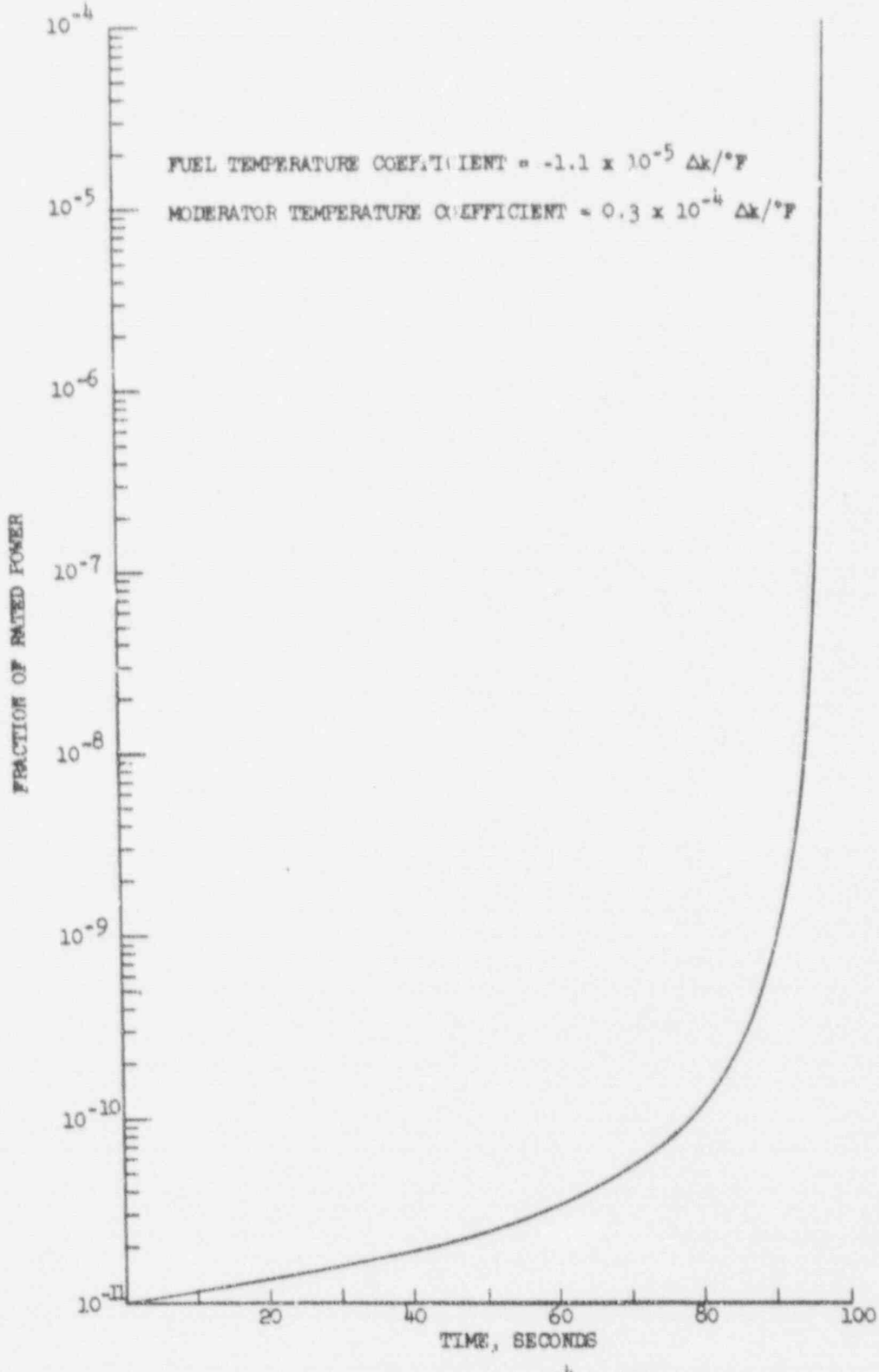

COLD STARTUP INCIDENT, 2.5×10^{-4} Δk/SEC INSERTION

FIGURE VI - B - 1

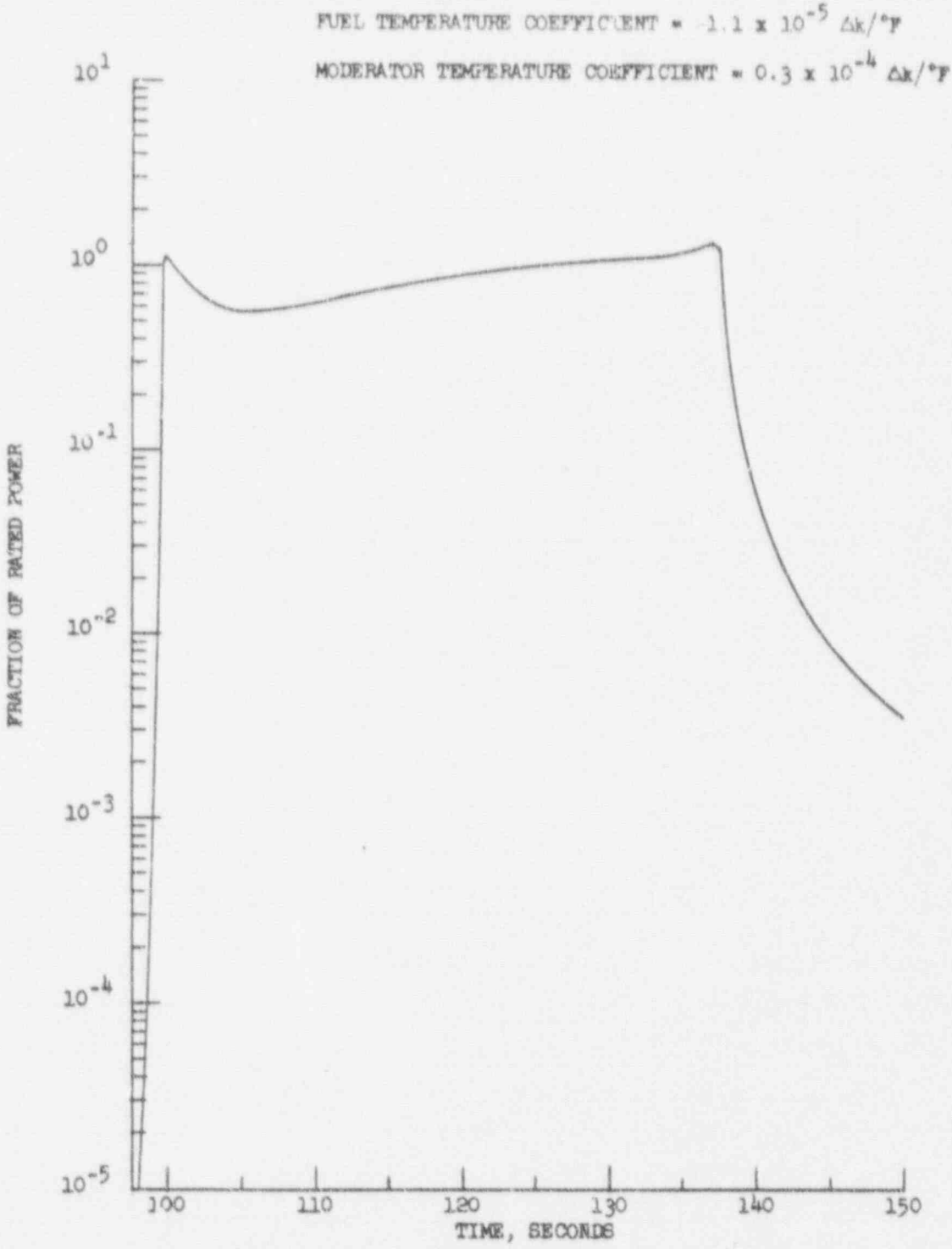

COLD STARTUP INCIDENT, 2.5 x 10^{-4} Δk/SEC INSERTION

FIGURE VI - B - 2

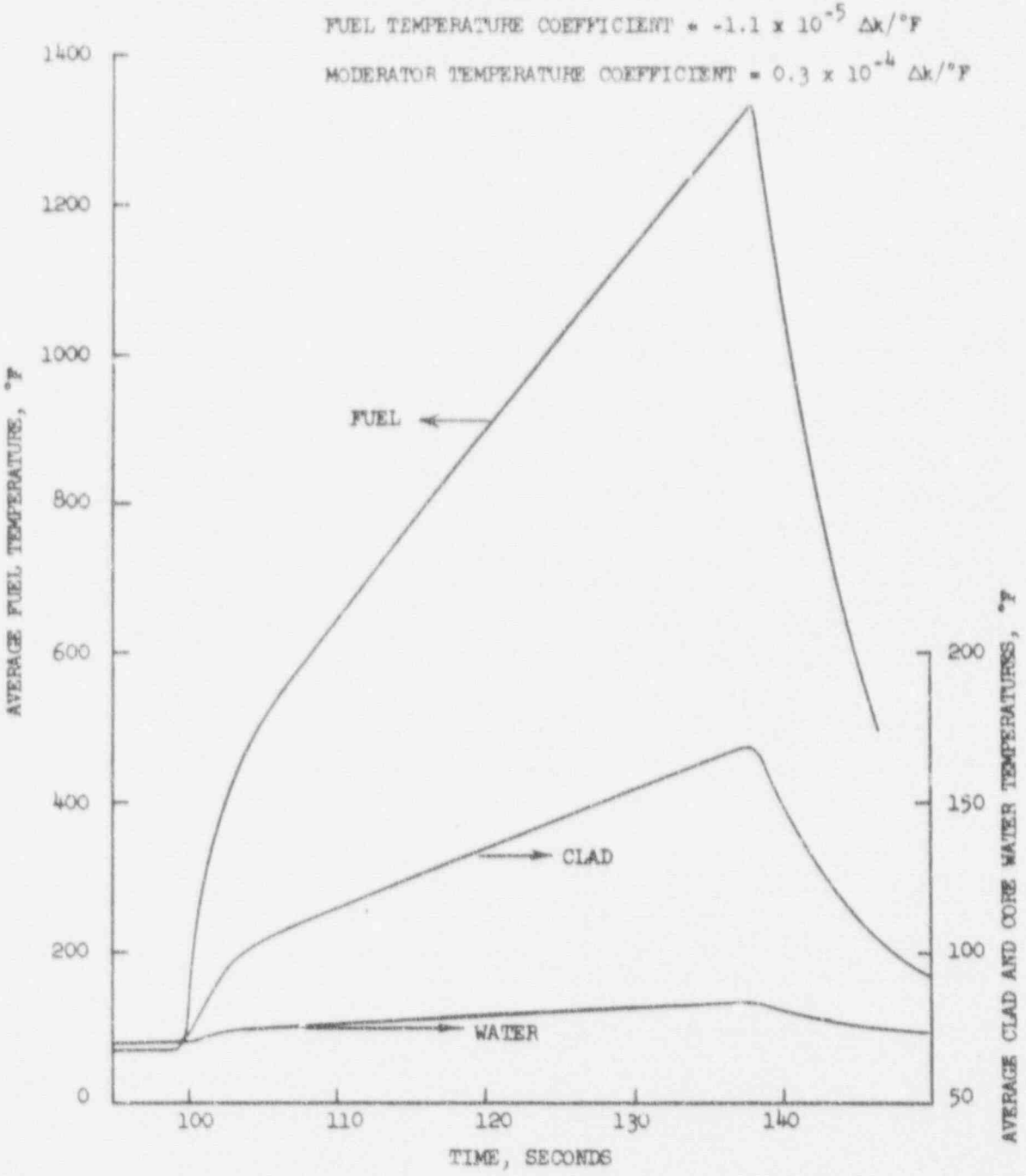

COLD STARTUP INCIDENT, 2.5 x 10^{-4} Δk/SEC INSERTION

FIGURE VI-B-3

FUEL TEMPERATURE COEFFICIENT = -1.1×10^{-5} $\Delta k/°F$

MODERATOR TEMPERATURE COEFFICIENT = 0.3×10^{-4} $\Delta k/°F$

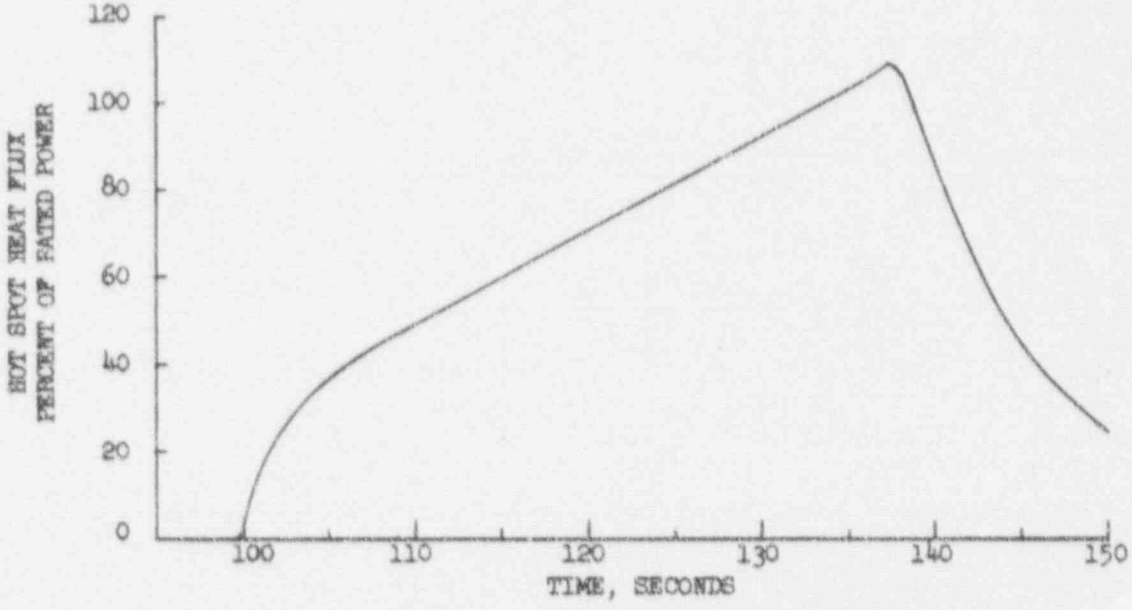

COLD STARTUP INCIDENT, 2.5×10^{-4} $\Delta k/SEC$ INSERTION

FIGURE VI-B-4

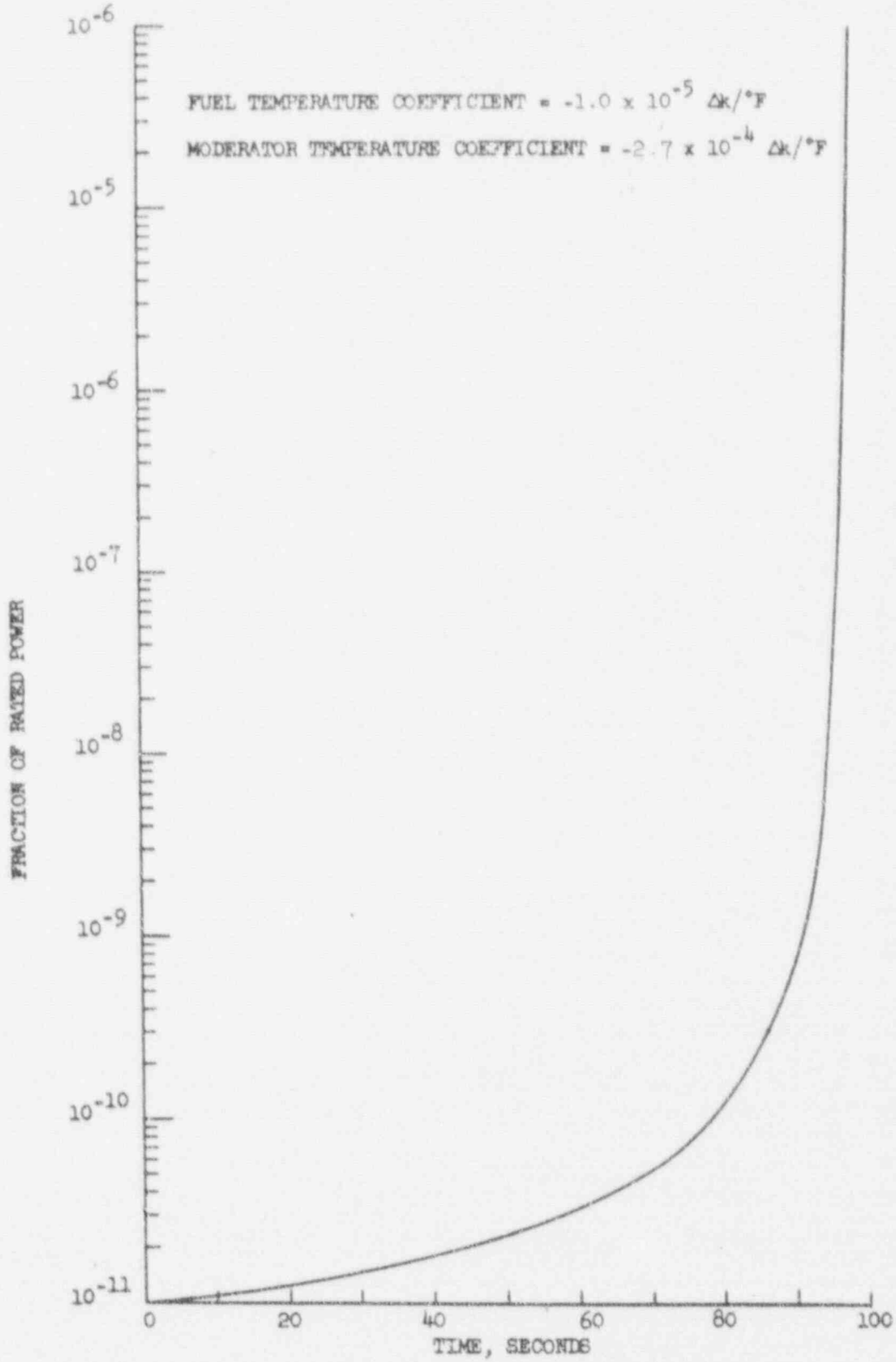

HOT STARTUP INCIDENT, 2.5 x 10^{-4} Δk/SEC INSERTION

FIGURE VI-B-5

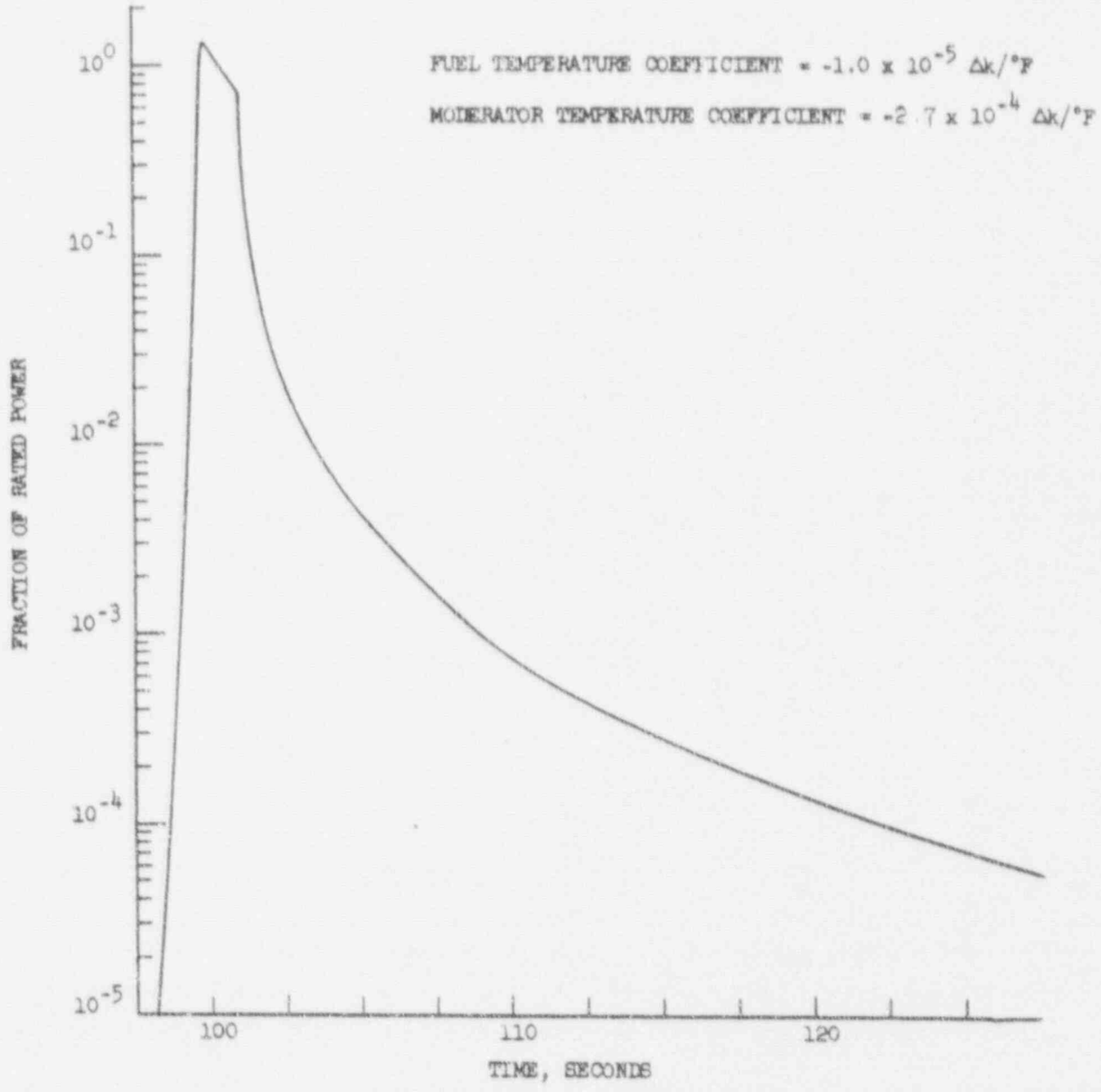

HOT STARTUP INCIDENT, 2.5 x 10^{-4} Δk/SEC INSERTION

FIGURE VI-B-6

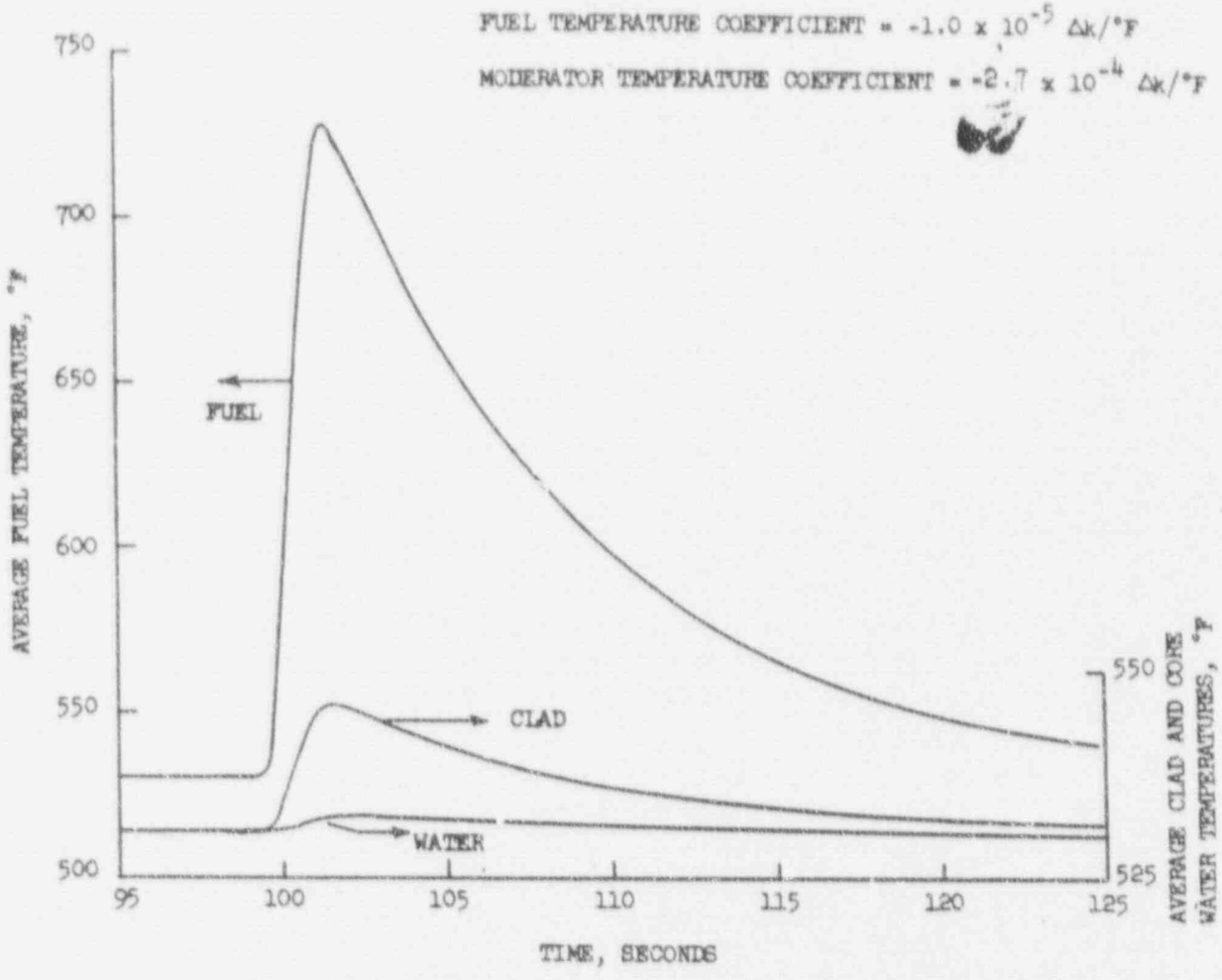

HOT STARTUP INCIDENT, 2.5 x 10^{-4} Δk/SEC INSERTION

FIGURE VI-B-7

FUEL TEMPERATURE COEFFICIENT = -1.0×10^{-5} $\Delta k/°F$

MODERATOR TEMPERATURE COEFFICIENT = -2.7×10^{-4} $\Delta k/°F$

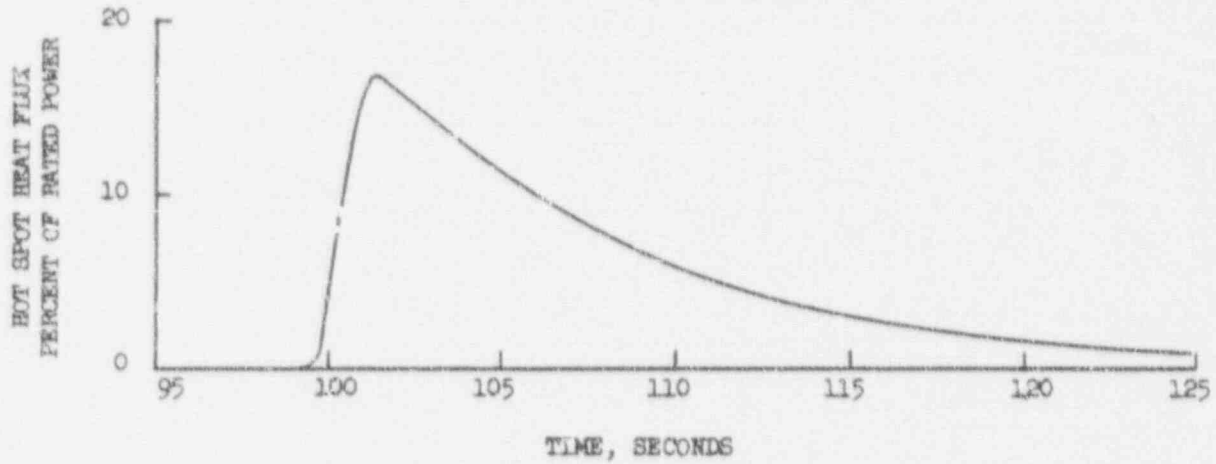

HOT STARTUP INCIDENT, 2.5×10^{-4} $\Delta k/SEC$ INSERTION

FIGURE VI-B-8

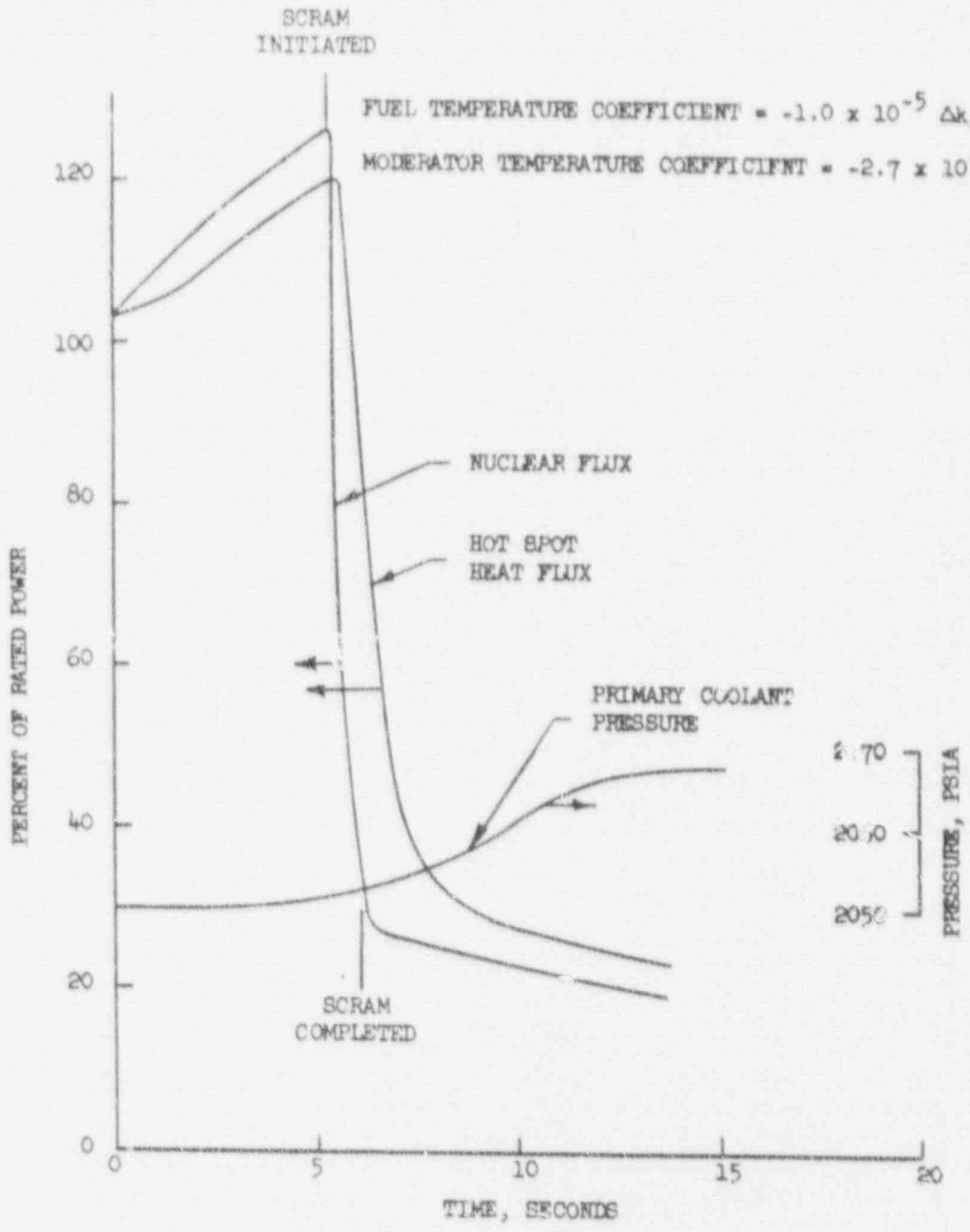

CONTINUOUS ROD WITHDRAWAL

(REACTIVITY INSERTION RATE = 2.5 x 10^{-4} Δk/sec)

FIGURE VI-B-9

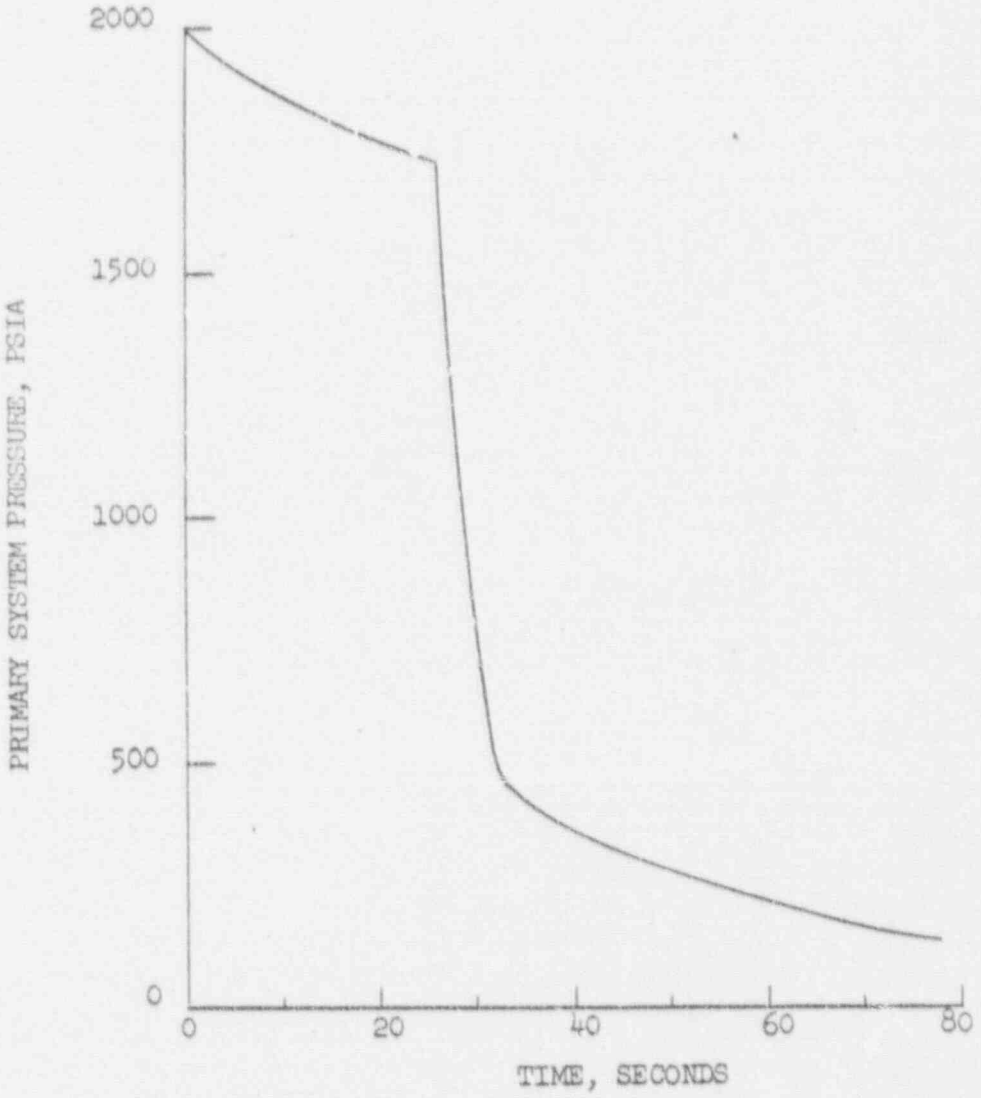

STEAM BREAK ACCIDENT

FIGURE VI-B-10

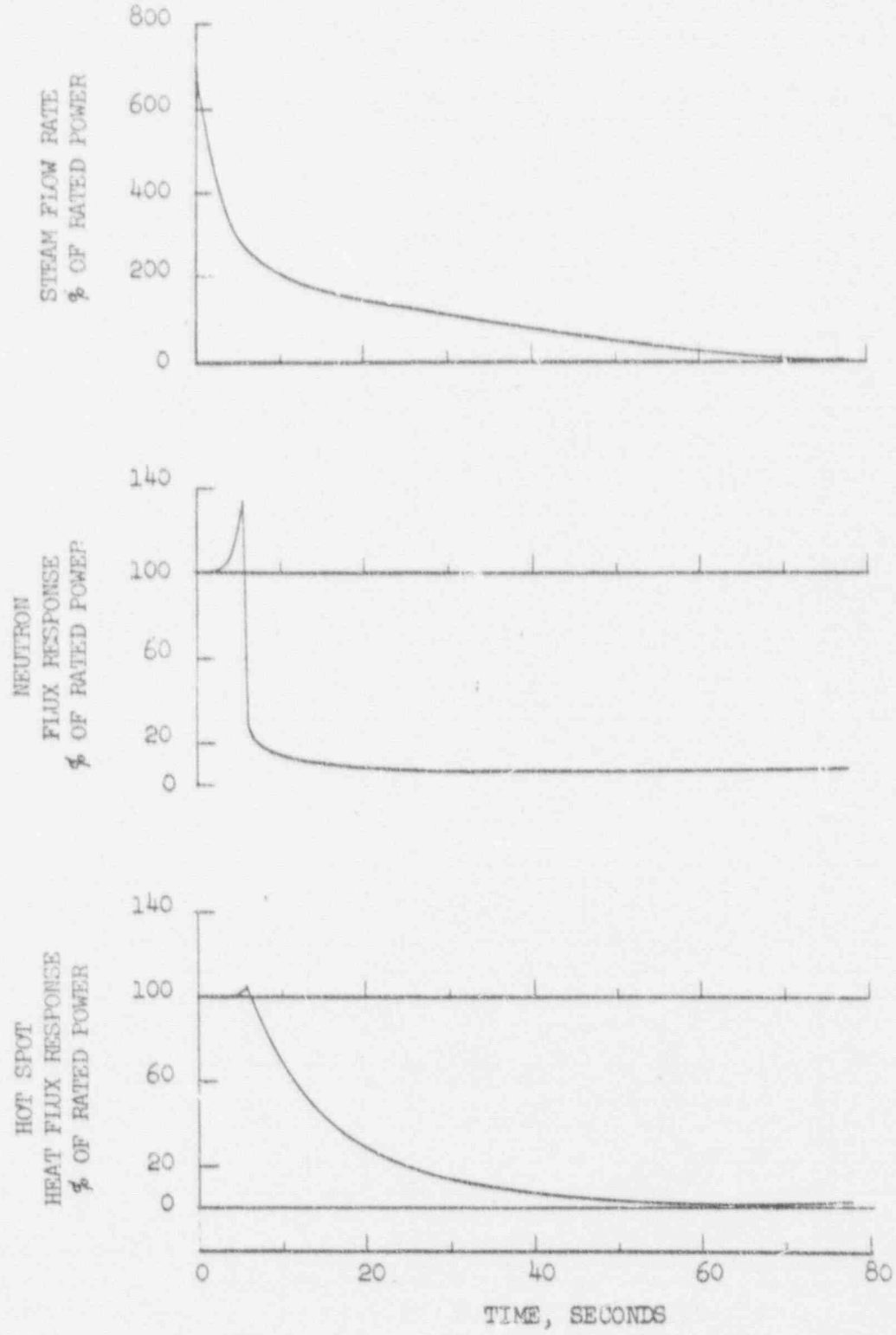

STEAM BREAK ACCIDENT

FIGURE VI-P-11

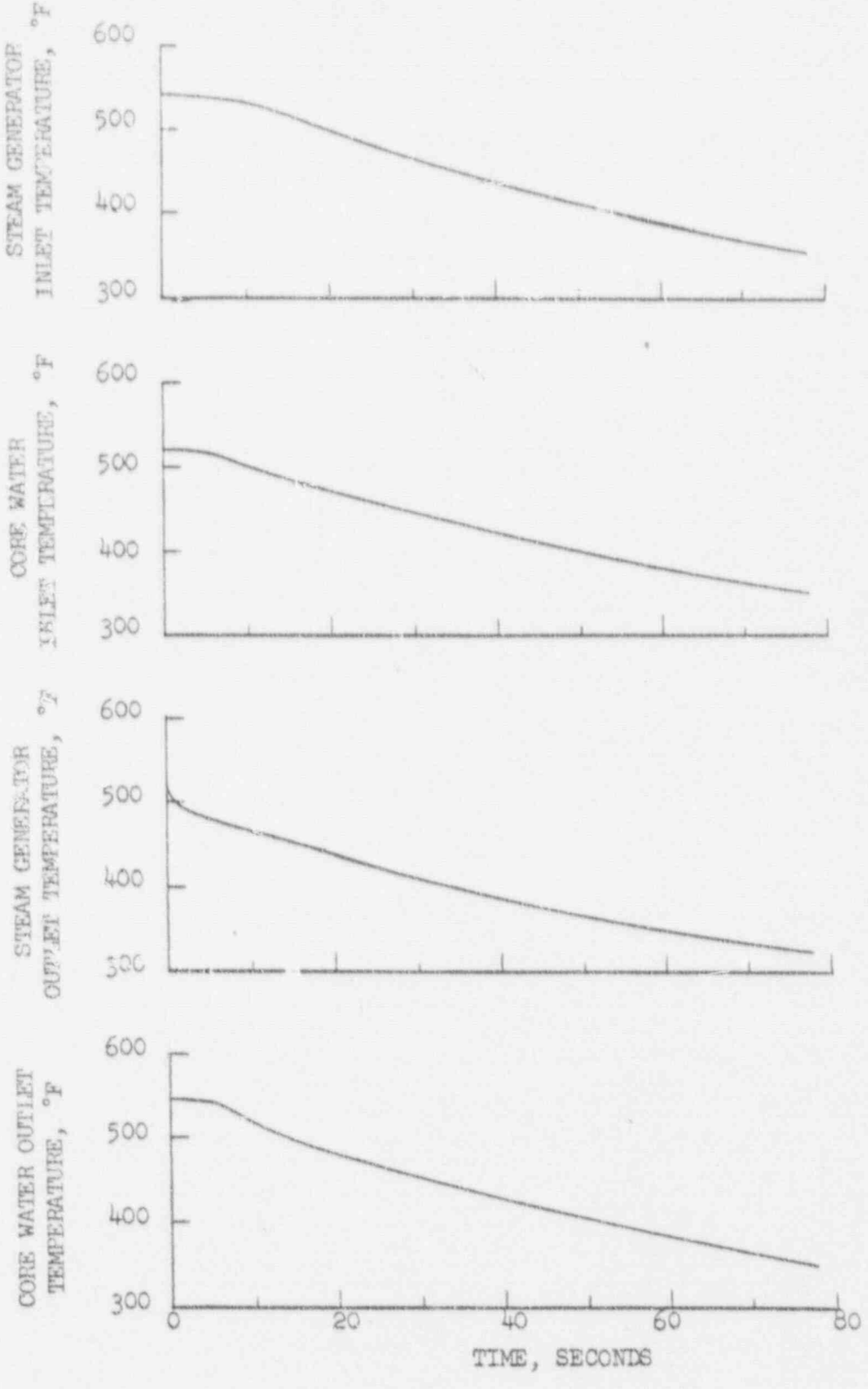

STEAM BREAK ACCIDENT

FIGURE VI-B-12

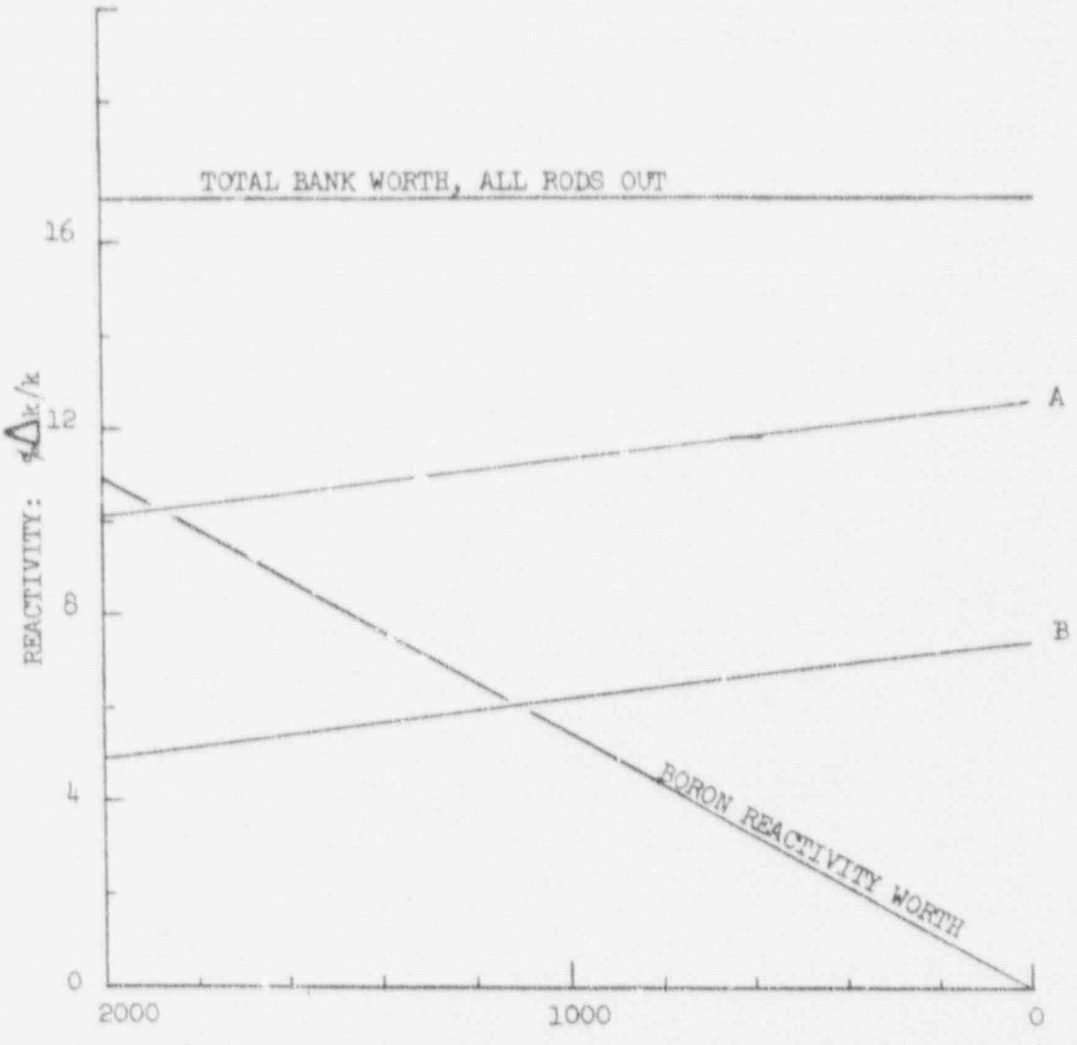

FIGURE VI-B-13

STEAM BREAK ACCIDENT, REACTIVITY INSERTION REQUIREMENTS

A - Reactivity required in control rods to maintain a shutdown margin of at least 0.5% $\Delta k/k$ if one rod sticks upon scram.

B - Reactivity required in control rods to maintain a shutdown margin of at least 0.5% $\Delta k/k$ if no rods stick upon scram.

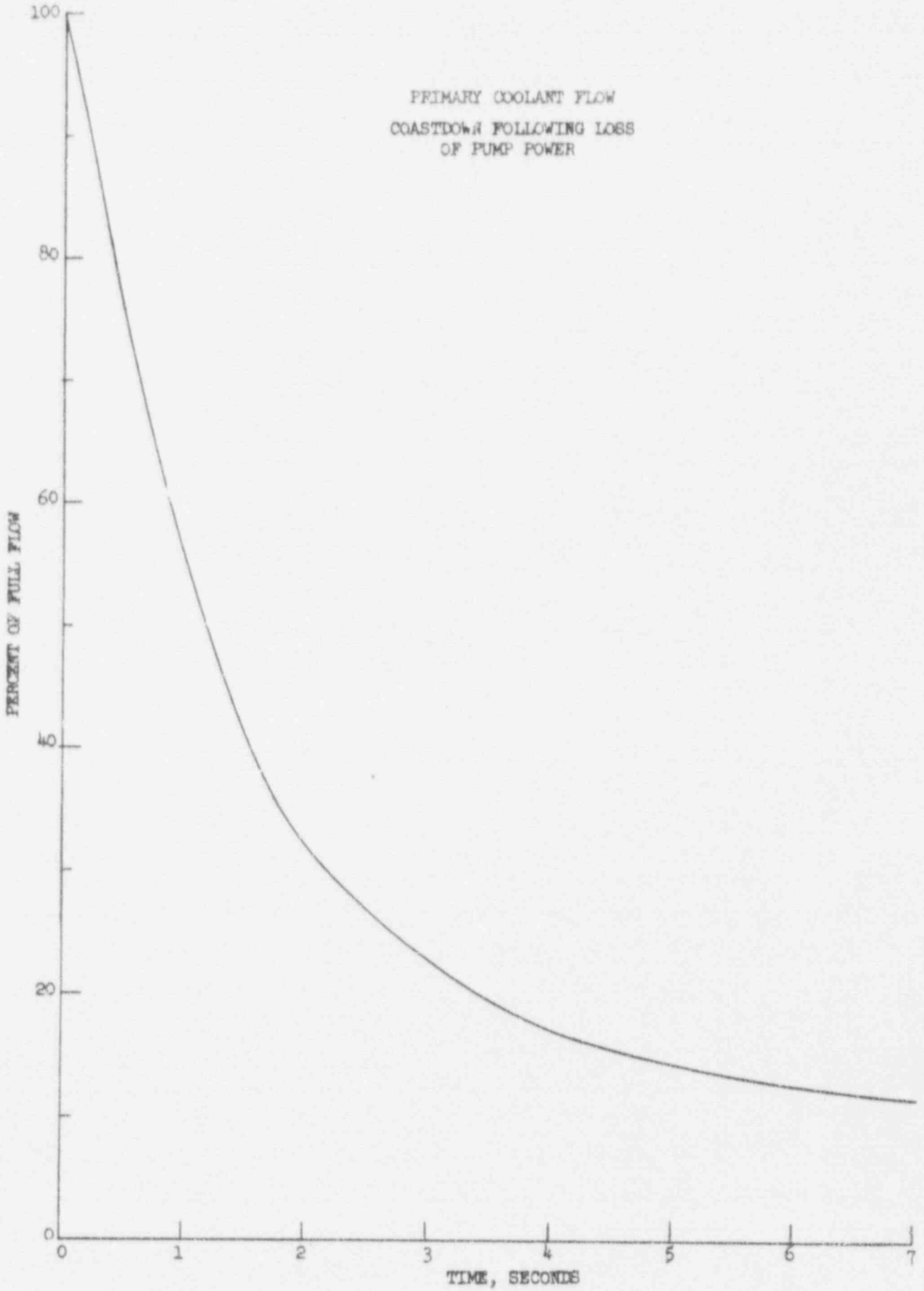
PRIMARY COOLANT FLOW
COASTDOWN FOLLOWING LOSS
OF PUMP POWER
PERCENT OF FULL FLOW
100
80
60
40
20
0
0
1
2
3
4
5
6
7
TIME, SECONDS

FIGURE VI-C-1

FUEL TEMPERATURE COEFFICIENT = -1.15×10^{-5} $\Delta k/k/F^{\circ}$

MODERATOR TEMPERATURE COEFFICIENT = -2.7×10^{-4} $\Delta k/k/F^{\circ}$

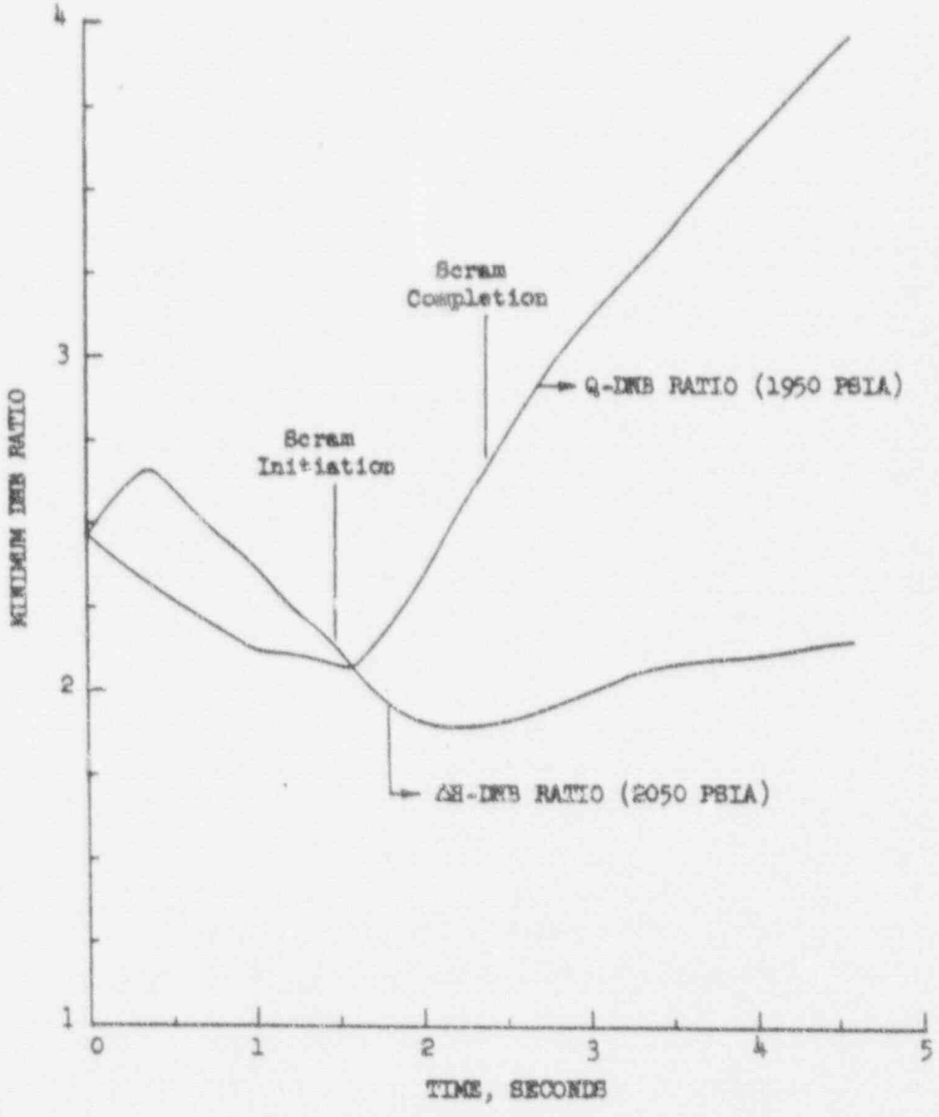

LOSS OF FLOW ACCIDENT

DNB RATIOS VERSUS TIME

FIGURE VI-C-2

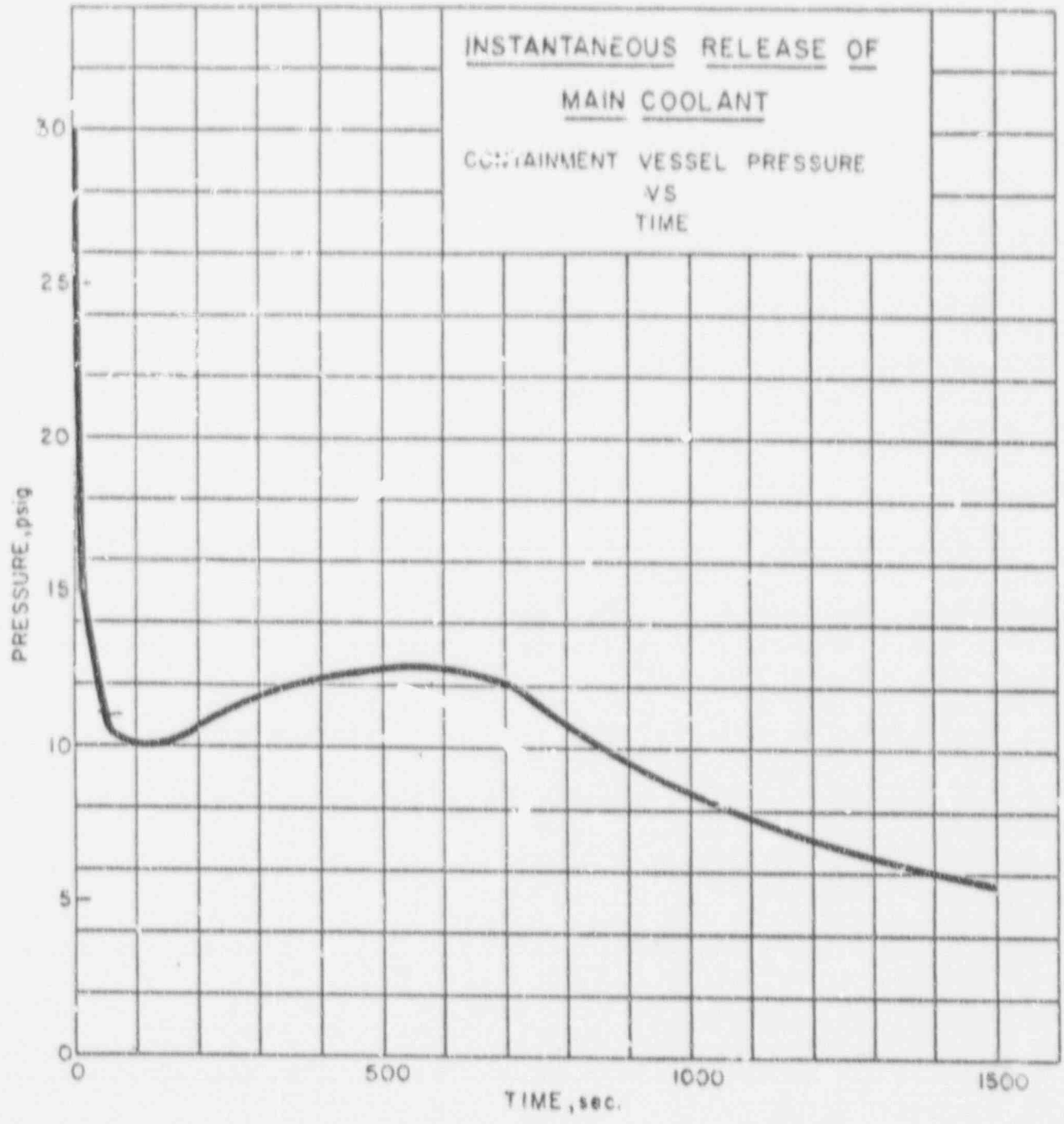
INSTANTANEOUS RELEASE OF
MAIN COOLANT
CONTAINMENT VESSEL PRESSURE
VS
TIME
PRESSURE, psig
30
25
20
15
10
5
0
0
500
1000
1500
TIME, sec.

FIGURE VI-D-1

VII. SAFETY CONSIDERATIONS

A. JUSTIFICATION FOR INCLUSION OF 9 x 9 ASSEMBLIES OF VIBRATIONALLY COMPACTED FUEL IN SAXTON PLUTONIUM PROGRAM

Evaluation of Defect Potential

Technical feasibility of the vibrational compaction process has been demonstrated by satisfactory in-pile performance of a number of test samples and by irradiation of bulk quantities of fuel rods in the PRTR.[1, 2, 3, 4] While a number of defects occurred during the early stages of these tests, the causes were identified in almost every case and the net result has been increased confidence in the use of vibrationally compacted fuels. This increased confidence is reflected in the choice of such fuel for the EBWR program. Under this program, 1,296 zircaloy clad fuel rods containing vibrationally compacted UO_2 - 1.5 w/o PuO_2 will be irradiated to exposures of 15,000 to 20,000 MWD/T.

Thirty-two of the thirty-three defects which occurred in PRTR have been attributed to fluoride contamination, excess moisture content, and traces of oil introduced by faulty powder attrition apparatus.[2,5,6,7,8,9] The defects occurred in both vibrationally compacted and swaged PuO_2-UO_2 fuel rods. The only defect which has not been explained to date occurred in a swaged rod. Investigation of this defect is continuing. The impurities cited are now being controlled and the results have been considered in developing specifications for the Saxton Plutonium Program. Since control of these impurities was initiated, one hundred and fifty seven fuel rods containing vibrationally compacted PuO_2-UO_2 fuel have been irradiated in PRTR to exposures of over 1,000 MWD/t (peak at 1600 MWD/T). These exposures are significant since all defects of vibrationally compacted rods prepared under old technology occurred at less than 400 MWD/T. Also, 560 rods from this latter group are still in pile and have attained exposures of 6,000 MWD/T without a defect.

Chloride, moisture, bad welds, and poor spacer design (resulting in fretting) were the main causes of the five defects which occurred at Savannah River during the early stages of the program.[10,11] Two defects which occurred in swaged rods[12,13] have not been explained to date and investigation is continuing. Since corrective measures were taken, they have had no defects in vibrationally compacted rods.[10,14] The rods have been irradiated to exposures of 9,000 MWD/T. While these rods contained only UO_2, there is no reason to suspect different behavior for PuO_2-UO_2 mixtures.

Evaluation of Water Logging and Washout Potential

During the early stages of development of loose powder fuels, fuel washout and waterlogging in the event of a defect were considered as possible performance limitations. These conjectures were based on (1) preliminary results of purposely defected fuel rods containing low density fuel (less than 85% T.D.) which was more susceptible to washout,[15,16] and (2) the reporting of a possible waterlogging failure of a swaged UO_2 fuel rod by Savannah River (details of this experiment are classified).[17,18] Apprehensions were greatly relieved when the former investigators reported the results of an unintentional defect in a swaged fuel rod containing UO_2 at 88% T.D.[19] Although the longitudinal split was 1.5 inches long and the reactor allowed to run at full power for 15 hours after the defect was detected, only a small amount of UO_2 (a maximum of 10% of the fuel in the area of the split) was eroded out of the rod. Apprehensions were further relieved when out-of-pile tests at the General Electric Laboratories indicated that vibrationally compacted, swaged and rolled UO_2 fuels had sufficient erosion resistance to prevent substantial losses to the coolant.[20, 21]

More recent results, however, have shown clearly that the potentials of these problems were greatly exaggerated during the early stages of development. No significant fuel washout and no waterlogging failures

were observed for the 33 defects which occurred in PRTR during the last two years.[2,5,6,7,8] Although cladding losses occurred in some cases, no severe reactor operating difficulties were reported. In some cases, the reactor underwent several pressure and power cycles after the defects were detected yet no waterlogging failures occurred.

The Hanford PRTR results are confirmed by the experience at the Savannah River Laboratories. They have never observed erosion of UO_2 from vibratory compacted or swaged fuel rods although they experienced seven defects including the previously mentioned possible waterlogging failure which had a 9 inch crack.[10,11,12,13,17,18]

The erosion resistance of loose powder fuels results from high density packing coupled with in-pile sintering. Evidence exists which indicates that in-pile sintering occurs at temperatures as low as 300°C.[22] Other evidence of enhanced sintering in a radiation field has also been reported.[23,24] These results may be explained by the following mechanism: (1) localized high temperatures resulting in increased rates for all sintering mechanisms (2) increased bulk and surface diffusion rates resulting from increased vacancy concentrations (3) enhancement of the vaporization-condensation mechanism through recoil processes.

Two waterlogging - washout type failures reported in 1962 should be mentioned since they caused some unnecessary anxiety. Neither failure can be considered applicable to the present situation. The first case reported was failure of a swaged, MgO-PuO_2 fuel rod exposed for 8 MWD/T in the PRTR.[25] Failure resulted from interaction between the MgO and water resulting in swelling and loosening of the fuel compact. No such reaction occurs in PuO_2-UO_2 fuels. The initial defect apparently resulted from fluoride contamination and release of absorbed water from the MgO. The second case reported was failure of a swaged UO_2 fuel rod undergoing transient tests in SPERT.[26] The failure occurred during a 7.5 sec-period power excursion test in which fuel temperatures rose by 300°C within

0.02 sec. It is certain that even a waterlogged rod containing pellets would burst under these conditions. The initial defects apparently resulted from broken epoxy resin seals used to insert eleven thermocouples into the center regions of the rod. The rod underwent several power excursion tests and remained in the reactor water for two days prior to the last test. Fuel washout occurred because of the large opening, 12 inches long and up to 0.5 inches wide, and because the fuel was not in-pile long enough to sinter.

The two cases cited cannot be employed to evaluate failure probabilities in loose powder fuels. Similarly one cannot employ the waterlogging failure reported by the Bettis Laboratories to evaluate failure potential in pelletized fuel.[27] The failure in this case was attributed to low pellet density (80% T.D.) and reaction of water with uranium carbide contaminant in the UO_2 pellet. The initial defect was intentional.

SUMMARY

1. Based on technology already developed at the national laboratories, no defects in vibrationally compacted fuel rods are anticipated.

2. The results of the national laboratory experiments show that no significant fuel washout and no waterlogging results from defects in rods containing loose powder fuel.

B. OPERATION WITH DEFECTIVE FUEL

As indicated in the previous section, there is a considerable amount of experience to indicate that clad failure under normal Saxton operating conditions is highly improbable. In addition, the available experience and information demonstrates that even under the conditions of clad failure and exposure of the fuel to the coolant that fuel washout is also highly improbable.

However, even in the event of clad failure while the plutonium core is in Saxton, there would be no danger to the plant personnel or undue hazard to the public. Unless caused by some violent transient, that is much less probable than the accidents postulated and analyzed in sections VI-A and VI-B, clad failure will be a gradual phenomena that would first manifest itself by an increase in the activity level of the reactor coolant. This increase would be due to the release of the gap activity of the failed rod into the coolant. If such an increase occurred, utilization of the alpha detection equipment described in Section V-B in conjunction with the normal Saxton primary coolant sampling techniques would be able to determine the extent, if any, of the plutonium contamination of the coolant. If no plutonium is detected and the coolant activity level is below the limit in the technical specifications, the continued normal operation of the reactor is possible. Continuing alpha analysis of the coolant during subsequent operation would detect any plutonium contamination increase. Significant plutonium contamination of the coolant would indicate gross clad failure and associated fuel washout and would require that reactor be shut down and procedures instituted to clean up the system and locate and remove the failed fuel.

REFERENCES

1. W. E. Roake, "Irradiation Alteration of Uranium Dioxide" Hanford HW 73072, March 1962.

2. "Quarterly Progress Report, Ceramics Research and Development Operation", HW 81600 January, February, March 1964.

3. J. J. Hawth, "Vibration-Compacted Ceramic Fuels" Nucleonics, Vol. 20, 9-1962, p. 50.

4. D. F. Babcock, et al., "An Evaluation of Heavy Water Moderated Power Reactors", DP 830, March 1963.

5. "Commercial Fabrication of Plutonium Fuel", Hanford Laboratories Invitational Meetings, April 2-3, 1964, p. 15, 18.

6. "Quarterly Progress Report, Ceramics Research and Development" HW-76302, pp. 4,5.

7. Ibid, HW-76304, pp. 4.1, 4.20.

8. "Unclassified Research and Development Programs, Division Reactor Development", HW-80308, November 63 and HW-81651, April 64.

9. Private communication, M. Freshly, S. Goldsmith, W. E. Roake.

10. Private communication, A. S. Ferrara.

11. Heavy Water Moderated Power Reactors Progress Report, DP-830, March 63.

12. Heavy Water Moderated Power Reactors Progress Report, DP-875, September-October 1963.

13. Heavy Water Moderated Power Reactors Progress Report, DP-905, March-April 1964.

14. Heavy Water Moderated Power Reactors Progress Report, DF-895, January-February.

15. M. M. Millhollen, A. R. Horn, J. L. Bates, "Hydriding in Purposely Defected Zircaloy-Clad Fuel Rods", HW 65465, 1961.

16. "Quarterly Progress Report, Fuel Development Operation" HW-69085, pp. 5.31-5.39, July-September, 1960.

17. R. R. Hood and L. Isokoff, "Heavy Water Moderated Power Reactors Progress Report, US AEC Report DP-505, p. 38 March 1960.

18. R. R. Hood and L. Isokoff, Ibid, DP-525, pp. 16-17, July 1960.

19. M. K. Millhollen, A. R. Horn, J. L. Bates, "Erosion Resistance of Swaged UO_2 Following an In-Reactor Fuel Rod Cladding Failure", HW-73015, 1961.

20. J. W. Lingafelter, E. A. Lees, R. J. Seely, GEAP-4020, 1962.

21. C. N. Spalaris, F. A. Comprelli, M. Siegler, GEAP-3698.

22. "Quarterly Progress Report, Ceramics Research and Development", HW-76304 pp. 4.10, October-December 1962.

23. E. A. Aitken, "Sintering Characteristics in a Radiation Environment", ASTM Meeting, June 28-29, 1961.

24. W. K. Barney, B. D. Wemple, Metallography of Irradiated UO_2 Containing Fuel Elements", KAPL 1836, 1958.

25. "Quarterly Progress Report, Fuel Development Operation", HW-76300 October-December 1962.

26. J. E. Houghtaling, T. M. Quegley, A. H. Spana, "Calculation and Measurement of the Transient Temperature in a Low-Enrichment UO_2 Fuel Rod During Large Power Excursions", IDO-16773, 1962.

27. J. D. Eichenberg et al., "Effects of Irradiation on Bulk UO_2," US AEC Report WAPD-183, Westinghouse Electric Company, October 1957.

28. J. J. Hawth, "Vibration-Compacted Ceramic Fuels" Nucleonics, Vol. 20, September 1962, p. 50.

29. V. W. Storhok, "Fabricating Plutonium for Better Performance", Nucleonics, Vol. 21, January 1963, p. 38.

30. United States-Euratom Joint Research and Development Program Report EURAEC 590, October 1962.

31. F. G. Dawson, "Plutonium As A Power Reactor Fuel", Hanford HW 75007, September 1962.

VIII. CONCLUSIONS

Based on the preceding report, it may be concluded that the proposed partial plutonium can be safely installed and operated as Core II in the Saxton reactor under chemical shim operating conditions or non-chemical shim conditions. The operating history of Saxton to date plus the results of the chemical shim experiment have clearly demonstrated the feasibility of such operation.

The accident analyses performed show that the results are no worse than for the previously analyzed Saxton Core I and that the present Saxton control and safety systems are more than adequate for use with the partial plutonium Core II.